1-1-2017

Optimal Capacity and Energy Efficiency of Massive MIMO Systems

Ahmed Alshammari
University of Denver

OPTIMAL CAPACITY AND ENERGY EFFICIENCY OF MASSIVE MIMO SYSTEMS

_____

A Dissertation

Presented to

the Faculty of the Daniel Felix Ritchie School of Engineering and Computer Science

University of Denver

_____

In Partial Fulfillment

of the Requirements for the Degree

Doctor of Philosophy

_____

by

Ahmed Alshammari

November 2017

Advisor: Dr. Mohammad Matin

Author: Ahmed Alshammari
Title: OPTIMAL CAPACITY AND ENERGY EFFICIENCY OF MASSIVE MIMO SYSTEMS
Advisor: Dr. Mohammad Matin
Degree Date: November 2017

Abstract

A lot of effort has been made during the last two decades to study and apply the concepts of MIMO technology in most of the wireless standards. Therefore, a huge improvement in the performance of wireless communications has been made. However, Demand for wireless services has exponentially increased during the past ten years. Hence, high throughput is very important for all users to get the best experience with the offered services. This creates many technical challenges that are difficult to handle with the existing technology. Therefore, massive multiple input multiple output (massive MIMO) is a new technology that has been proposed as one of the solutions that can overcome these challenges and fulfill the requirements of the next generation of wireless communications. The main concept of massive MIMO is that the base station (BS) equipped with a large number of antenna elements serve terminals over the same time-frequency resources. It is going to be one of the key tools that can satisfy and handle the exponential growth in data traffic. Massive MIMO was introduced as a modified and scalable version of multiuser MIMO. Massive MIMO improves systems capacity and energy efficiency using simple linear processing.

Despite the promising benefits of massive MIMO, a lot of aspects must be tackled before it can be practically used. This dissertation investigates issues that affect the performance massive MIMO such as the angle spread, angle of arrival, pilot length and antenna spacing. Results show that the low angle spread of negatively affects the channel capacity and energy efficiency (EE). This effect can be reduced by increasing the transmit power to increase the signal to noise ratio. Moreover, it is shown that and adding more antennas in the BS and increasing the spacing between them can also diminish the impact of the imperfect channel by improving the channel capacity and the EE. This research also analyzes the relationship between the number of terminals and the capacity in a single cell scenario. Results show that the sum capacity of the system can increase when the number of users is increased. However, allocating too many users can negatively affect the performance of massive MIMO.

Acknowledgements

First and foremost, I thank my god for the all the blessings and the gifts that I enjoy in my life.

I would also like to thank and appreciate the efforts of my advisor Professor Mohammad Matin for his tremendous support and encouragements that have always inspired and helped me throughout my PhD journey. I would also like to thank my supervisory committee members, Professor Jack Donnelly, Professor Jun Jason Zhang and Professor Yun-Bo Yi for their time and support. To all the faculty, staff members and fellow students at the Department of Electrical and Computer Engineering of the University of Denver, Thank you. It has been an honor to have met you all and worked with you.

Last but not least, I am deeply indebted to my family for everything, especially my parents who allowed me to realize my own potential. Their support and gaudiness over the years is the reason I have come to this point in my education. Also, I would like to thank my wife and my son for their patience, understanding and support while I spent countless hours preparing this dissertation.

Table of Contents

List of Figures

List of Acronyms

5G (Fifth Generation)

MIMO (Multiple Input Multiple output)

BS (Base Station)

LMMSE (Linear Minimum Mean Square Error)

MSE (Mean Square Error)

DL (Downlink)

UL (Uplink)

UE (User Equipment)

TDD (Time Division Duplex)

FDD (Frequency Division Duplex)

CSI (Channel State Information)

i.i.d. (Independent and Identically Distributed)

SINR (Signal-to-Interference-Plus-Noise Ratio)

AOA (Angle of Arrival)

EE (Energy Efficiency)

SCM (Spatial Channel Model)

RX (Receiver)

SU-MIMO (Single-User MIMO)

MU-MIMO (Multi-User MIMO)

SNR (Signal to Noise Ratio)

GB (Gigabyte)

EB (Exabyte)

PDF (Probability Density Function)

LTE (Long Term Evolution)

Chapter One: Introduction

1.1 Motivation

The last few years have witnessed a huge increase in the wireless data traffic. Introducing smart hand-held devices in the last decade has led the tremendous growth in the number of applications that are hungry for bandwidth. Also, many services like file sharing and video streaming are already pushing the limits of the current wireless networks. 400 million times is the reported increase in mobile data traffic between the years 2000 and 2015, from less than 10 GB per month to 3.7 EB per month respectively [1]. It is not expected that this trend is stopping any time soon. In the next decade, required data rates will grow significantly to a level that cannot be supported by the fourth generation (4G) networks. Figure 1.1 shows the mobile data traffic between the year 2015 and 2020. Clearly, an acceleration is forecasted in the next few years, as the data traffic is expected to exceed 30 EB per month in the year 2020 which represent an 8-fold increase over the year 2015 [1]. Sources of this demand will not only come from data exchange by smartphones, computers and tablets but also from the emerging kinds of communications, such as the multimedia rich applications like 3D holography, tele-presence and communications between machines [2]. Figure 2.2 shows the number of connected devices between the years 2015 and 2020. It is estimated that the number of connected devices will be around 11 billion devices by the year 2020. Moreover, most of the future devices will

be equipped with a lot of technologies that require very advanced wireless communication capabilities. Hence, researchers are trying to find ways to handle 1000 times the current data traffic, provide service for 10 or even 100 times more users and lower the latency for mobile user by a factor of 5 in comparison with the Long-Term Evolution (LTE).

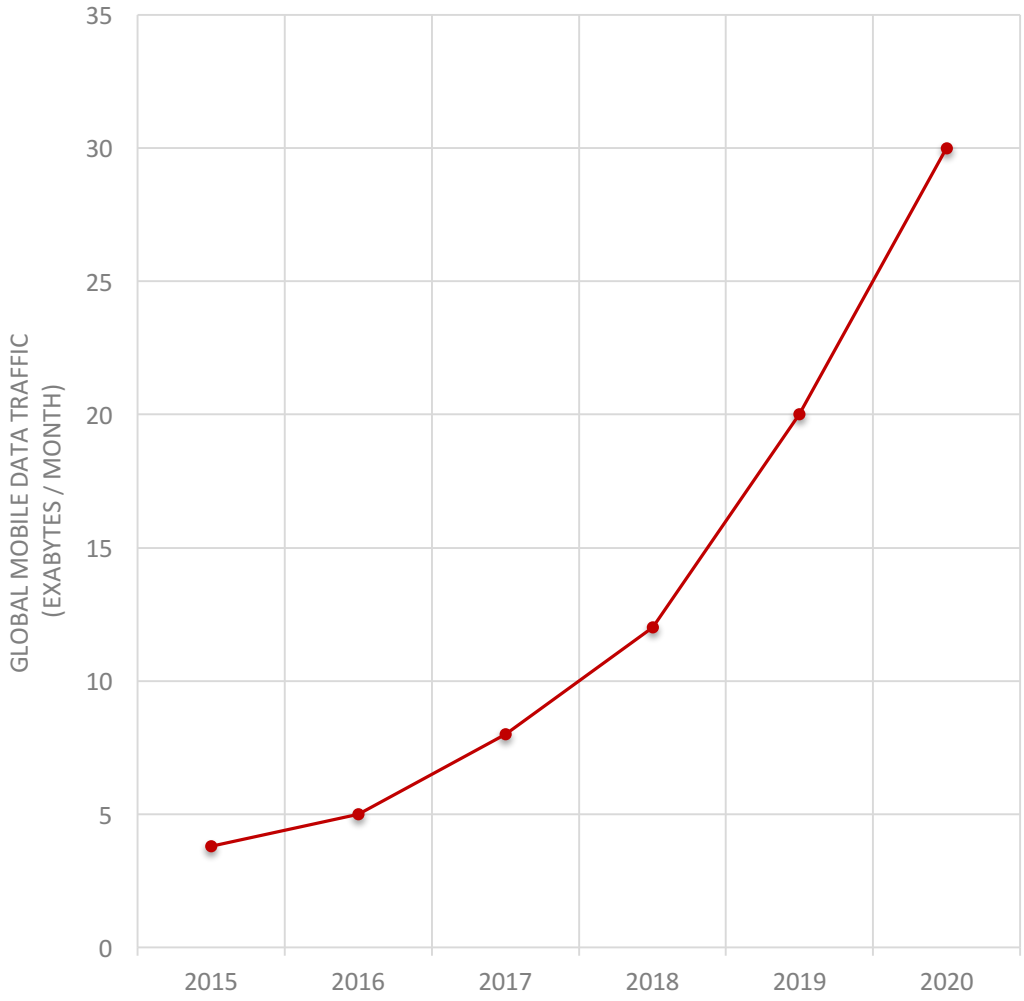

Figure 1.1 Global mobile data traffic (source: Cisco [3]).

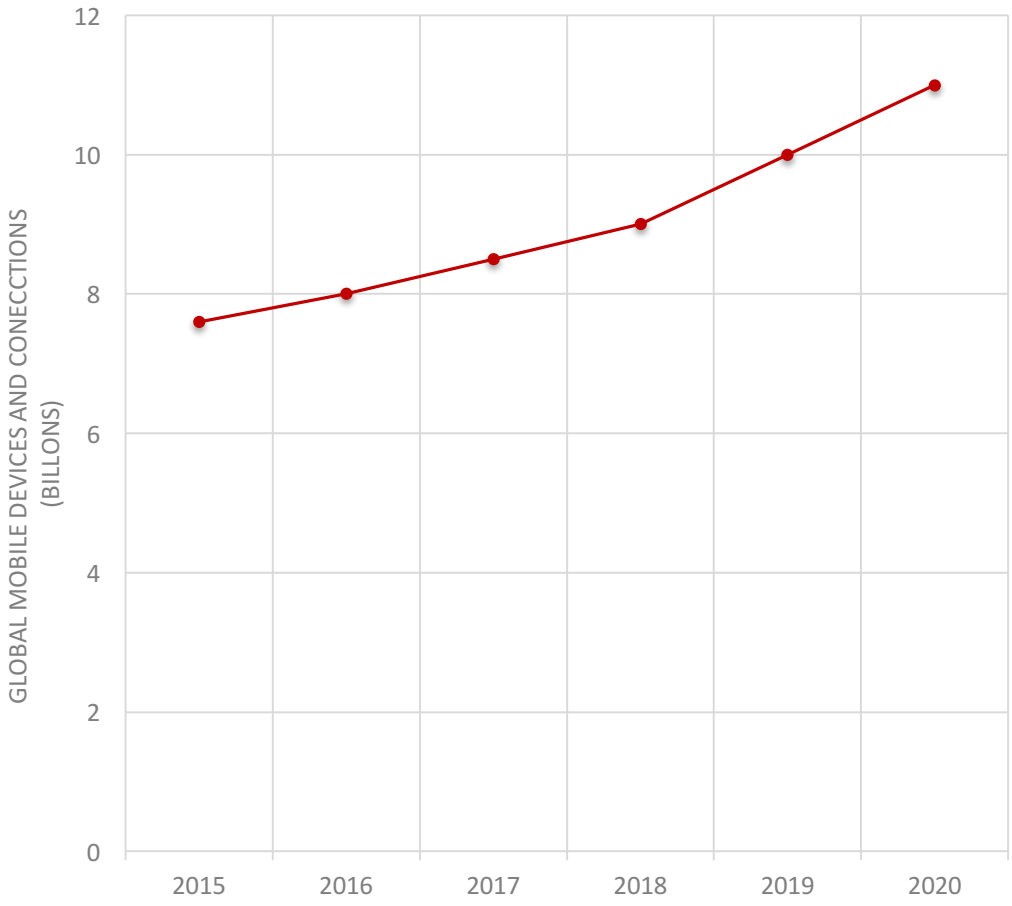

Figure 1.2 Global mobile devices (source: Cisco [3]).

The most important parameter to measure the performance of any wireless network is its throughput in (bits/s):

$$\text{Throughput} = \text{Bandwidth (Hz)} \times \text{Spectral efficiency (bits/s/Hz)}.$$

Obviously, improving the throughput can be done either by increasing the spectral efficiency or using more bandwidth. Increasing the frequency spectrum is the simplest way to meet the demand for higher throughput. However, the effectiveness of this option has recently become less attractive due to many reasons. First, the fact that spectrum is a natural resource makes it constrained. Multiple communications services must share fixed portions of the spectrum. Already, various operators and services occupy most part of the available spectrum. Thus, portions of the spectrum dedicated for other services must be reallocated for mobile commutations to increase the frequency spectrum of operations. However, this can be done to a very limited extent that cannot satisfy the future demand for mobile data traffic. Also, not all bands of the spectrum are suitable for wireless communications due to their high attenuation and unfavorable propagation. Moreover, spectrum is one of the most valuable resources in the world which makes this option very expensive for mobile operators. It is obvious that more spectral efficient technologies are needed to sustain the evolution of wireless communications. For example, data rates in certain areas can be increased using more aggressive spectrum reuse strategies. Small cells is one of these strategies. However, high-mobility users and wide area coverage are two reasons that makes the small cell option less efficient [4].

Attenuation of the transmitted signals in wireless communications results from the fading which can be caused by multipath propagation or by obstacles between the receiver and the transmitter that cause shadowing, yielding a serious challenge for the reliability of wireless communications. One of the well-known diversity techniques used to enhance the reliability of communications is the transmission through multiple input multiple output (MIMO) antennas. It has been proven in MIMO technology that deploying multiple antennas at the receiver and transmitter increase the amount of data that can be transmitted and received through a certain frequency band. The gains in this case are linearly proportional to the minimum number of antennas in the transmitter or the receiver if the scattering environment is rich and the channel knowledge is the available at the receiver [5]–[13]. Unfortunately, Due to its complex transmission strategies and the requirement for accurate channel state information (CSI) at the BS, the adoption of multi-user MIMO (MU-MIMO) in current standards does not take full advantage of the available research in literature [14] .

The 5th generation of wireless communication systems (5G) promises much higher capacity and speeds under limited spectrum and tight power compared to the current systems [14]–[26] . Hence, signal processing techniques and system configurations must be fundamentally changed to support efficient signal transmission. Although the enabling technologies of 5G are not finally identified yet, massive MIMO is a strong candidate technology. This technology was introduced Back in 2010 when Tom Marzetta from bell labs published the paper "*Noncooperative Cellular Wireless with Unlimited Numbers of Base Station Antennas"* which have been cited over 1300 times. Since then, he and his colleagues have made many contributions in this area such as [27]–[31]. Massive MIMO

proposes new strategies to practically implement concepts from MU-MIMO, where non-cooperative single antenna users, K are served simultaneously through a BS with a very large number of antenna elements, M [32], [33] . When M is much larger than K, low complexity linear signal processing can be optimal, while instantaneous channel state information (CSI) is available to the BS though the uplink (UL) training. It has been shown that significant improvements in the radiated energy and channel capacity can be achieved using massive MIMO [29], [34]–[36].

Massive MIMO can be considered as a gold mine of research problems. Despite the huge advantageous that massive MIMO is bringing to the next generation of wireless communication such as the ability to accommodate high number of users with very high data rates and reliability with very low power consumption, a lot of aspects must be addressed before it can be practically used. In fact, many of the traditional communication problems are now considered less relevant, however, an entirely new class of problems that must be considered have been uncovered. Many recent work in literature have discussed the tremendous improvements that massive MIMO can bring to the capacity and energy efficiency [29], [30], [37], [38]. Also, impairments that might affect the performance of massive MIMO have been investigated in [37], [39]–[41]. Hence, interest in this technology is growing as the numbers of published research in this area increases.

1.2 Fifth Generation (5G)

Interest in the 5G standard is increasing as the long-term evolution (LTE) which is part of the 4G standards is reaching a maturing level where the only improvements that can be made are incremental. Many engineering challenges must be dealt with in 5G. Hence,

it is very important to understand and recognize the expected capabilities of a 5G system to meet these challenges. Although many requirements are imposed by different applications, they do not have to be satisfied simultaneously. The following is a summary of the 5G requirements.

1.2.1 Data Rate

Meeting the tremendous mobile data traffic is undoubtedly the main reason why 5G is needed. There will be different targets for the various metrics used to measure the data rate:

a) **Aggregate data rate** that indicates the total amount of data that can be handled by the network, measured in bits/s per unit area. The upgrade from 4G to 5G will roughly result in 1000x increase in this quantity

b) **Edge rate, which** is also known as the 5% rate, represents the least data rate one can expect to be served within the range of the network. The edge rate is one of the most important metrics that has a logical engineering meaning. The aim for 5G is to improve the edge data rate to range between 100 Mbps (sufficient to stream high definition videos) and 1 Gbps [42]. This means that 5G must ensure that 95% of users get 100 Mbps which is very challenging because it would require around 100 times improvement over the current 4G systems where the 5% rate is typically around 1 Mbps.

c) **Peak rate** is the ultimate amount of data rate that can be achieved under any possible system configuration. It is usually considered to be a number dedicated

for marketing purposes that engineers do not typically care about. The peak rate is usually in the range of tens of Gbps.

1.2.2 Latency

The latency of the existing 4G systems is around 15 ms with 1 ms sub-frame time including the overheads required for access and resource allocations [42]. Even though this latency is adequate for 4G applications, new cloud based technologies and two way gaming are expected in 5G [43]. Therefore, 5G must have the capabilities of providing 1 ms latency which is almost an order of magnitude faster than the contemporary systems. As a result, this constraint on latency will greatly shrink down the sub-frame time and may also impose critical design choices at various components of the protocol.

1..2.3 Cost and Energy

Ideally, energy consumption and costs are supposed decrease with 5G or at least the per link costs and energy should not increase. The cost per bit and the joules per bit must at least drop by 100x because the data rates on per link basis will be increased around 100x. Many technologies have the potential of reducing power consumption and cost [42]. For example, the spectrum of the millimeter wave will be almost 10-100x cheaper than the spectrum below 3 GHz used in 3G and 4G. Also, small cells solution will also be 10-100x cheaper and more efficient in energy consumption than macro-cells.

1.2.4 Devices Types

More diverse range of devices are going to be efficiently supported in 5G. A single macrocell must be able to support at least 10,000 low rate terminals beside the usual high-rate devices especially with the rise of machine to machine communications. Therefore, the network management and control plans relative to 4G must be fundamentally changed because their state machines and overhead cannot handle such large and diverse subscriber base.

1.3 Problem Statement

Massive MIMO will be included among many other technologies in the 5G standards. However, there are a lot of problems that must be considered before finalizing the 5G standards. Thus, a lot of recent research is aiming for that goal. Capacity and energy efficiency are one of the most important performance metrics of any wireless system. This dissertation investigates the performance of massive MIMO using these two metrics. While it is challenging to maintain ideal channel conditions when a large number of antennas are located in tight space, many work in literature ignore that issue and just assume a perfect channel conditions [38]. Hence, a channel model that takes into account the angle spread, antenna spacing and angle of arrival is considered to explore the capacity and EE of Massive MIMO systems. This dissertation also investigates the influence of serving too many users simultaneously in the same geographical area on the performance of massive MIMO. This effect can vary based on the cell size and the number of antennas in the BS and the spacing between them.

1.4 Methodology

The simulation capabilities of MATLAB are exploited to inspect the effect of the imperfect channel knowledge and user allocation on UL channel estimation, capacity and EE using the mathematical model of massive MIMO. The channel covariance matrix, which is necessary for the LMMSE estimator, is generated in MATLAB. A closed form expressions of the probability density function (PDF) for the Signal-to-Interference-Plus-Noise Ratio (SINR) is derived. The estimated channel is used to calculate the capacity and energy efficiency of massive MIMO.

1.5 Chapters Organization

The rest of this dissertation is organized as the following:

Chapter 2: reviews the concept of multi-antenna communications. It summarizes the main characteristics of Point to Point MIMO and Multi-Users MIMO and the differences between them. It also introduces the massive MIMO technology and discusses its potential advantages and the possible challenges that must to be dealt with.

Chapter 3: analyzes the capacity and EE of massive MIMO using the one ring channel model.

Chapter 4: investigates the relationship between the number users of massive MIMO and the sum capacity.

Chapter 5: concludes the dissertation and highlights some of future work ideas.

Chapter Two: Literature Review

2.1 Introduction

As technologies are becoming more advanced, it can be taken for granted that more wireless throughput is always going to be needed. It is expected that, within few years, millions of users will want to use mobile multimedia applications such as online gaming, e-healthcare, streaming videos and communicating through holographic videos [44]. Thus, hundreds of megabits per second will be essential for every user.

Availability of spectrum which will never increase, fundamentals of information theory and the electromagnetic laws of propagation are all aspects that impact the amount of information that can be transferred wirelessly. Hence, the performance of wireless networks is always limited at the physical layer [31]. Improving the efficiency of a wireless networks is typically done by 1) utilizing the free or underutilized areas of the spectrum 2) increasing the density of access points 3) improving the spectral efficiency by increasing the number of bits that can be carried in each Hertz [45]. Millimeter wave and small cells are used to handle the first two respectively [46]. It is likely that the tradition of using new bands and deploying more access points will continue in the future, but the necessity to maximize the spectral efficiency is inevitable [47].

Using MIMO technology is the only way to substantially improved channel capacity. The original form of this technology is Point to point MIMO [5] that was theoretically developed later to Multiuser MIMO [48] and recently Massive MIMO is evolving to be the optimal and most useful form of the multi antennas communications [30], [38], [49].

2.2 History of MIMO

There is a remarkable history behind the phrase "Multiple Input Multiple Output". Even though it is used to refer to one of the communication techniques, it was used in the 1950s in filters theory and electric circuit [50].

The term MIMO was used to indicate circuits with multiple input and multiple output ports in its original context. During the 90s, however, this term has been adopted by communication systems researchers and information theorists to denote a novel signal processing technique that was developed for wireless systems with multiple antennas. The reference point in this different use of the term was the communication channel. The term multiple input was used to denote the signals that were entering the communication channel from the multiple antennas. Also, the word multiple output implied signals received at the multiple antennas of the receiver, which were regarded as the output of the communication channel. It was in the paper published in 1999 by Gerry faschini and Peter Driessen where the term MIMO used in wireless communications as part of analyzing the theoretical communication capacity of a wireless system with multiple transmit and receive antennas [51].

Although multiple antennas are required in MIMO communications, it is not the first technique that utilizes multiple antennas to be developed. In fact, using multiple antenna technology to enhance the performance of radars and other aspects of communications dates back to the early 1900s. During 1905 Karl Braun showed the first application of multiple antennas which uses phased array antennas to enable rapidly steerable radar, and later, in AM radio broadcasting to switch between sky-wave and ground-wave propagations [52].

Fading has been combated in wireless communications using the multi antennas technology for more than 70 years through the receive diversity. The idea of receive diversity showed up in 1931 in a paper published by H. Peterson and H. Beverage [53]. The receive diversity was used in military applications such as the troposcatter during the 1950s.

During the early 1990s, two technologies that employ the multi antennas techniques were introduced. The first technology is the transmit diversity which also combat fading. This technique was initially introduced in two papers published in 1991 and 1993 [54], [55]. Later, Alamouti published his well-known paper where he proposed a novel technique to achieve transmit diversity with a very much less processing requirements at the receiver [56]. His paper explained how to achieve transmit diversity using a simple space time coding technique. Since its introduction, Alamouti's method has become the most preferable MIMO scheme almost by all wireless systems.

There was another form of multi antenna techniques being introduced, while research on transmit diversity was in progress. Instead of using multi antennas to ease the effect of fading, different group of researchers were looking for new methods of exploiting fading to satisfy the demand for more throughput. The paper on layered space time communication published by Gerry Foschini in 1996 who works at AT&T research Labs illustrated the main concept for the series of spatial multiplexing techniques that were later known as the Bell-Labs layered Space Time (BLAST) schemes [57]. Two years later, the team of Foschini were the first to come up with a laboratory prototype system based on a certain type of BLAST technology known as Vertical BLAST or V-Blast for short [58].

Since these developments in spatial multiplexing and spatial diversity in the late 1990s, a huge amount of research has been done. The emerging MIMO techniques from this research using the means of spatial multiplexing and spatial diversity led to increasing the number of wireless standards used commercially. In 2001, Iospan introduced the first MIMO technology that can be used commercially. Most of commercial communications standards now include MIMO technology after it was included in the WiMAX standard in 2005.

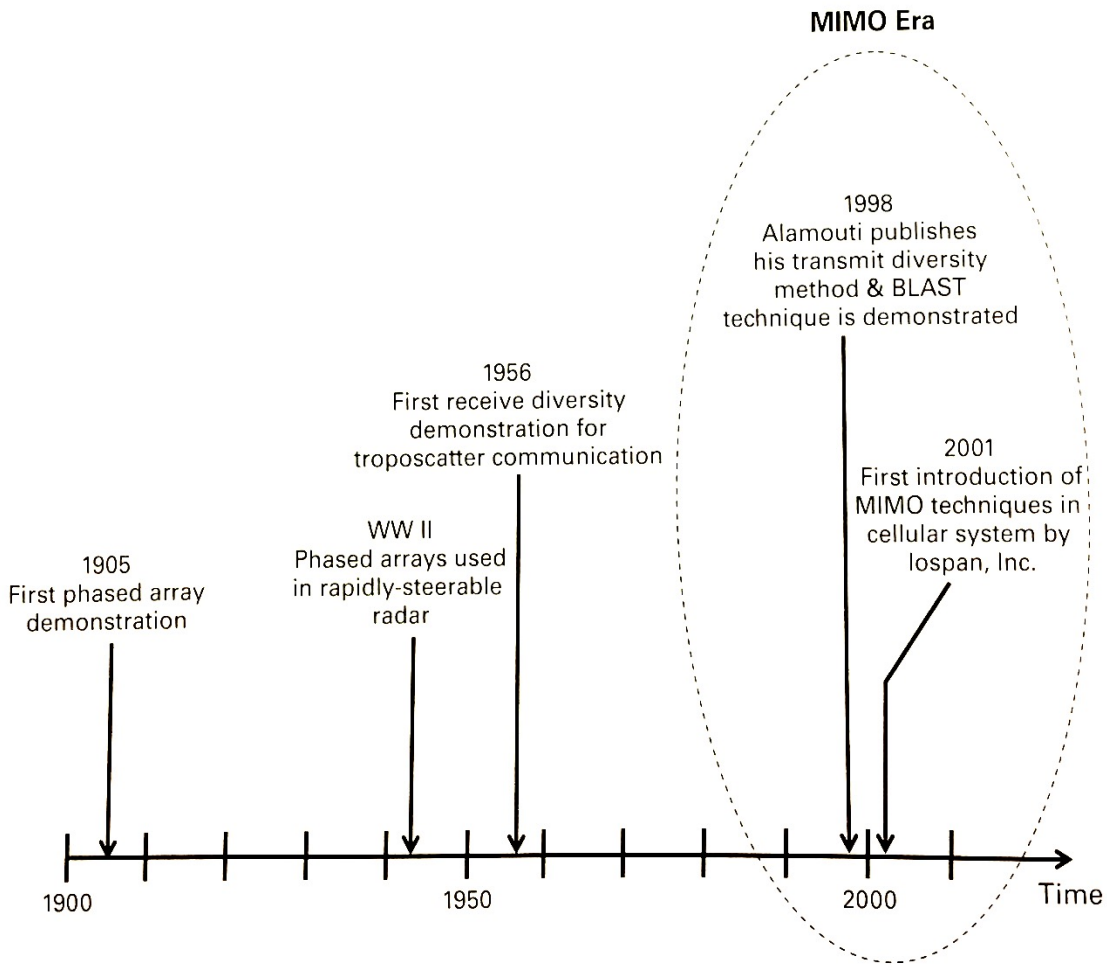

Figure 2.1 Summary of the history of Multi-antenna technology [59]

Some of the most important historical events in the use of multi antenna technology over the past one hundred years are summarized in Figure 2.1. This timeline along with the previous discussion proofs that MIMO is the most recent form of exploiting the multi-antenna technology.

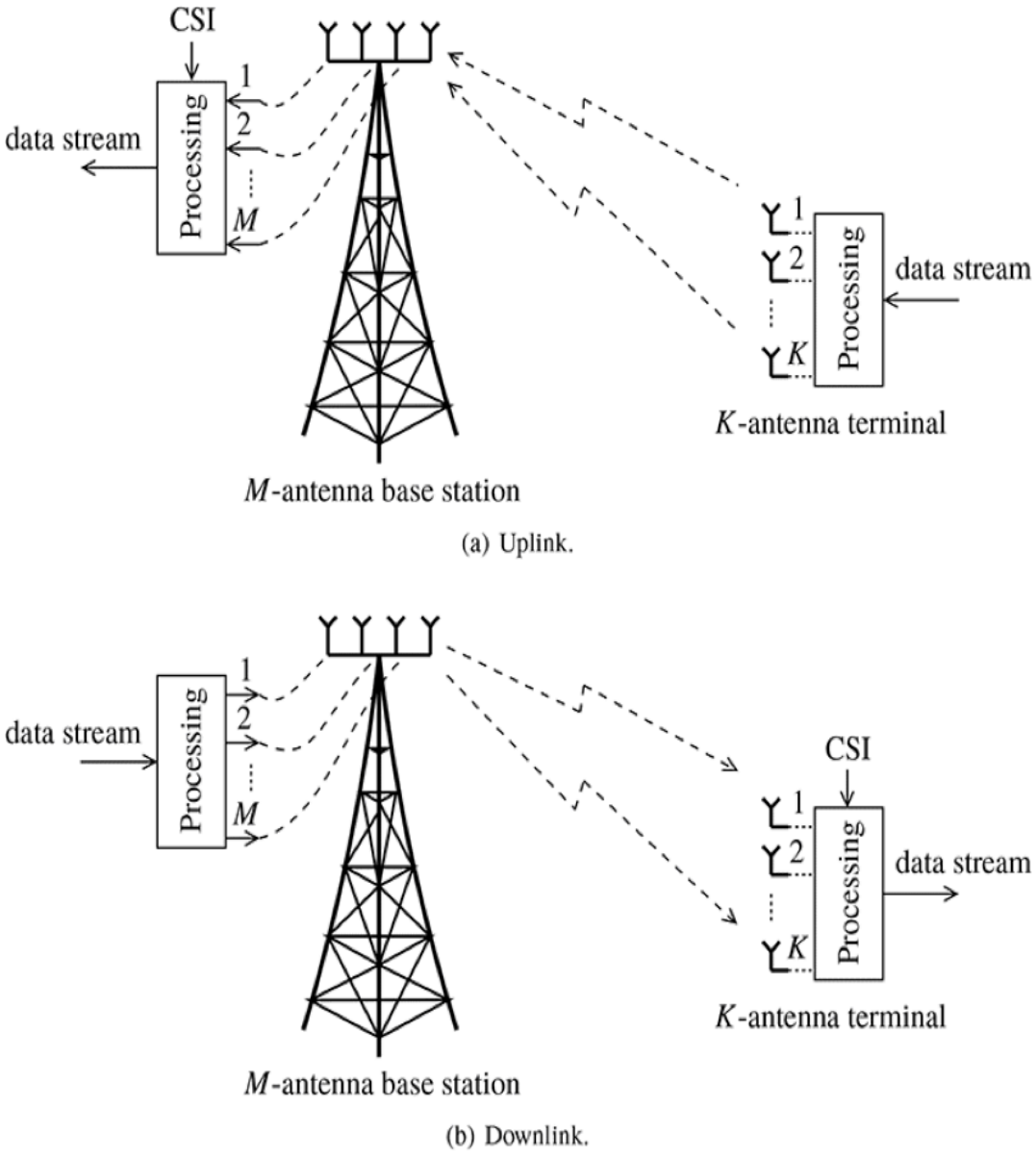

Figure 2.2 Point to Point MIMO [31]

2.3 Point to Point MIMO

During the late 90s, point to point MIMO which is the first form of the MIMO technologies was introduced [31], [13]. As shown in Figure 2.2, each terminal with multiple antennas is served with a BS equipped with an array of antennas. Combination between frequency/time division multiplexing is used to serve different users in distinct time/frequency blocks [37], [60]. Therefore, throughput is increased without using more bandwidth or pumping higher power. In what follow, some of the basic facts about Point-to-Point MIMO are summarized. Vectors are transmitted and received in every channel use. The channel capacity (in b/s/Hz) with the existence of additive white Gaussian noise at the receiver according to Shannon theory is [31]:

$$\mathrm{C}^{\mathrm{Ul}} = \log_2 \left| \boldsymbol{I}_M + \frac{\rho_{\mathrm{Ul}}}{\boldsymbol{K}} \boldsymbol{G}\boldsymbol{G}^{\mathrm{H}} \right| \quad 2.1$$

$$\mathrm{C}^{\mathrm{dl}} = \log_2 \left| \boldsymbol{I}_K + \frac{\rho_{\mathrm{dl}}}{\boldsymbol{M}} \boldsymbol{G}^{\mathrm{H}}\boldsymbol{G} \right| \quad 2.2$$

Where G is frequency response of the channel between the BS and the terminal that is denoted by an M*K dimensional matrix. ρ_{dl} and ρ_{Ul} are the DL and the UL SNRs that vary in proportion to the total radiated power. M & K are the number of BS and UE antennas respectively. While channel knowledge is required at the receiver to satisfy the capacity in 2.1, transmitter is not required to have any knowledge about the channel. For high SNRs, $\mathrm{C}^{\mathrm{dl}}$and C^{Ul} scale logarithmically with the SNR and linearly with min (*M, K*) in rich scattering propagation environments. Therefore, capacity of the link can be improved by simultaneous use of a large number of antennas at the transmitter and the receiver.

There are many issues preventing Point to Point MIMO of being scalable beyond eight antennas. First, eight streams of data may not always be supported by the propagation environment especially under line of sight conditions [37]. The time needed for training is proportional to the number of antennas [47]. Third, complicated terminals require independent electronics for every antenna [31]. Fourth, the signal processing that can achieve close to Shannon limit performance is very complicated. Finally, users who are around the cell edge where SNR is usually low as a result of the high path loss would struggle because of the slow improvement with min(*M,K*). Table 2.1 illustrates this situation on the DL capacity for user with *K*=4 operating at SNR of -3 dB for M=1,2,4,8 BS antennas. It is obvious that only two streams are supported in this situation.

Table 2.1: Capacity (bits/s/Hz) for four antenna users vs. Number of base station antennas operating at -3 dB

M	1	2	4	8
C	1.51	1.83	2.06	2.19

2.4 Multiuser MIMO

The MU-MIMO system shown in Figure 2.3 where multi-antenna BS serves multiple UE is more practical than point to point MIMO. The main principle of multiuser MIMO is that each BS with multiple antennas can use the same frequency-time resources to serve a multiplicity of single antenna terminals that share the multiplexing gain [48]. One can intuitively understand the multiuser MIMO scenario as if the *K*-antennas terminal in the point to point MIMO was broken up into multiple autonomous terminals [61]. Cooperation between the antennas of the UE is possible in the case of the point to point MIMO, however UEs in MU-MIMO cannot communicate with each other. Although the poor-quality channels can sometimes severely influence the throughput achieved by individual users, the break up actually improves the sum throughput of the system[49]. Hence, the impact of the propagation environment on MU-MIMO system is less than the case of point to point MIMO due to the multi-user diversity. As a result, many communication standards such as 802.16 (WiMAX), 802.11 (WiFI) and LTE have included MU-MIMO. The BS usually is equipped with only few number of antennas (i.e. 10 antennas or less) for most MIMO application. Thus, only modest improvement is brought to the spectral efficacy using the MIMO technology so far.

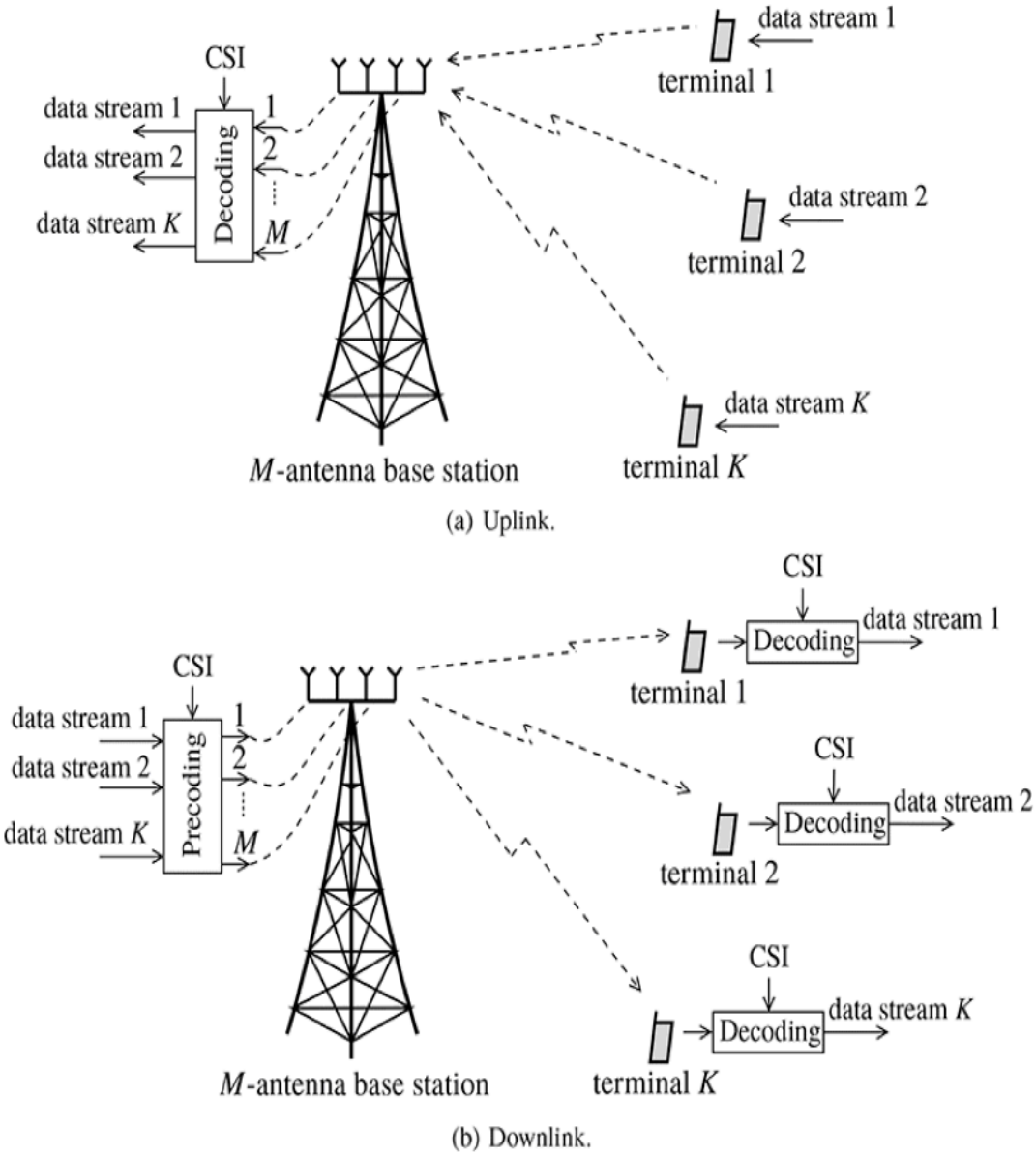

Figure 2.3 Multiuser MIMO [31]

The performance of MU-MIMO system if the terminals in Figure 2.3 with a single antenna each, *K* are served by the BS is better than the case of point to point MIMO. Knowing that G is the *M*K* matrix that represent the frequency response between the BS antennas and the *K,* the sum capacities of the UL and DL are given by

$$\mathrm{C}^{\mathrm{Ul}} = \log_2\left|\boldsymbol{I}_M + \rho_{\mathrm{Ul}}\boldsymbol{G}\boldsymbol{G}^{\mathrm{H}}\right| \qquad 2.3$$

$$\mathrm{C}^{\mathrm{dl}} = \max_{\substack{v_k \geq 0 \\ \sum_{k=1}^{K} v_k \leq 1}} \log_2\left|\boldsymbol{I}_M + \rho_{\mathrm{dl}}\boldsymbol{G}\boldsymbol{D}_{\boldsymbol{v}}\boldsymbol{G}^{\mathrm{H}}\right| \qquad 2.4$$

Where $v = [v_1, \ldots., v_K]^{\mathrm{T}}$, ρ_{dl} is the DL SNR, and ρ_{Ul} is the UL SNR for every terminal. The total UL transmit power of multiuser MIMO is greater than the transmit power of the point to point MIMO by a factor of *K* [62]. Computing the capacity of the DL in 2.4 depends on solving a convex optimization problem. CSI knowledge is important for both 2.3 and 2.4. On the UL only the BS is required to know the channel while every terminal must be separately informed about their permissible transmit rate. On the DL, however, CSI knowledge is required in the BS and the terminals.

The most import thing to note is that cooperation between UE antennas is possible in the point to point case, whereas terminals cannot cooperate in the multiuser case [61]. However, the lack of cooperation between the terminals in the multi user system does not affect the UL sum capacity when comparing 2.1 and 2.3. Moreover, the DL capacity 2.4 can exceed the DL capacity in 2.2 of point to point MIMO.

There are two reasons that make multiuser MIMO better than Point to Point MIMO. First, multiuser MIMO is less sensitive to the propagation environment. It shows a good performance even when line of sight conditions is present. Second, single antennas terminals can be sufficient. However, Multiuser MIMO cannot be scalable for two reasons. First, the complexity of dirty paper coding and decoding grows exponentially [37]. Second, the time needed for training to acuire the channel state information (CSI) increases in proportion with the number of users and the BS antennas [38].

2.5 Massive MIMO

Massive MIMO is a newest form of the MIMO technology that has yet to be employed in the next generation of wireless systems [28], [63] due to its many advantages that will enhance the wireless communications. The name of this technology refers to the concept of equipping the BS with a very large number of antennas [64]. It is going to be an important solution to handle the exponential growth in data traffic. When this technology was introduced in [49] and [65], It was presented as a modified and scalable version of multiuser MIMO. Simple linear processing is sufficient for massive MIMO to add orders of magnitude of improvement to energy and spectral efficiency [64].

Considering its capacities in 2.3 and 2.4 based on the Shannon theory, increasing M in multiuser MIMO result in logarithmically growing throughputs. The total time spent for training , however, increases linearly [66], [67]. Massive MIMO avoid this problem by taking measures to ensure that operations do not approach Shannon limit, however achieving a performance that overtake any typical multiuser MIMO system.

There are three main differences that distinguish between massive MIMO and multiuser MIMO. First, knowledge of the channel is only required at the BS [68]–[70]. Second, the number of antennas M at the BS is usually much larger than the number of users K [71]. Third, both the DL and the UL use simple linear signal processing [72]. Therefore, scaling up this technology can be easily done when it comes to the number of antennas at the BS.

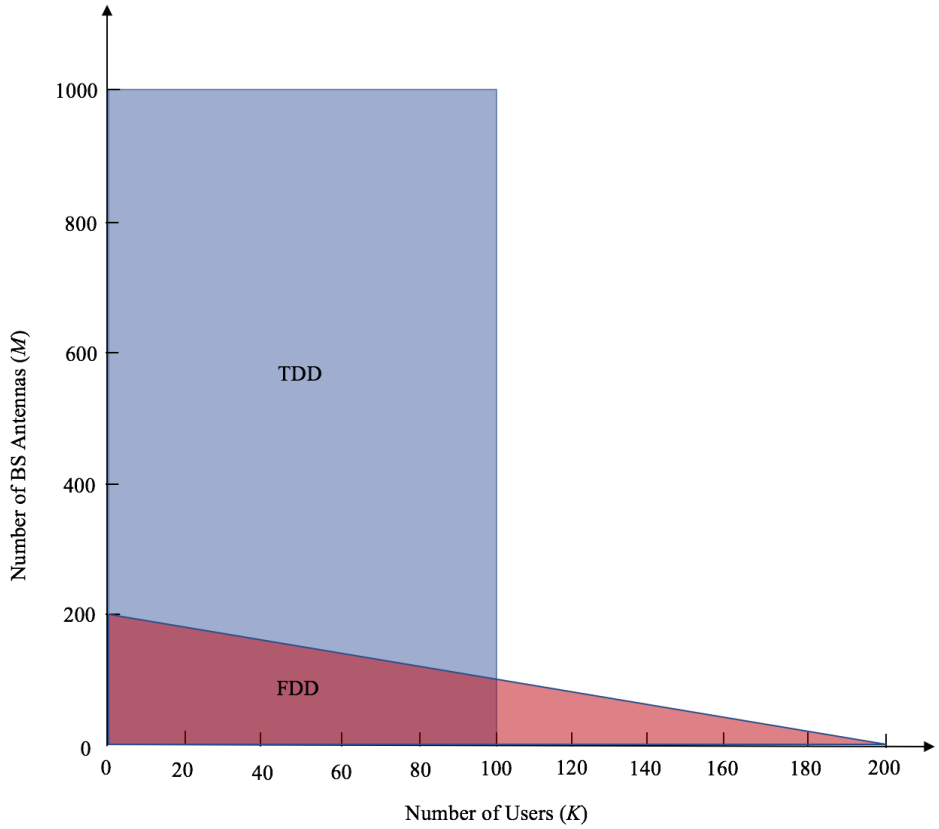

Figure 2.4 Comparison between possible (M,K) in TDD and FDD systems [34]

In massive MIMO, hundreds of terminals can be simultaneously served with a BS equipped with hundreds of antennas over the same time/frequency resources. Some key enabling characteristics for this technology are:

2.5.1 Time Division Duplex

On the contrary of the frequency division duplex (FDD), The overhead required to estimate the channel does not depend on the number of BS antennas M under time division duplex (TDD) protocol [47], [73]. Hence, it is preferred to use TDD protocol in massive MIMO. Exploiting the channel reciprocity can considerably reduce the overhead required for CSI acquisition [74]. Figure 2.4 illustrate the advantage of TDD over FDD [34]. It shows that the possible (M,K) dimensions in TDD is much more than FDD. Therefore, the resources necessary for channel estimation are not affected by increasing the number of BS antennas when TDD is used. For example, when the coherence interval T is 200 symbols, the constraint for the number of users and BS antennas is $M+K < 200$ in FDD system, while the constraint for TDD systems is $2k<200$.

2.5.2 Linear processing

Linear processing: signal processing at the terminals in massive MIMO must be able to handle large dimensional channels. Hence, one of the advantages of massive MIMO is linear decoding and precoding [28]. For example, UL data transmission can be decoded with simple matched filter and DL data transmission can be pre-coded with conjugate beamforming as illustrated in Figure 2.5.

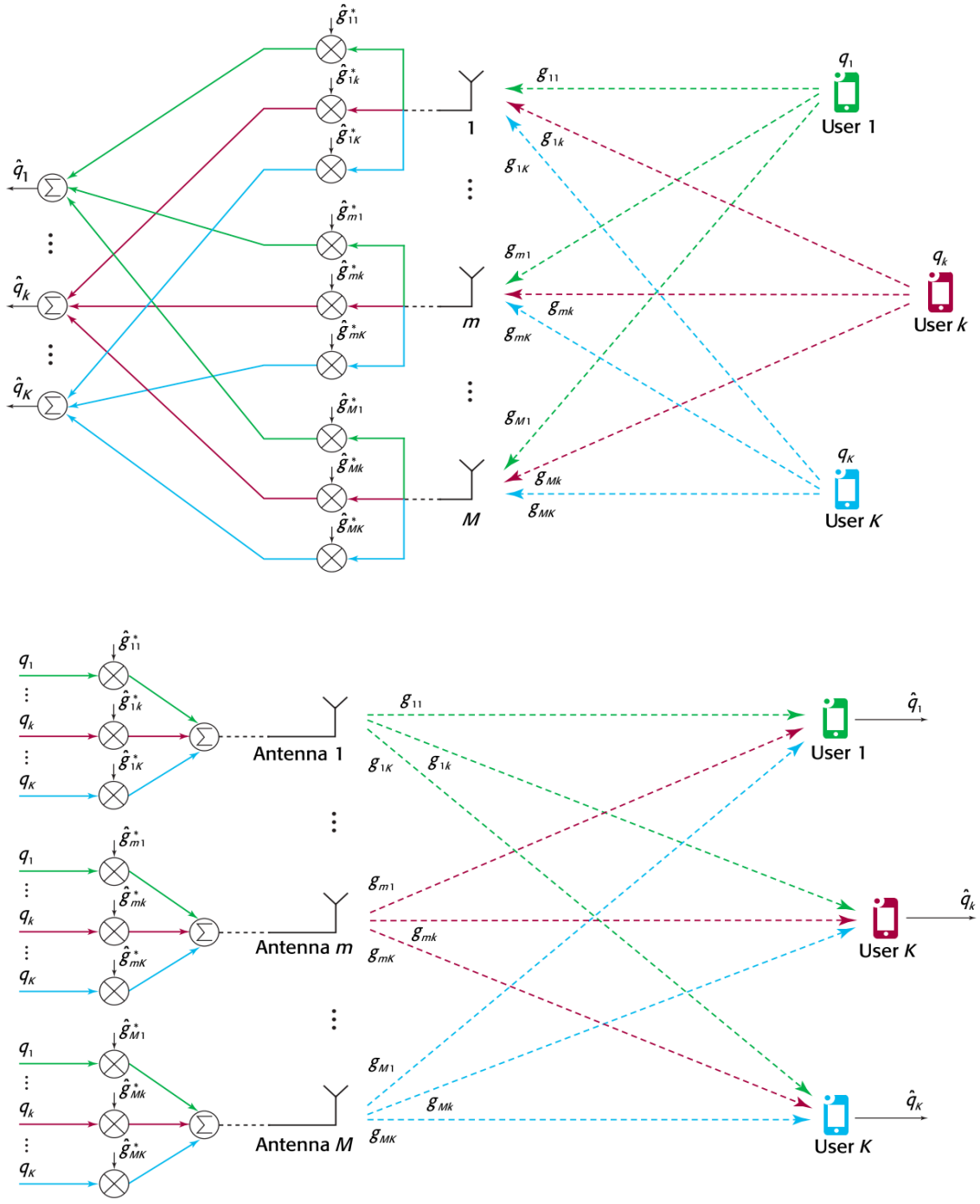

Figure 2.5 linear processing of Massive MIMO [47]

2.5.3 Favorable propagation

Due to the law of large numbers, the channel between the terminals and the BS can be well conditioned. Therefore, massive MIMO exploits the assumption that the channel vectors are almost orthogonal. This phenomenon is called favorable propagation where only linear processing is needed for optimal performance. Figure 2.5 illustrates that the interference and noise can be canceled out on the UL using simple linear detector like the matched while the BS can exploit linear beamforming techniques to beamform various streams of data to numerous users without mutual interference.

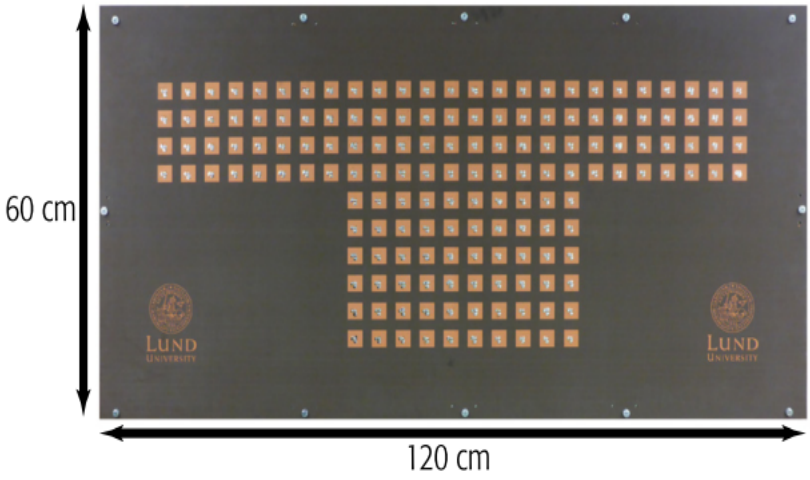

Figure 2.6 LuMaMi Massive MIMO testbed

2.5.4 Array Size

One of the characteristics of massive MIMO is that the antenna array does not occupy a big space because they are physically small. For example, the spacing between antennas is about 6 cm at 2.6 GHz. Thus 128 antennas occupy a cylindrical array has a dimension of a 28cm×29cm only [75]. Another example is shown in Figure 2.6 which is a photo of massive MIMO testbed of LuMaMi at Lund university [76]. The array which is designed for carrier frequency 3.7 GHz contains 160 patch antennas that are dual-polarized. The panel size is 60*120 cm and the spacing between the antenna elements is 4 cm which leaves a plenty of space for adding more antenna elements. One of the possible deployment scenarios for such a panel can be on buildings facades.

3.1.5 Scalability

Massive MIMO is a scalable technology: since the BS acquires the channel through UL pilot when operating in TDD protocol, the time spent on channel estimation does not depend on the number of BS antennas. Thus, the number of BS antennas can be increased without adding more time to the estimation process. Furthermore, because multiplexing and demultiplexing are not needed at the user ends, signal processing on each terminal is independent of the other users

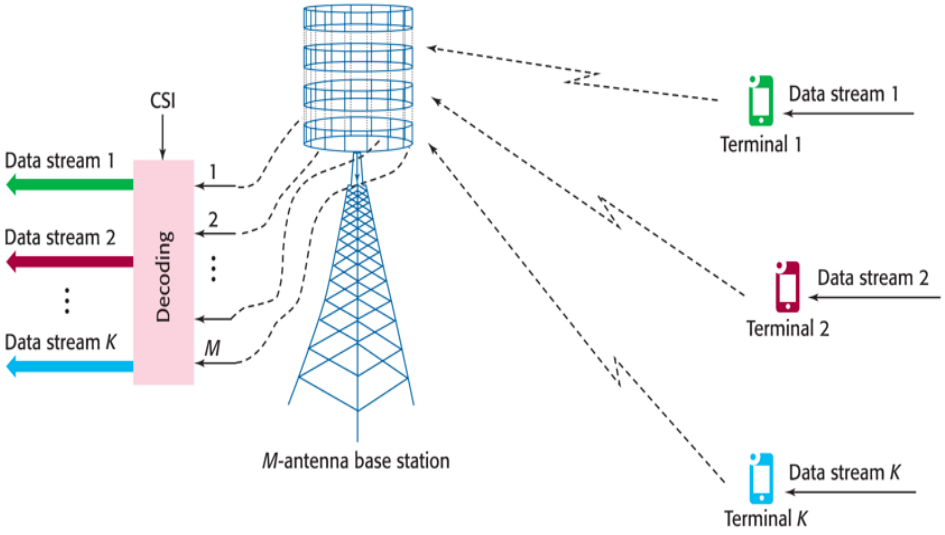

(a) Uplink

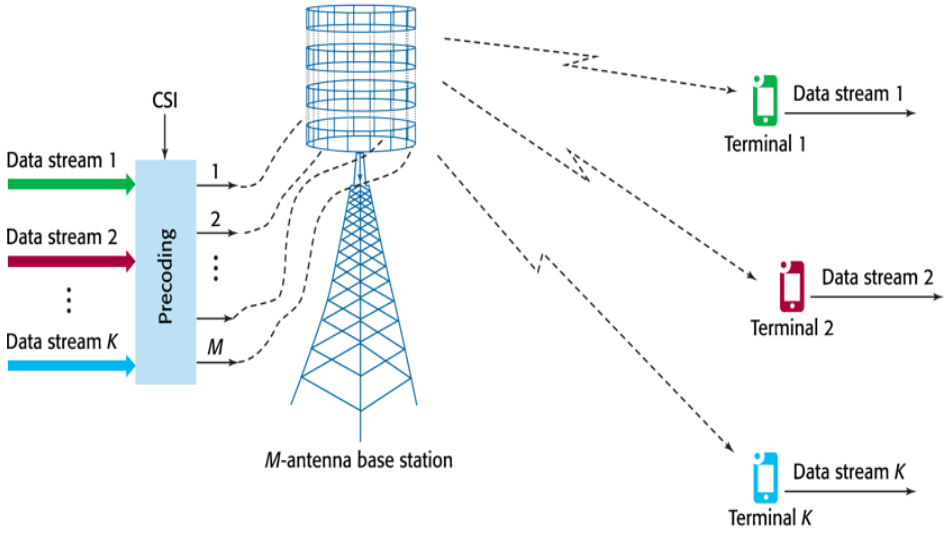

(a) Downlink

Figure 2.7. Massive MIMO. (a) Uplink operation. (b) Downlink operation [47].

2.6 How Does Massive MIMO Operate

UL and DL operations of massive MIMO are illustrated in Figure 2.7 [31]. This setup might represent a single cell site, or cell taken out of a network. A large number of UE K inside the cell are served through an array of antennas in the BS. Each terminal usually have a single antenna [77], [78]. Other cells are served by different BSs that do not cooperate among each other except for pilot assignment and power control [79]. All terminals use the full frequency-time resources simultaneously for UL/DL transmissions [80]. On the UL, individual signal sent by the terminals are recovered at the BS. The BS, on the DL, makes sure that every UE receives only the signal that was intended for it. Multiplexing/demultiplexing processing at the BS are possible because of the available knowledge of the CSI.

The BS creates an arrow beam towards the direction of the terminal under line of sight (LOS) propagation environment as shown in figure 2.8 (a). The concentration of these beams become more accurate (i.e. they become narrower) as the number of antennas is increased. In the case of the existence of a local scattering, the signal received at any UE consists of the superposition of many independent components as a result of scattering and reflections which can add up destructively or constructively. These components add up constructively exactly at the location of the user if the transmitted waveforms are perfectly selected as shown in Figure 2.8 (b). The precision of the power concentration to a certain terminal can be increased by adding more antennas to the BS. Therefore, it is very important to have CSI at the BS that is sufficiently accurate to focus the power [81].

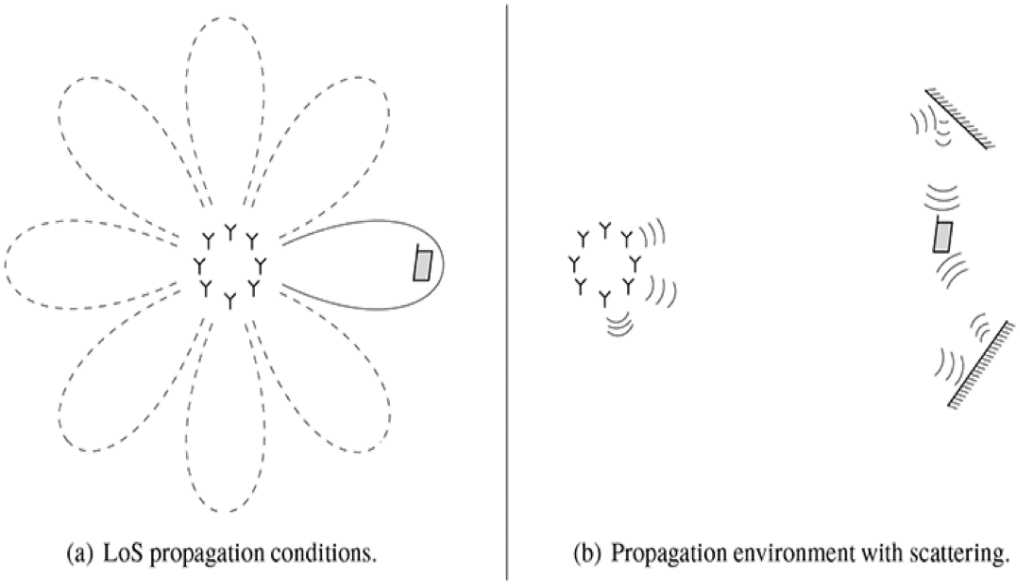

Figure 2.8 The effect of precoding in different propagation environments [31] .

TDD operation shown in Figure 2.9 is preferred in massive MIMO. The coherence period divides into three operations that include channel estimation (UL/DL training), UL data transmission, and DL data transmission.

2.6.1 Channel Estimation

One of the most essential tasks of the BS is detecting the users transmitted signals on the UL and precoding the DL signals. Hence, the BS requires the CSI which can be obtained using the UL training. Terminals that are assigned orthogonal pilot signal each, send these pilot to the BS. The pilot sequences transmitted from all terminals are already known to the BS. Thus, the BS can estimate the channels using these pilot signals.

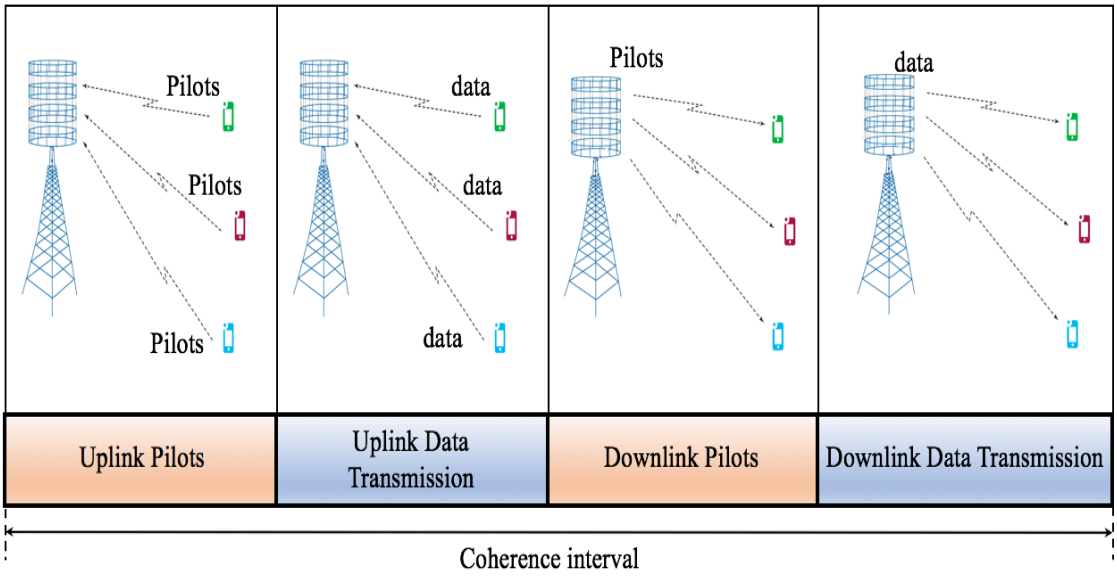

Figure 2.9 TDD protocol of Massive MIMO transmission

Moreover, partial knowledge of CSI might be required at every terminal for coherent detection of the transmitted signals from the BS. This partial knowledge can be either obtained using DL training or through some algorithm that can blindly estimate the channel. To detect its intended signal, the terminal only requires the effective gain of the channel because the signals performing is conducted using linear precoding techniques at the BS.

2.6.2 UL Data Transmission

UL data transmission occupies part of the coherence interval. In the UL, the BS receives the transmitted data from all K terminals in the same frequency-time resource. The BS detect the signals transmitted from all terminals exploiting the channel estimates and the linear combining techniques.

2.6.3 DL Data Transmission

The BS transmits the DL data to all the terminals on the same frequency/time resource. In specific, the BS creates *M* pre-coded signal and feed them to *M* antennas. This can be done using the estimated channel and the symbol intended for the *K*th user.

2.7 Benefits of Massive MIMO

The need for more reliable communications and the demand for wireless throughput will always increase. Hence, new technologies in the future are required to simultaneously serve many users with a very high throughput [82]. These requirements can by met with massive MIMO. The capacity of the UL transmission under favorable propagation conditions is (DL transmission follows the same argument):

$$C_{\text{sum}} = \log_2 \det\left(\boldsymbol{I}_K + p_u M \boldsymbol{I}_K \right) = K \log_2(1 + M p_u) \qquad 2.1$$

Where *M* and *K* represent the array gain and multiplexing gain respectively. It is obvious that large *K* and *M* result in a very high energy and spectral efficiency. Hence, by increasing *K* and *M,* higher number of users can be served over the same frequency band without the need the increase the transmit power of every terminal. Therefore, the throughput of every user increases. Moreover, the transmit power can be reduced 3 dB by doubling the number of antennas in the BS without compromising the quality of service.

Favorable propagation conditions and Optimal processing at the BS are necessary to get the array and the multiplexing gain. These gains can also be achieved using linear processing with massive MIMO instead of the usual low dimensional point to point MIMO with very complicated processing schemes [83]. In fact, when the number of BS antennas is increased to a very large number in massive MIMO, the channel becomes favorable because of the low of large numbers. Therefore, linear processing is considered almost optimal for massive MIMO. Therefore, array and multiplexing gains can be achieved using simple linear processing. Also, the throughput can always be improved by increasing the number of users and the BS antennas.

Figure 2.10 shows the capacity as a function of the number of BS antennas for optimal receivers and linear receivers at K=10. The capacity for MRC, ZF and MMSE are also shown in the figure. It is clear that the capacity approaches the Shannon sum capacity of the optimal receivers when M is large. For example, the largest sum rate that can be obtained with optimal receiver and M=K=10 is 8.5 bits/s/Hz. However, when M is large, say 60, the sum rate of 38 bits/s/Hz can be obtained with simple ZF receivers.

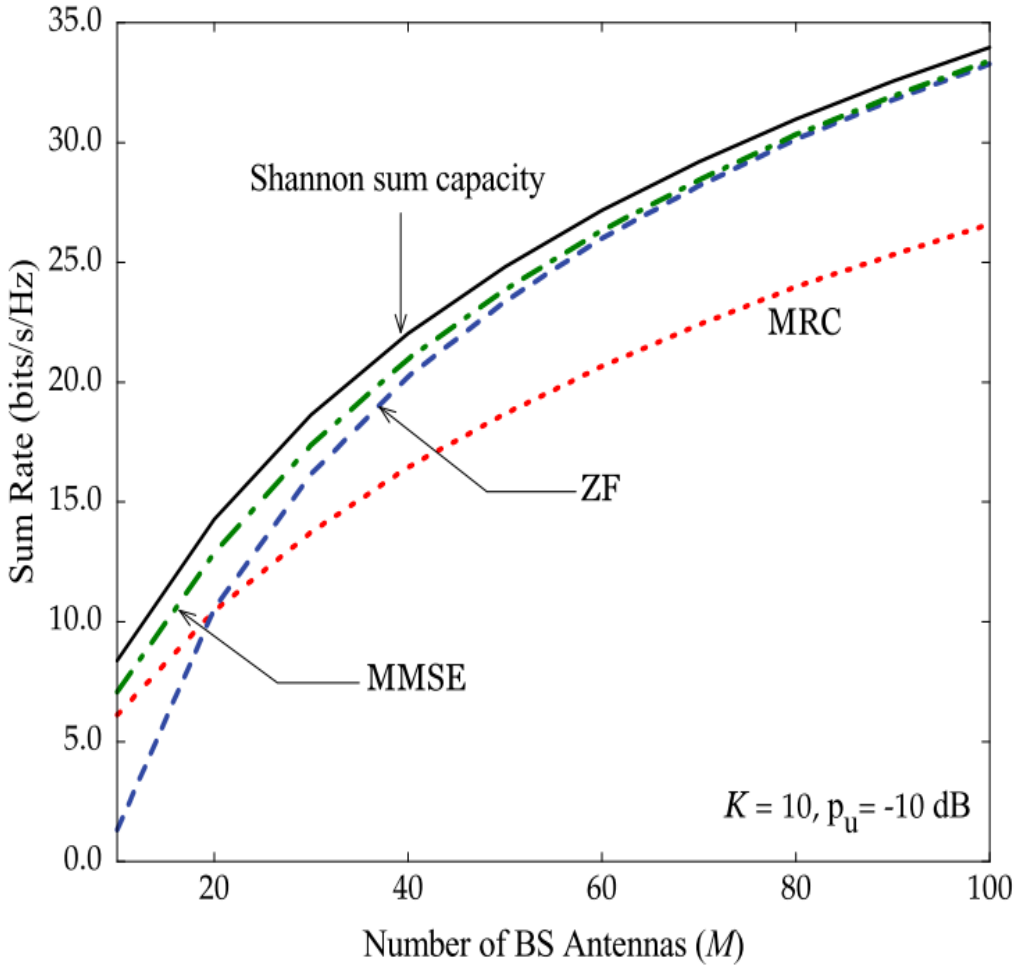

Figure 2.10 UL capacity for different linear receivers in comparison with the optimal receiver [34]

2.8 Challenges of Massive MIMO

Although massive MIMO have great advantages, many challenges still need to be dealt with. The most important issues are listed below:

2.8.1 Unfavorable propagation

It is assumed that massive MIMO operates under favorable propagation conditions. In practice, however, there many circumstances that makes the propagation of the channel unfavorable. For example, the propagation environment when the number of users is much more than the number of scatters, or if the scatters between the BS and the channels of different users are common. Disturbing the antennas of the BS over a large area is one possible solution to this problem.

2.8.2 Pilot Contamination

Cellular networks in practice consist of a large number of cells. Due to the scarcity of the frequency spectrum, frequency resources are shared between many cells. Thus, assigning orthogonal pilots for all the users is difficult because of the restricted channel coherence period. These orthogonal sequences are usually reused between the different cells. Hence, the process of channel estimation in a certain cell can be affected with the pilot sequences transmitted on the other cells. The system performance can be reduced by this phenomena known as “pilot contamination” [84].

Pilot contamination is one of the major issues that imposes limitations on the performance of massive MIMO systems. Even if the number of BS antenna grows to a very large number, this effect cannot be eliminated. A lot of research is being made to reduce this effect. In order to reduce the impact of inter cell interference that leads to the pilot contamination, many solutions have been proposed. Pilot contamination precoding schemes, the eigenvalue decomposition based channel estimation as well as pilot

decontamination are proposed in [85]–[87]. It has been shown in [88] that pilot contamination could be decreased using pilot assignment schemes between the cells that are aware of the channel covariance in a specific types of channels. A lot of research is still trying to consider this issue from many prospective.

Although the focus of current research is on non-orthogonal pilots as the main cause of pilot contamination, there are other causes for pilot contamination that have been identified recently [89]. Various sources that can cause pilot contamination include non-reciprocal transceivers due to the structure of the internal clock of the radio frequency chains and hardware impairments causing out of band and in band distortions that affect training signals.

2.8.3 The Need for New Designs and Standard

Deploying massive MIMO using the current standard such as LTE would be very efficient. However, the maximum number of antennas at the BS allowed by the LTE standard are only 8 antennas. Moreover, the CSI used by LTE are assumed rather than measured. For example, one of the possibilities for the DL in LTE is to transmit the pilot signals from the BS through many fixed beams. The strongest beam is then reported back to the BS to be used for the DL transmission. Massive MIMO, on the other hand, exploit measured (estimated) channel information. Thus, new standards are needed before massive MIMO is reduced to practice.

There are other changes necessary to adjust to massive MIMO. For example, the expensive transceivers in the current communication systems must be replaced with a large number of inexpensive and low power consuming antennas. a special consideration must be given to the hardware designs. Huge efforts on the industrial and academic levels are needed for this purpose.

Chapter Three: The Impact of Angle Spread, Angle of Arrival and Antenna Spacing on Massive MIMO Systems

3.1 Introduction

A BS equipped with a large number of antennas is one of the main characteristics of massive MIMO. The UEs *K* can operate with one antenna only [39], [90]. Also, using the TDD protocol in massive MIMO enable UL and DL transmission on the same subcarrier. Therefore, the process of channel estimation can be more efficient especially when *M* is large because the time needed for training is independent of the number of antennas *M* at the BS [71], [41], [91]. The reciprocal channel between the single antenna terminal and the BS is illustrated in Figure 3.1.

The channel matrix in the analysis of massive MIMO usually consists of independent identically distributed (iid) complex Gaussian gains. However, this is not always the case in real world. Specifically, the correlation between the transmitting or receiving pair of antennas, or the presences of a direct LOS paths in the received signal causes $\mathrm{H} \neq \mathrm{H}_w$. Therefore, the effects of realistic channel conditions on the performance of massive MIMO are investigated in this dissertation.

***Notations**:*

x: lower case boldface is used to indicate column vectors

X: matrices are represented with uppercase boldface

$\mathbf{X}^{T}$: transpose

$\mathbf{X}^{*}$: conjugate

$\mathbf{X}^{H}$**:** conjugate transpose

$\mathbf{X}^{*}$: conjugate

$\mathrm{tr}(\mathbf{X})$: trace of matrix **X.**

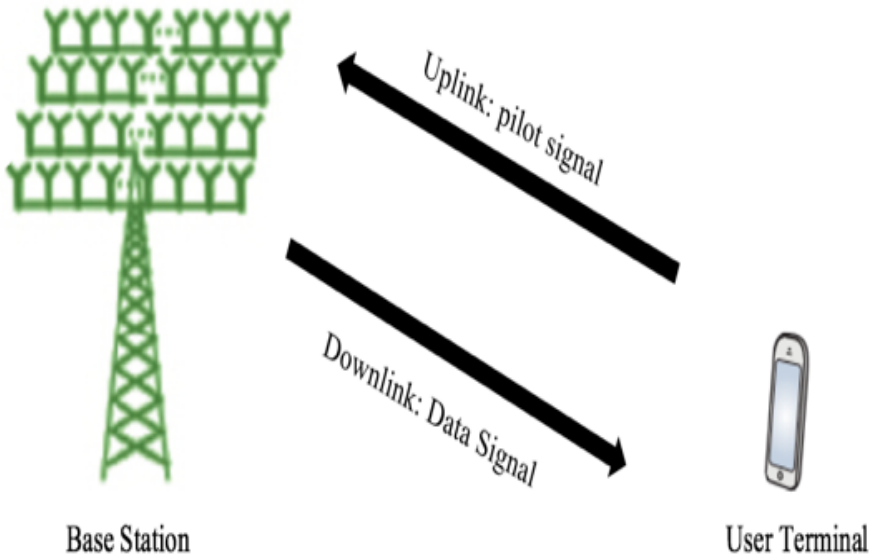

Figure 3.1. Channel reciprocity in massive MIMO based on TDD protocol

3.2 Channel and System Model

3.2.1 Time Division Duplex (TDD)

The process of the TDD protocol is shown in Figure 3.2. During the coherence period T_{coher}, the channel is static [92]. The coherence period is divided as the following: for $T_{\text{pilot}}^{\text{UL}}$ channel uses, UL pilot signaling starts each fading block followed by T_{data}^{UL} channel uses of UL data transmissions. Then, the DL pilot signaling for T_{pilot}^{DL} channel uses enable the terminals of estimating their actual channels and the present interference conditions to coherently recover the DL data. Irrespective of the number of antennas M, the number of pilots is scalar, hence the DL pilot signaling does not necessarily grow as M increases. The coherence period finishes with DL data transmission for T_{Data}^{DL}. TDD satisfy the following relation $T_{\text{pilot}}^{\text{UL}} + T_{data}^{UL} + T_{pilot}^{DL} + T_{Data}^{DL} = T_{coher}$.

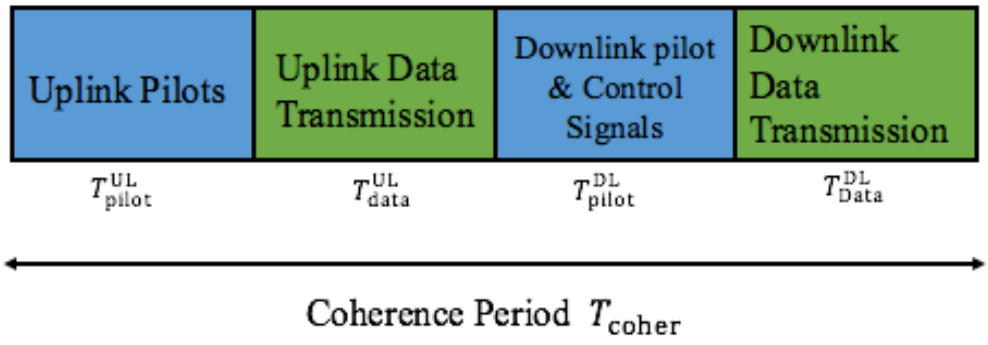

Figure. 3.2 Illustration of TDD protocol and data transmissions.

3.2.2 One Ring Model

The one ring model describes the environment where most of the scatters are concentrated around the UE in a ring shape. This model is suitable for suburban areas where the UE and the BS are separated with a high distance. The one ring model has been widely used to investigate outdoor MIMO communications were the UE is placed at the center of a ring of scatters. In general, every scatter on the ring is a representation of many scatters that form the incident ray in a certain direction. The angular spread with respect to the BS in the UL controls the radius of the ring [93].

The one ring model SISO model in [94] was used to investigate a narrowband Rayleigh fading channel in [94], [95]. The reference model of the MIMO channel has been derived using the one ring model in [96].

The channel covariance matrix is generated using the one ring model in [97] to analyze the influence of non-ideal channel conditions on the performance of massive MIMO systems. The one ring model shown in Figure 3.3 assumes that a ring of scattering objects of radius r surrounds the terminal while no scattering objects are located around the BS. The azimuth angle between the terminal and the BS is denoted θ and they are located at distance d of each other. The multipath components arrive to the terminal with an angle spread Δ. The covariance matrix $\mathbf{R}$ of the channel is generated using 3.1 [98].

$$[\mathbf{R}]_{n,p} = \frac{\mathbf{1}}{\mathbf{2}\Delta}\int_{-\Delta}^{\Delta} e^{jk^T(\alpha+\theta)(u_n-u_p)}\, d\alpha \qquad 3.1$$

where $u_n,\ u_p$ denote the position vectors of the BS and $k(\alpha) = -\frac{2\pi}{\lambda}(\cos(\alpha), \sin(\alpha))^{\mathrm{T}}$

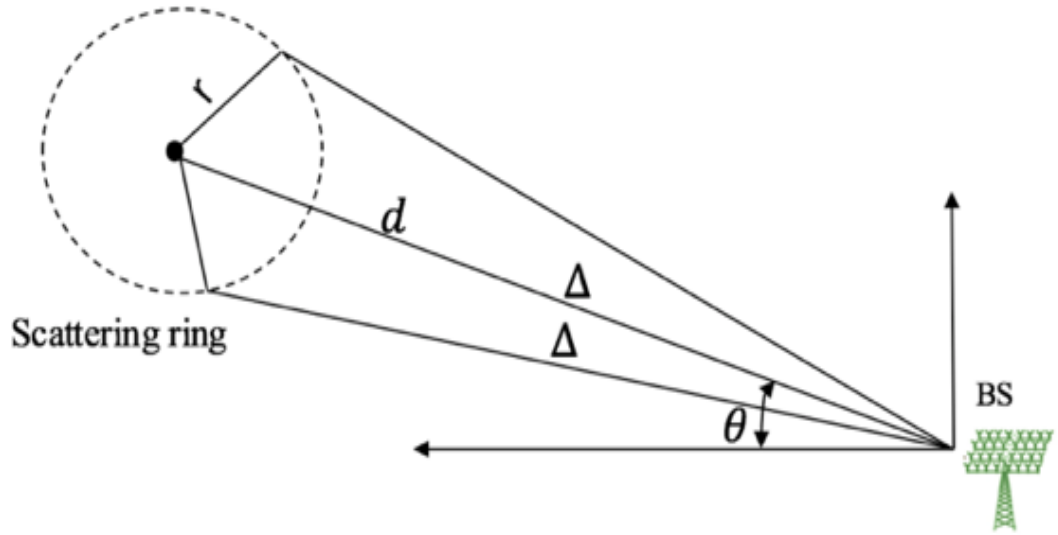

Figure. 3.3. The one ring model

The Toeplitz form of the channel covariance matrix is given as

$$[\mathbf{R}]_{n,p} = \frac{\mathbf{1}}{\mathbf{2}\Delta}\int_{-\Delta+\theta}^{\Delta+\theta} e^{-j2\pi D(n-p)sin(\alpha)}\, d\alpha \qquad 3.2$$

3.2.3 Downlink transmission

The DL channel is either used to transmit data or to estimate the channel using training pilots. The model of a downlink signal z ∈ ℂ received at the terminal for multiple input single outputs system is

$$z = \mathbf{h}^{T}\mathbf{d} + v \tag{3.3}$$

where $\mathbf{d} \in \mathbb{C}^{N\times 1}$ indicates the pilot signal or the zero-mean random signal. $\mathbf{X} = \mathbb{E}\{\mathbf{d}\mathbf{d}^{H}\}$ denotes the covariance matrix where the average power is $p^{\mathrm{BS}} = \mathrm{tr}(\mathbf{X})$. Due to precoding, the design parameter $\mathbf{X}$ is dependent on the channel realization $\mathbf{h} \in \mathcal{H}$ where the set of channel realizations is denoted $\mathcal{H}$. Hence, during each coherence period, $\mathbf{h}$ remains constant but changes between blocks because $\mathcal{H}$ changes. The additive term v is receiver noise which composed of the receiver noise $v_{noise} \sim \mathcal{CN}(0, {\sigma_{\mathrm{UE}}}^2)$ and the interference v_{interf} from transmitting simultaneously to other terminals. The interference and the data signal are independent of each other and both have zero mean.

$$v = v_{noise} + v_{interf} \tag{3.4}$$

3.2.4 Uplink Transmission

The reciprocal UL channel is used for data transmission and pilot signaling to estimate the channel; see Figure 3.1. like 3.3, the received signal $\mathbf{y} \in \mathbb{C}^N$ at the BS is modeled as

$$\mathbf{y} = \mathbf{h}s + \mathbf{n} \tag{3.5}$$

where $s \in \mathbb{C}$ indicates the stochastic data signal or the deterministic pilot signal used to estimate the channel; in any case, $p^{UE} = \mathbb{E}\{|s|^2\}$ is the average power. The additive term $\mathbf{n} \in \mathbb{C}^{N\times 1}$ in 4.5 is composed of the interference from simultaneous transmissions and the receiver noise $\mathbf{n}_{noise}$.The interference is independent of s but can be dependent on the channel realization $\mathcal{H}$.

$$\mathbf{n} = \mathbf{n}_{noise} + \mathbf{n}_{interf} \tag{3.6}$$

3.3 Uplink Channel Estimation

Comparison between the received UL signal **y** in 3.5 and the UL pilot s is made to estimate the current channel realization **h**. The typical channel estimation (pilot-based) considers Rayleigh fading channel with a known statics which is affected with independent complex Gaussian noise [49]. At the BS, linear minimum mean square error (LMMSE) estimator is used to estimate the channel based on the observation of the received uplink signal **y** in (3.5).

$$\hat{\mathbf{h}} = \underbrace{s^{*}\mathbf{R}\bar{\mathbf{Y}}^{-1}}_{\mathbf{A}}\mathbf{y} \tag{3.7}$$

where $\bar{\mathbf{y}}$ and $\mathbf{R}$ denote the covariance matrices of $\mathbf{y}$ and the channel

$$\bar{\mathbf{Y}} = \mathbb{E}\{\mathbf{y}\mathbf{y}^{H}\} = p^{UE}\boldsymbol{R} + \boldsymbol{S}+\sigma_{BS}{}^{2}\mathbf{I} \tag{3.8}$$

The mean square error (MSE) is

$$\text{MSE} = \text{tr}(\mathbf{G}) = \mathbb{E}\left\|\hat{\mathbf{h}} - \mathbf{h}\right\|_{\mathbf{2}}^{\mathbf{2}} \tag{3.9}$$

The error covariance matrix $\mathbf{G}$ is given in 3.10.

$$\mathbf{G} = \mathbb{E}\{(\hat{\mathbf{h}} - \mathbf{h})\big(\hat{\mathbf{h}} - \mathbf{h}\big)^{H}\} = \mathbf{R} - p^{UE}\mathbf{R}\bar{\mathbf{Y}}^{-1}\mathbf{R} \tag{3.10}$$

The channels consists of the LMMSE estimate in 3.7 pulse an unknown estimation error $\mathbf{h} = \hat{\mathbf{h}} + \boldsymbol{\epsilon}$ where $\boldsymbol{\epsilon} \in \mathbb{C}^{N\times 1}$ indicate the estimation error. $\hat{\mathbf{h}}$ and $\boldsymbol{\epsilon}$ both have zero mean and uncorrelated, but are independent. Thus, the covariance matrix of the estimated channel is $\mathbb{E}\big\{\hat{\mathbf{h}}\hat{\mathbf{h}}^{H}\big\} = \mathbf{R} - \mathbf{G}$ where $\mathbf{G}= \mathbb{E}\{\boldsymbol{\epsilon}\boldsymbol{\epsilon}^{H}\}$ is given in 3.10.

Suppose that the pilot signal is $\mathbf{y} \in \mathbb{C}^{1\times B}$ where $1 \le \boldsymbol{B} \le \boldsymbol{T}_{pilot}^{UL}$. Then, for every element of $\boldsymbol{B}$, Separate LMMSE estimate is computed, $\hat{\mathbf{h}}_i = \mathbf{h} - \boldsymbol{\epsilon}_i$ **for** $i = 1, \dots, B$, using 3.7. Taking the average results in

$$\widehat{\hat{\mathbf{h}}} = \frac{1}{B}\sum_{i=1}^{B}\hat{\mathbf{h}}_i = \mathbf{h} - \frac{1}{B}\sum_{i=1}^{B}\boldsymbol{\epsilon}_i \tag{3.11}$$

Then the MSE of $\widehat{\hat{\mathbf{h}}}$ is

$$\mathbb{E}\left\{\left(\frac{1}{B}\sum_{i=1}^{B}\boldsymbol{\epsilon}_i\right)^{H}\left(\frac{1}{B}\sum_{i=1}^{B}\boldsymbol{\epsilon}_i\right)\right\} = \frac{\text{tr}(\mathbf{G})}{B} \tag{3.12}$$

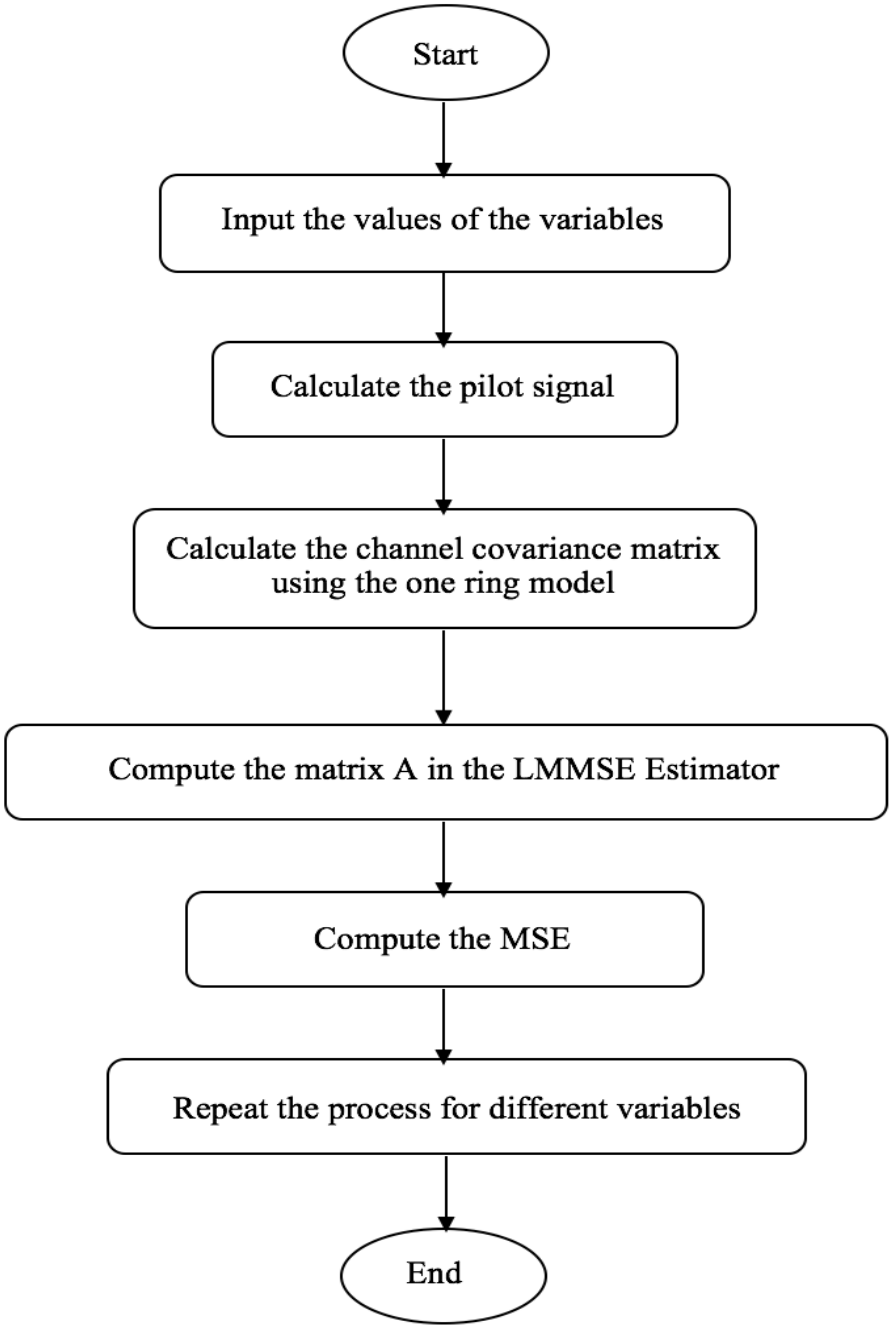

Figure 3.4 Flowchart of the simulation of massive MIMO channel estimation accuracy.

4.3.1 Results and Discussion

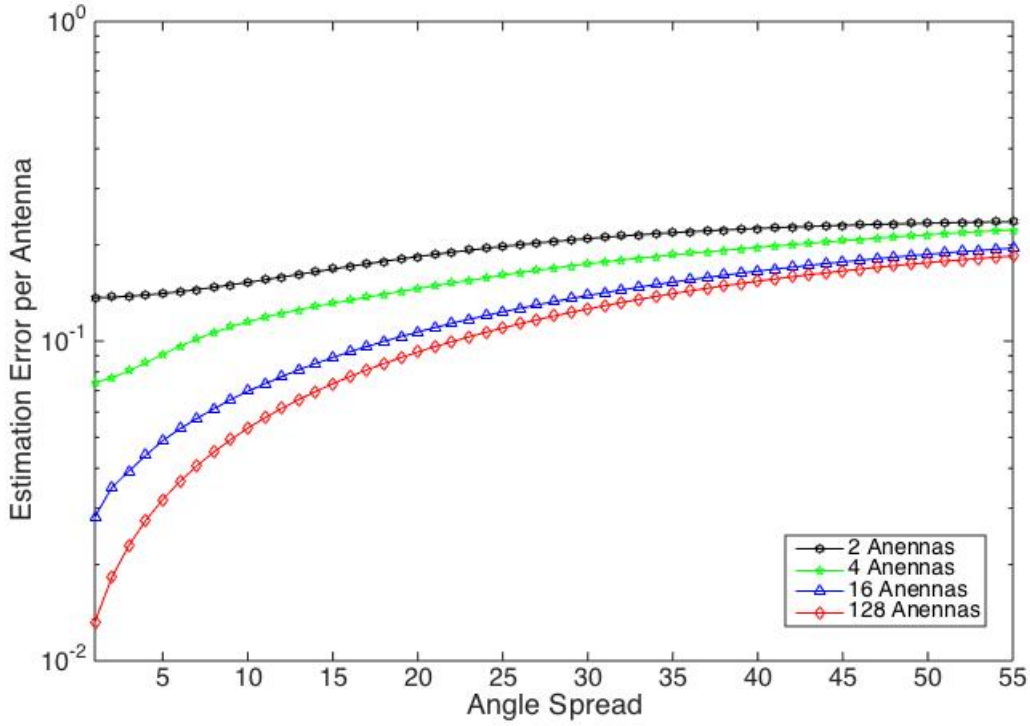

Figure 3.5 Estimation error as a function of angle spread UL SNR: 5 dB [69] .

The flowchart in Figure 3.4 describes the main steps to simulate and analyze the channel estimation accuracy of massive MIMO systems. All simulation and figures are generated in MATLAB.

Figure 3.5 shows the relative estimation errors per antenna for an angle spread that varies between 10 and 55 degrees. Four different BS antennas have been considered with no interference (**S** = 0). The covariance matrix **R** of the channel is generated with the one ring model form [97]. The angle of arrival (AOA) considered is 30 degree which reasonable assumption especially for an array with half-wavelength spacing between antennas.

Figure 3.5 proves that it is easier to estimate channels with less error per antenna when the angle spread is low. This can be noted when the number of BS antennas is high; reducing the angle spread of the one ring model result in less estimation errors. Hence, The BS with large number of antennas is more sensitive to the variations in angle spread.

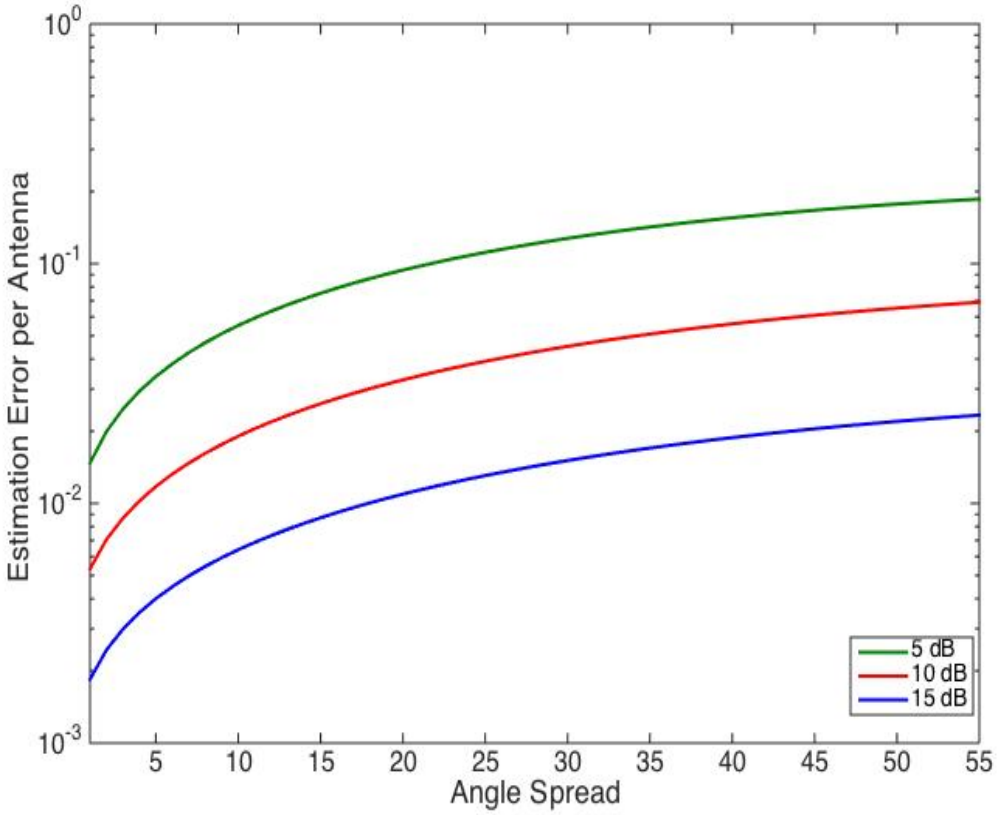

Figure 3.6 Estimation error as a function of angle spread for different SNRs with BS of 50 antennas [69].

Figure 3.6 illustrate the possibility of improving the estimation accuracy of the massive MIMO channel by increasing the SNR. The figure considers the impact of three different values of UL SNRs on the channel estimation accuracy when the BS is equipped

with 50 antennas. Estimation error per antenna is also shown as a function of angle spread. High SNR increases the accuracy of channel estimation by reducing the number of errors. Therefore, high UL SNR is needed to fully utilize massive MIMO because accurate CSI is necessary for coherent reception/transmission. Also, high angle spread can compensate for the lower SNRs.

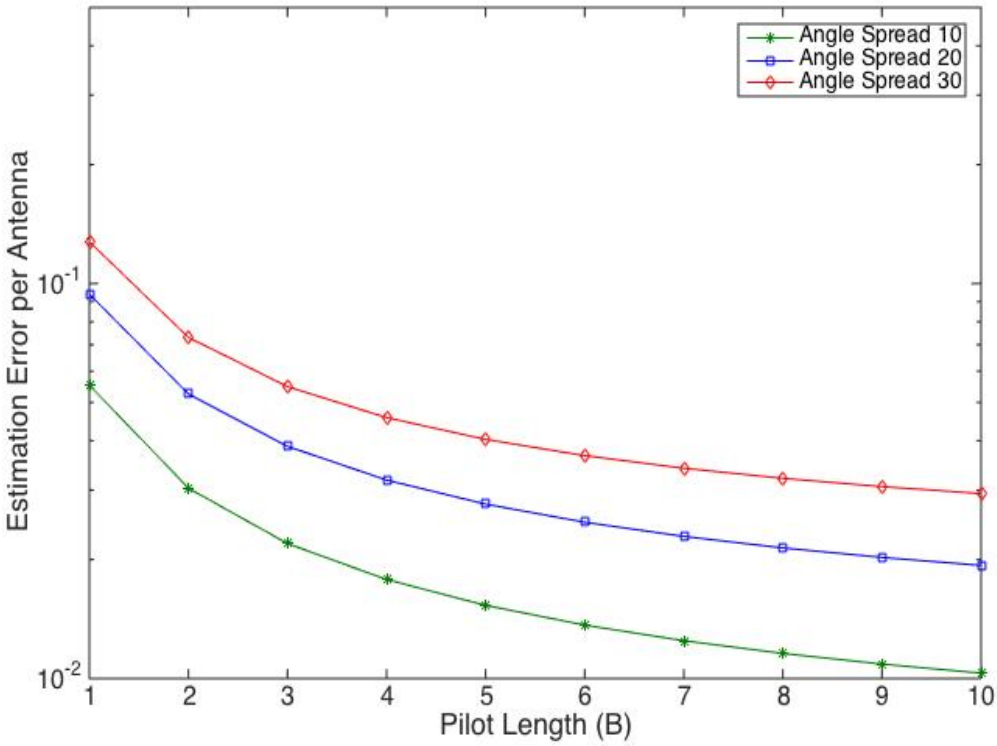

Figure 3.7 (a) Estimation error per antenna as a function of the pilot length UL SNR of 5 dB [69].

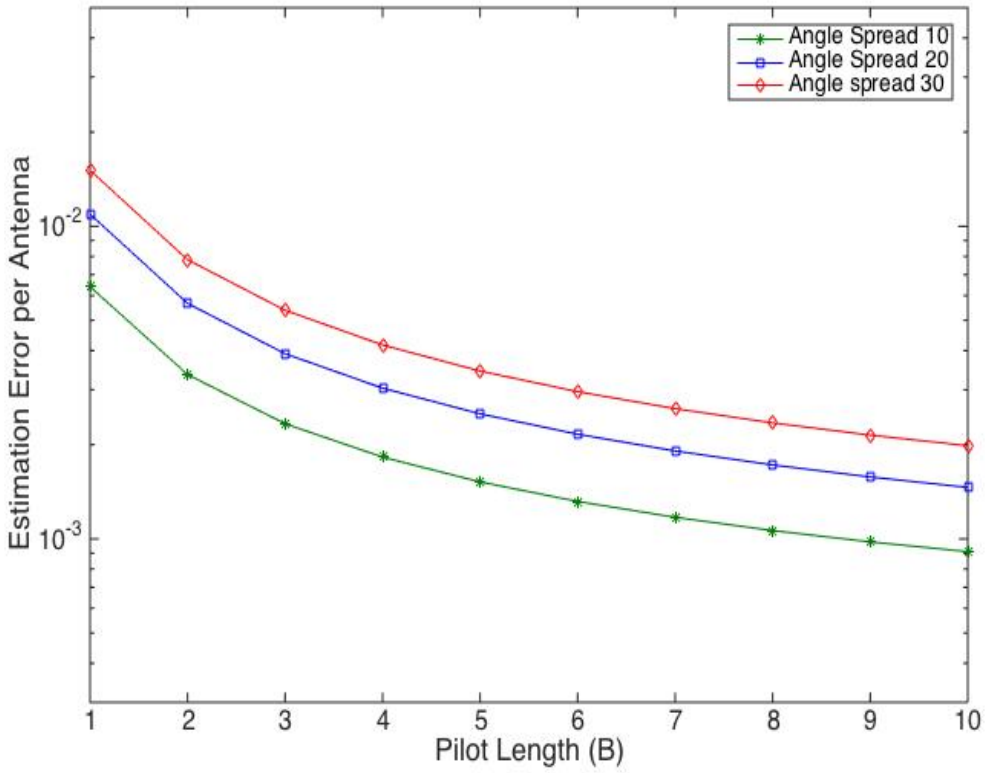

Figure 3.7 (b) Estimation error per antenna as a function of the pilot length UL SNR of 15dB [69].

Increasing the length of the pilot signal can also be used to improve the estimation accuracy. This is illustrated in Figure 3.7 (a,b) where the relative estimation error per antenna shown for different angle spread with variable pilot lengths. There is a clear gain in the accuracy of channel estimation that can be achieved by increasing the length of the pilot. Figure 3.7 also shows reduction in estimation errors occurs when channels are highly correlated along with increasing the pilot length.

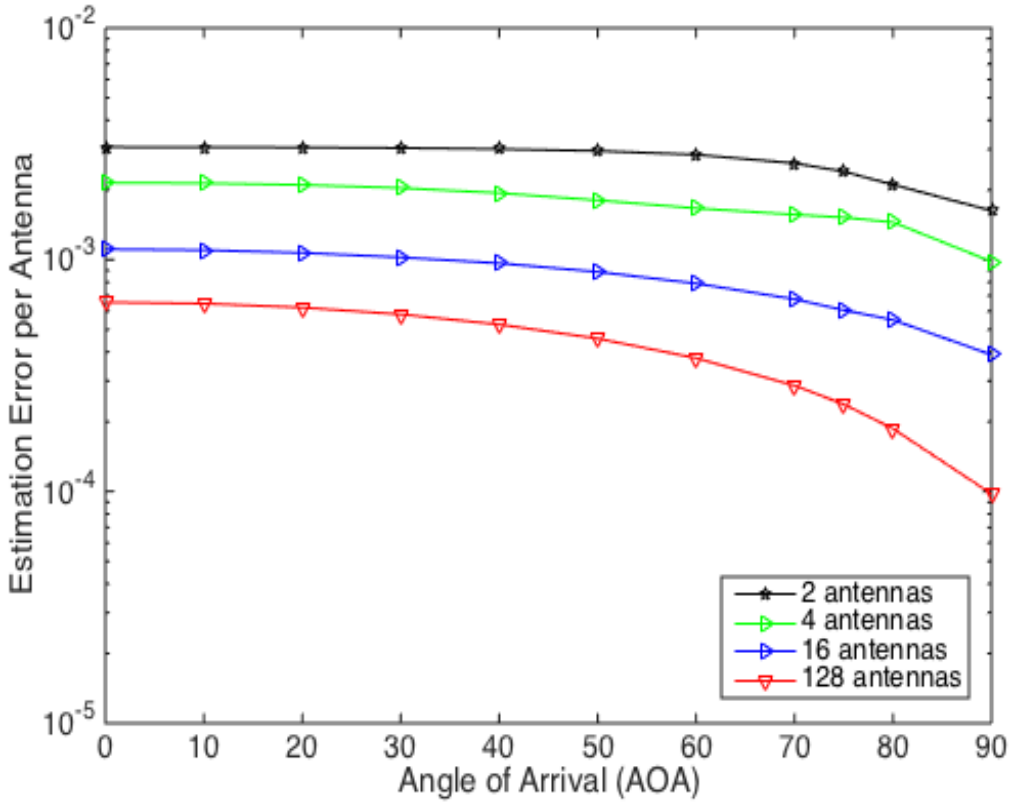

Figure 3.8 Estimation error for the LMMSE estimator as a function of the angle of arrival (AOA); uplink SNR of 25dB [99].

Angle of arrival can also affect the estimation accuracy of massive MIMO. This is illustrated in Figure 3.8 where the relative estimation error is shown as a function of the angle of arrival (AOA) to the BS with half wavelength spacing between antennas. The estimation accuracy increases as the angle of arrival to the BS increases. This improvement can be noticed when the number of BS antennas is 128 where the least number of errors per antenna happens at 90-degree AOA.

The impact of antenna spacing on the channel estimation accuracy is shown in Figure 3.9. The antenna spacing in the figure ranges between half the wavelength to four times the wavelength. Obviously, Varying the antenna spacing can affect the quality of the channel estimation when the number of BS antenna is very high.

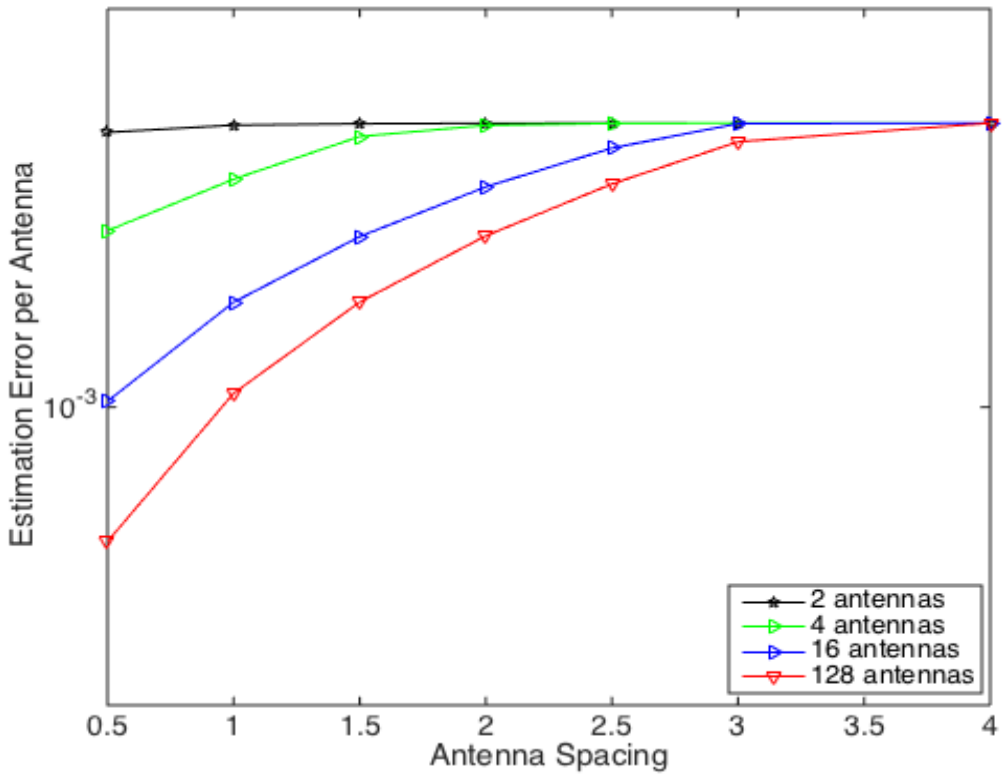

Figure 3.9 Impact of antenna spacing on the channel estimation accuracy. uplink SNR of 25dB [99].

3.4 DL/UL Data Transmission

Under the TDD protocol, the ergodic capacities of the DL data transmission 3.3 and the UL data transmission 3.5 are investigated in this section. These capacities are derived based on the estimated channel using the LMMSE estimator in 3.7. Arbitrary knowledge $\mathcal{H}^{\mathrm{BS}}$ of the channel $\mathcal{H}$ is available at the BS in every coherence period. The conditional distribution $f = (\mathbf{d}|\mathcal{H}^{\mathrm{BS}})$ of the signal $\mathbf{d}$ is selected based on that knowledge. Different arbitrary knowledge $\widetilde{\mathcal{H}}^{UE}$ of the channel $\mathcal{H}$ is used at the terminal to decode data. The ergodic DL capacity (in bit/s/Hz) is [39]

$$\mathrm{C}^{\mathrm{DL}} = \frac{T_{\mathrm{data}}^{\mathrm{DL}}}{T_{\mathrm{coher}}} \mathbb{E}\left\{ \max_{f = (\mathbf{d}|\mathcal{H}^{\mathrm{BS}}): \mathbb{E}\|\mathbf{d}\|_2^2 \le p^{\mathrm{BS}}} \mathfrak{I}\left(\mathbf{d}; z|\mathcal{H}, \mathcal{H}^{\mathrm{BS}}, \widetilde{\mathcal{H}}^{\mathrm{UE}}\right) \right\} \quad (3.13)$$

where $\mathfrak{I}\left(\mathbf{d}; z|\mathcal{H}, \mathcal{H}^{\mathrm{BS}}, \widetilde{\mathcal{H}}^{\mathrm{UE}}\right)$ represents the mutual information between the transmitted and received signals $\mathbf{d}$ and z respectively for a certain channel knowledge of ($\widetilde{\mathcal{H}}^{UE}$,$\mathcal{H}^{\mathrm{BS}}$) and a certain channel realization $\mathcal{H}$. The ratio $\frac{T_{\mathrm{data}}^{\mathrm{DL}}}{T_{\mathrm{coher}}}$ denotes the allocated portion of channel uses for the DL.

The ergodic capacity (bit/s/Hz) of the uplink channel in (3.3) is

$$\mathrm{C}^{\mathrm{UL}} = \frac{T_{\mathrm{data}}^{\mathrm{UL}}}{T_{\mathrm{coher}}} \mathbb{E}\left\{ \max_{f = (s|\mathcal{H}^{\mathrm{UE}}): \mathbb{E}\{\|s\|_2^2\} \le p^{\mathrm{BS}}} \mathfrak{I}\left(\mathbf{d}; \mathbf{y}|\mathcal{H}, \mathcal{H}^{\mathrm{BS}}, \widetilde{\mathcal{H}}^{\mathrm{UE}}\right) \right\} \quad (3.14)$$

where $\mathfrak{I}\left(\mathbf{d}; \mathbf{y}|\mathcal{H}, \mathcal{H}^{\mathrm{BS}}, \widetilde{\mathcal{H}}^{\mathrm{UE}}\right)$ is the mutual information between the transmitted and received signals s, $\mathbf{y}$ respectively for a given channel knowledge ($\mathcal{H}^{\mathrm{UE}}$,$\mathcal{H}^{\mathrm{BS}}$) and a given channel realization $\mathcal{H}$. The joint distribution of $\mathcal{H}, \mathcal{H}^{\mathrm{BS}}, \mathcal{H}^{\mathrm{UE}}$ is used to find the expectation in 3.14 and the conditional distribution of the data signal $f = (\mathbf{d}|\mathcal{H}^{\mathrm{UE}})$. The

ratio $\frac{T_{\text{data}}^{\text{UL}}}{T_{\text{coher}}}$ denotes the allocated fraction of channel uses for the UL channel. $\widetilde{\mathcal{H}}^{UE}$ and $\widetilde{\mathcal{H}}^{BS}$ are the channel available at the receiver for the DL/UL respectively which can be degraded compared to $\mathcal{H}^{\text{UE}}$ and $\mathcal{H}^{\text{BS}}$. The DL capacity in 3.13 and the UL capacity in 3.14 become

$$\text{C}^{\text{DL}} = \frac{T_{\text{data}}^{\text{DL}}}{T_{\text{coher}}} \mathbb{E}\left\{\log_2(1 + \text{SINR}^{\text{DL}}(\mathbf{x}^{\text{DL}}))\right\} \quad 3.15$$

$$\text{C}^{\text{UL}} = \frac{T_{\text{data}}^{\text{UL}}}{T_{\text{coher}}} \mathbb{E}\left\{\log_2(1 + \text{SINR}^{\text{UL}}(\mathbf{x}^{\text{UL}}))\right\} \quad 3.16$$

where $\mathbf{x}^{\text{DL}} = [u_1^{\text{DL}} \dots u_k^{\text{DL}}]^{\boldsymbol{T}}$ denotes the beamforming vector and $\mathbf{x}^{\text{UL}} = [u_1^{\text{UL}} \dots u_k^{\text{UL}}]^{\boldsymbol{T}}$ indicate the receive combining. Both vectors have a unit norms and are functions of $\hat{\mathbf{h}}$. The expressions for the DL and the UL SINR are given in 3.17 and 3.18 respectively.

$$\text{SINR}^{\text{DL}}(\mathbf{x}^{\text{DL}}) = \frac{\left|\mathbb{E}\left\{\mathbf{h}^H \mathbf{x}^{\text{DL}} | \widetilde{\mathcal{H}}^{\text{UE}}\right\}\right|^2}{\mathbb{E}\left\{|\mathbf{h}^H \mathbf{x}^{\text{DL}}|^2 | \widetilde{\mathcal{H}}^{\text{UE}}\right\} - \left|\mathbb{E}\left\{\mathbf{h}^H \mathbf{x}^{\text{DL}} | \widetilde{\mathcal{H}}^{UE}\right\}\right|^2 + \frac{\mathbb{E}\left\{I_{\mathcal{H}}^{\text{UE}} \middle| \widetilde{\mathcal{H}}^{UE}\right\}}{p^{\text{BS}}} + \frac{\sigma^2{}_{\text{UE}}}{p^{\text{BS}}}} \quad 3.17$$

$$\text{SINR}^{\text{UL}}(\mathbf{x}^{\text{UL}})$$

$$= \frac{\left|\mathbb{E}\left\{\mathbf{h}^H \mathbf{x}^{\text{UL}} | \widetilde{\mathcal{H}}^{\text{BS}}\right\}\right|^2}{\mathbb{E}\left\{|\mathbf{h}^H \mathbf{x}^{\text{UL}}|^2 | \widetilde{\mathcal{H}}^{\text{BS}}\right\} - \left|\mathbb{E}\left\{\mathbf{h}^H \mathbf{x}^{\text{UL}} | \widetilde{\mathcal{H}}^{BS}\right\}\right|^2 + \frac{\mathbb{E}\left\{(\mathbf{x}^{\text{UL}})^H (\text{Q}_{\mathcal{H}} + \sigma_{\text{BS}}^2 \text{I}) \mathbf{x}^{\text{UL}} \middle| \widetilde{\mathcal{H}}^{\text{BS}}\right\}}{p^{\text{UE}}}}$$

3.18

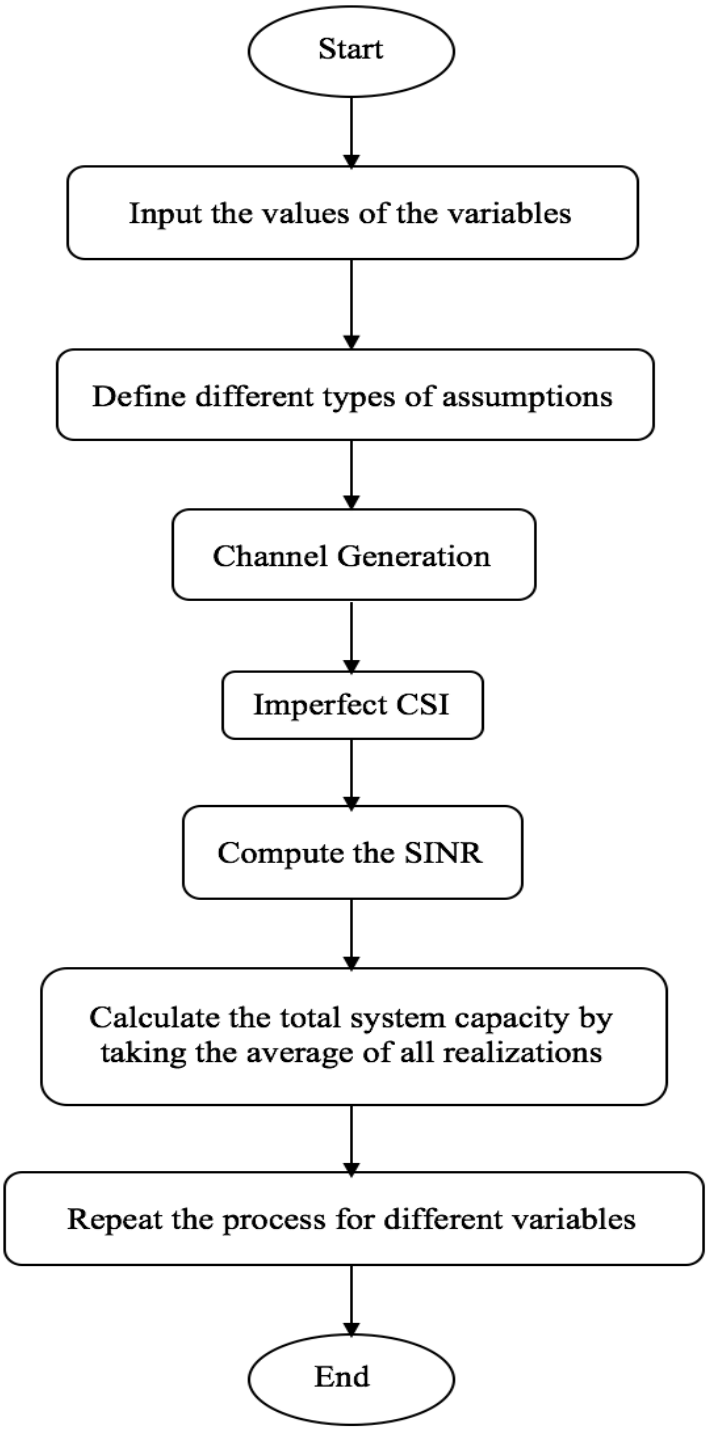

Figure 3.10 Flow chart of the simulation of massive MIMO capacity analysis.

3.4.1 Results and Discussion

In this section, the effect of channel anngle spread, angle of arrival and antenna spacing on the capacity of massive MIMO is illustrated. The average SNRs considered for the DL and the UL are defined as $p^{\mathrm{BS}} \frac{\mathrm{tr}(\mathbf{R})}{N\sigma^2{}_{\mathrm{UE}}}$ and $p^{\mathrm{UE}} \frac{\mathrm{tr}(\mathbf{R})}{N\sigma^2{}_{\mathrm{BS}}}$ respectively. The angle spread and the number of antennas are varied under fixed SNR. To make the DL and UL capacities identical, the ratio of the DL and UL data is fixed at $\frac{T_{\mathrm{data}}^{\mathrm{DL}}}{T_{\mathrm{coher}}} = \frac{T_{\mathrm{data}}^{\mathrm{UL}}}{T_{\mathrm{coher}}} = 0.45$. The flowchart in figure 3.10 describes the main steps to numerically generate and analyze the capacity of massive MIMO systems.

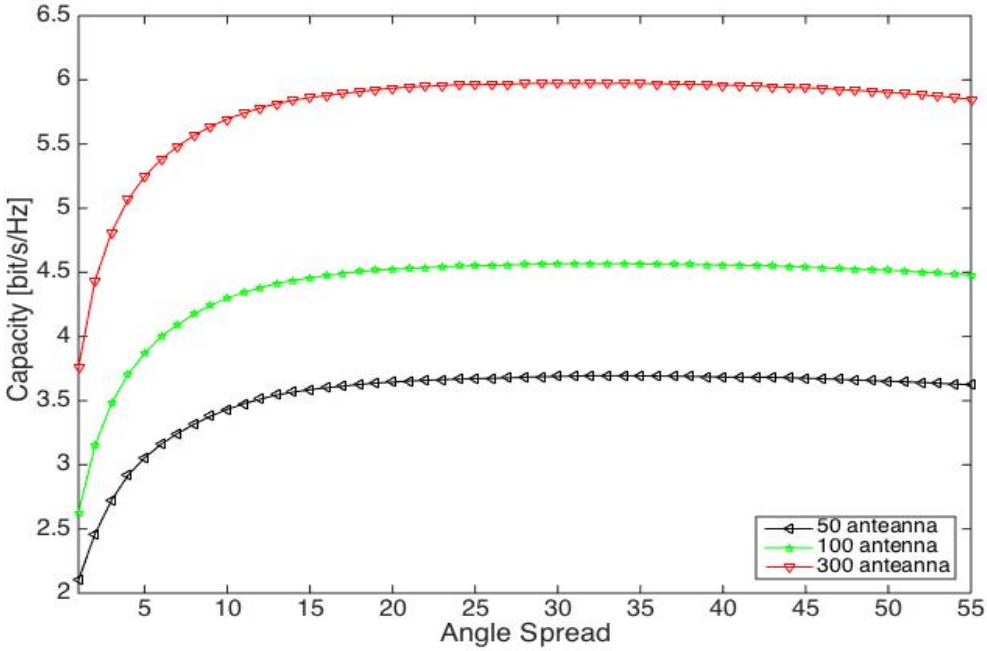

Figure 3.11(a) Channel capacity as a function of the angle spread ; SNR:0 dB [63].

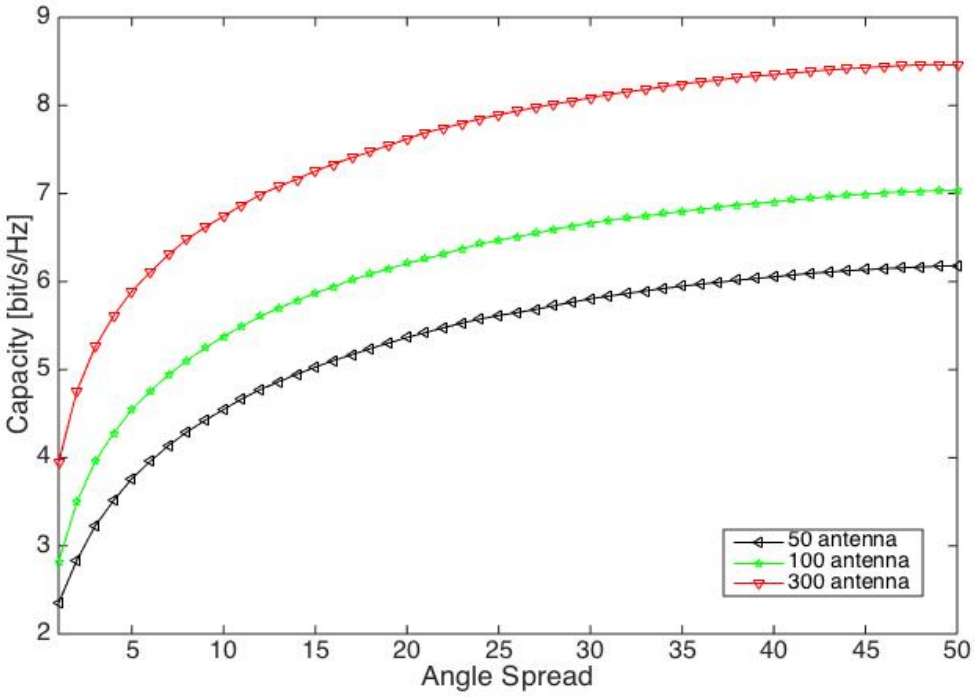

Figure 3.11 (b) Channel capacity as a function of the angle spread ; SNR:25 dB [63].

Figure 3.11 (a & b) considers three different numbers of antennas: 50,100 and 300 with SNRs of 0 and 25 dB respectively. Results show the channel capacity in bit/s/Hz as a function of angle spread for the three cases. The capacity grows as the angle spread is increased. Hence, the least correlated channels give the best performance while the lowest performance happens with the strongly correlated channels. Note that adding more antennas to the BS increases the channel capacity which is consistent with one of the main advantages of Massive MIMO. Figure 3.11 (b) shows the capacity is more sensitive to variations in the angle spread at high SNR.

Figure 3.12 shows the relation between the channel capacity and the number of BS antennas and the angle spread. Results indicate that as the number of BS antenna increases the capacity increases as will. Also, the channel capacity is negatively affected by the low angle spread even when the number of antennas is very high. Distinguishing between the various transmitted signals becomes difficult for the BS because of the difference in the length of the paths between the scatters and the transmitting antennas gets smaller as the angle spread decreases.

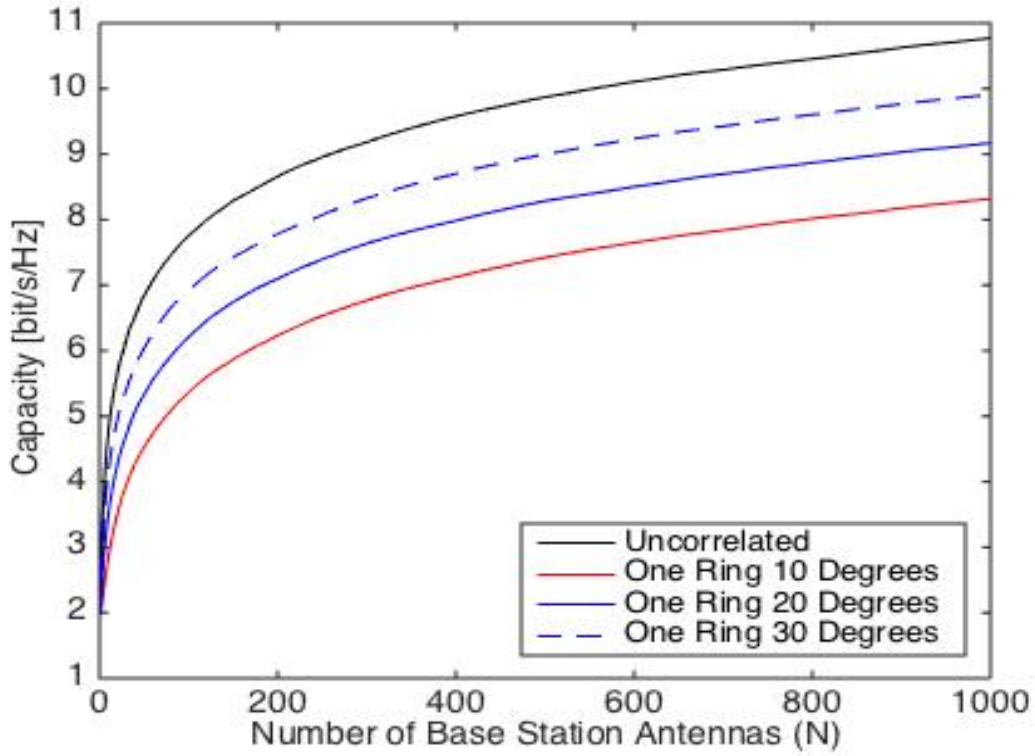

Figure 3.12 Channel capacity as a function of the number of antennas for different angle spread scenaros SNR:25 dB [99].

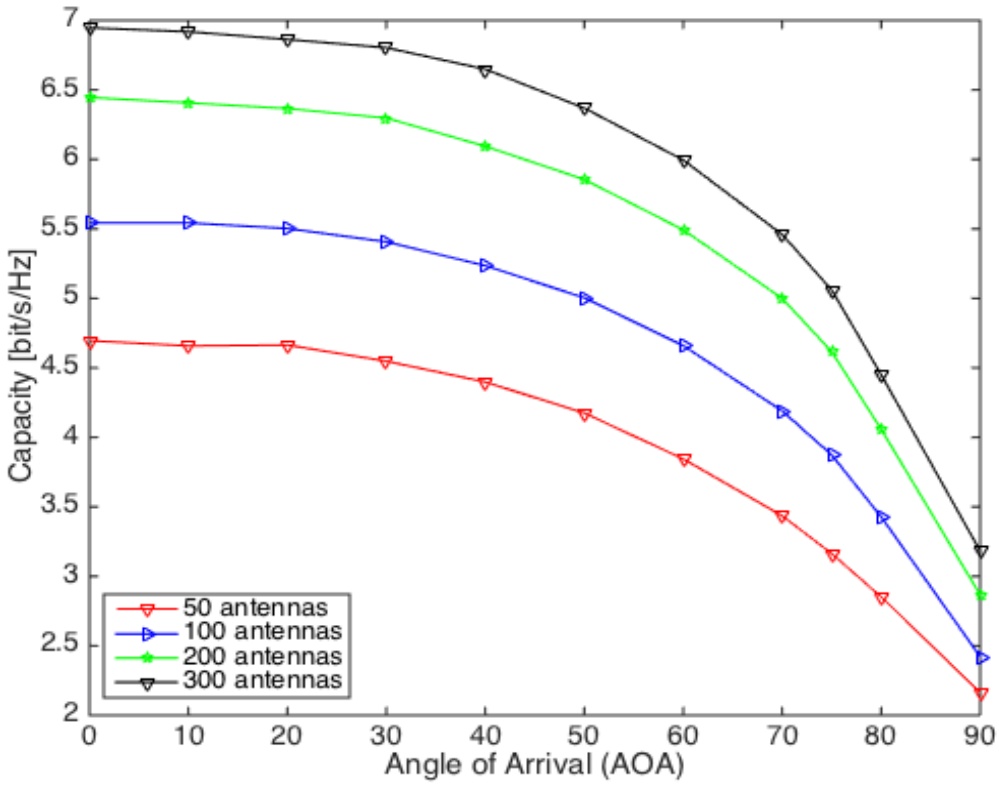

Figure 3.13 Channel capacity as a function of the AOA for different BS antennas SNR:25 dB [99].

Figure 3.13 considers the channel capacity of massive MIMO for three different numbers of antennas: 50,100 and 300 with SNR of 25 dB. Results show the channel capacity in bit/s/Hz as a function of AOA for the three cases. The channel capacity decreases as the AOA increases. Therefore, it can be concluded that the capacity of the channel is inversely proportional to the AOA. Note that that the impact of AOA on the capacity can be much higher when the number of BS is very high.

Spacing between the antenna elements in the BS can also affect the capacity of missive MIMO systems. Figure 3.14 shows the capacity as the antenna spacing is varied for different number of BS antennas. The channel capacity is improved as the separation between the antennas elements is increased. However, the effectiveness of increasing the antenna spacing stops after a certain point which makes any further separation between the antennas pointless.

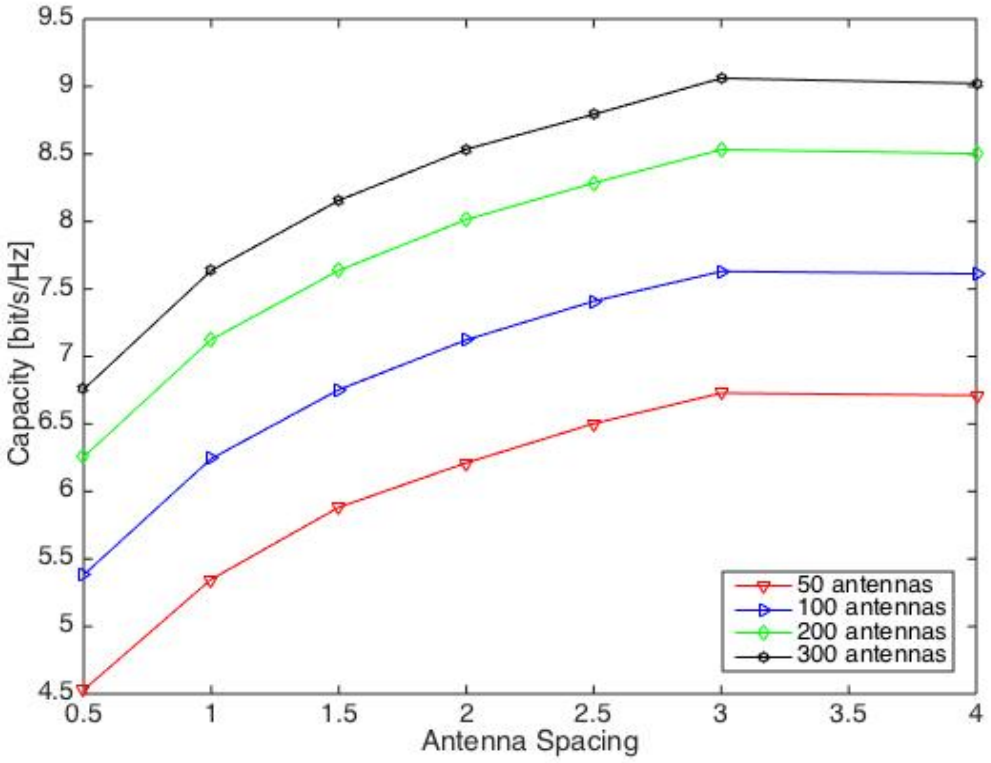

Figure 3.14 Channel capacity as a function of the antennas spacing for different corelation scenaros SNR:25 dB [99].

3.5 Energy efficiency

The energy efficiency (EE) in bit/Joule of the massive MIMO is defined as the ratio capacity (in bit/channel use) and to the transmit power that is measured in (joule/channel use). The energy consumption at the amplifiers in the transmitters in each coherence period under the TDD protocol is

$$E_{\text{amp}} = \left(T_{\text{pilot}}^{\text{DL}} + T_{\text{data}}^{\text{DL}}\right)\frac{p^{\text{BS}}}{\omega^{\text{BS}}} + \left(T_{\text{pilot}}^{\text{UL}} + T_{\text{data}}^{\text{UL}}\right)\frac{p^{UE}}{\omega^{\text{UE}}} \tag{3.18}$$

where $\omega^{\text{BS}}, \omega^{\text{UE}}$ denote the efficiency of the amplifiers at the BS and the UE respectively. The average power (Joule/channel use) is given as

$$\frac{E_{\text{amp}}}{T_{\text{coher}}} = \underbrace{\alpha_{\text{DL}}\left(\frac{T_{\text{pilot}}^{\text{DL}}}{T_{\text{coher}}}\frac{p^{\text{BS}}}{\omega^{\text{BS}}} + \frac{T_{\text{pilot}}^{\text{UL}}}{T_{\text{coher}}}\frac{p^{\text{UE}}}{\omega^{\text{UE}}}\right) + \frac{T_{\text{data}}^{\text{DL}}}{T_{\text{coher}}}\frac{p^{\text{BS}}}{\omega^{\text{BS}}}}_{\text{DL power}} \quad +$$

$$\underbrace{\alpha_{\text{UL}}\left(\frac{T_{\text{pilot}}^{\text{DL}}}{T_{\text{coher}}}\frac{p^{\text{BS}}}{\omega^{\text{BS}}} + \frac{T_{\text{pilot}}^{\text{UL}}}{T_{\text{coher}}}\frac{p^{\text{UE}}}{\omega^{\text{UE}}}\right) + \frac{T_{\text{data}}^{\text{UL}}}{T_{\text{coher}}}\frac{p^{\text{UE}}}{\omega^{\text{UE}}}}_{\text{UL power}} \tag{3.19}$$

where α_{DL} and α_{UL} are the ratios of the DL and the UL transmission respectively

$$\alpha_{\text{DL}} = \frac{T_{\text{data}}^{\text{DL}}}{T_{\text{data}}^{\text{DL}} + T_{\text{data}}^{\text{UL}}} \tag{3.20}$$

$$\alpha_{\text{UL}} = \frac{T_{\text{data}}^{\text{UL}}}{T_{\text{data}}^{\text{DL}} + T_{\text{data}}^{\text{UL}}} \tag{3.21}$$

The EE (in bit/Joule) of massive MIMO system is defined as the following.

$$\text{EE}^{\text{DL}} = \frac{\text{C}^{\text{DL}}}{\alpha_{\text{DL}}\left(\frac{T_{\text{pilot}}^{\text{DL}}}{T_{\text{coher}}}\frac{p^{\text{BS}}}{\omega^{\text{BS}}} + \frac{T_{\text{pilot}}^{\text{UL}}}{T_{\text{coher}}}\frac{p^{\text{UE}}}{\omega^{\text{UE}}} + N\rho + \zeta\right) + \frac{T_{\text{data}}^{\text{DL}}}{T_{\text{coher}}}\frac{p^{\text{BS}}}{\omega^{\text{BS}}}} \tag{3.22}$$

$$\text{EE}^{\text{DL}} = \frac{\text{C}^{\text{UL}}}{\alpha_{\text{UL}}\left(\frac{T_{\text{pilot}}^{\text{DL}}}{T_{\text{coher}}}\frac{p^{\text{BS}}}{\omega^{\text{BS}}} + \frac{T_{\text{pilot}}^{\text{UL}}}{T_{\text{coher}}}\frac{p^{\text{UE}}}{\omega^{\text{UE}}} + N\rho + \zeta\right) + \frac{T_{\text{data}}^{\text{UL}}}{T_{\text{coher}}}\frac{p^{\text{UE}}}{\omega^{\text{UE}}}} \tag{3.23}$$

where $N\rho + \zeta$ denote the baseband circuit power consumption

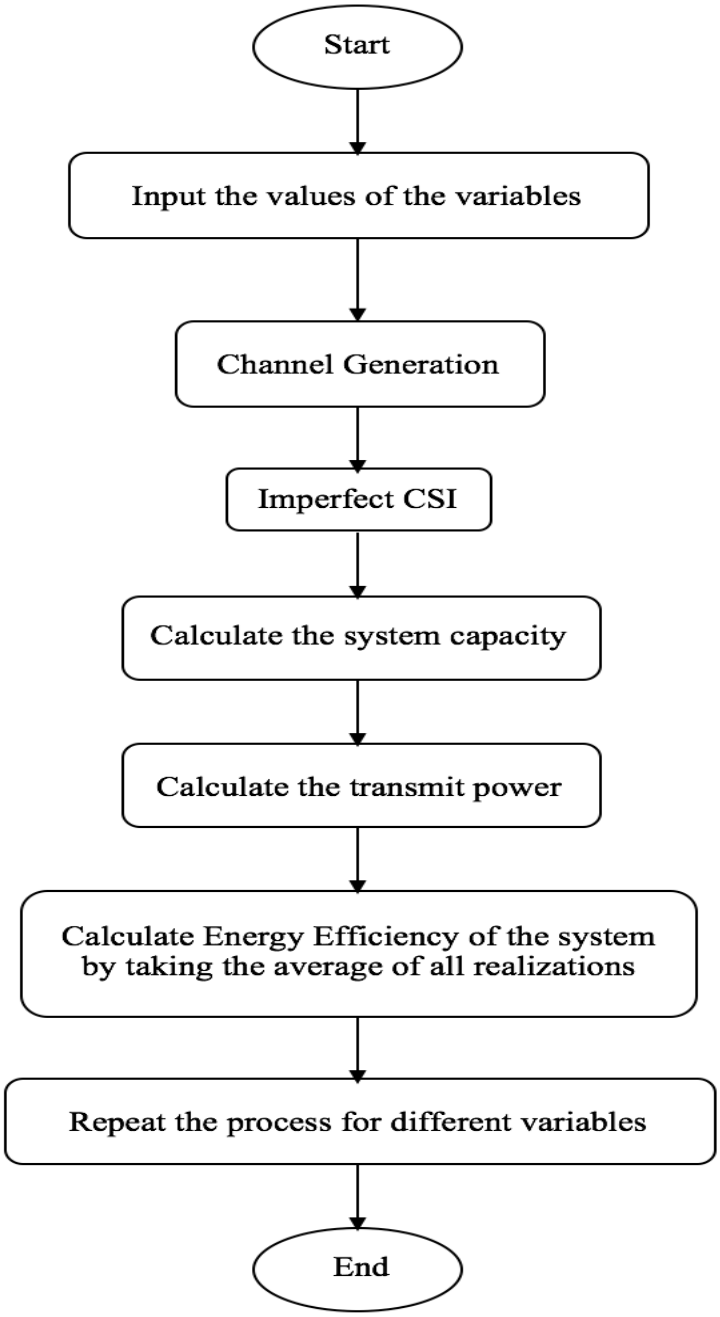

Figure 3.15 Flowchart of the simulation of massive MIMO EE analysis.

3.5.1 Numerical Results

The relation between the performance of Energy Efficiency (EE), the number of BS antennas, imperfect channel conditions and transmit power of massive MIMO is presented in this section. The power consumed by the circuit if only one antenna is used is $\rho + \zeta = 0.02 \frac{\mu J}{\text{Channel use}}$. However, the circuit power for any number of antennas N is $N\rho + \zeta$. Therefore, splitting between ρ and ζ is : $\frac{\rho}{\rho+\zeta} = 0$. Also, the amplifiers efficiencies are $\omega^{\text{BS}} = \omega^{\text{UE}} = 0.3$. The covariance matrix of the channel is produced using the one ring model in 3.6 with angel spread that varies between 10 to 50. To make the EE of the downlink and the uplink identical, we let $\alpha_{\text{DL}} = \alpha_{\text{UL}} = 0.5$ and $\frac{T_{\text{data}}^{\text{UL}}}{T_{\text{coher}}} = \frac{T_{\text{data}}^{\text{DL}}}{T_{\text{coher}}} = 0.05$. The flowchart in figure 4.15 describes the main steps followed to numerically generate and analyze the EE of massive MIMO systems.

The average EE of the DL and the UL for three different number of BS antennas using the capacities in 3.12 and 3.13 are shown in Figure 3.16 (a). EE improves as the number of antennas goes up. Hence, EE is very important feature of massive MIMO. The figure also shows that the performance improves as the angle spread is increased.

Figure 3.16 (b) shows the power allocations corresponding to the curves in Figure 3.16 (a). Although higher number of antennas N is more energy efficient, more transmit power is required as the number of antennas is increased. The transmit power grows as the angle spread of the channels increased.

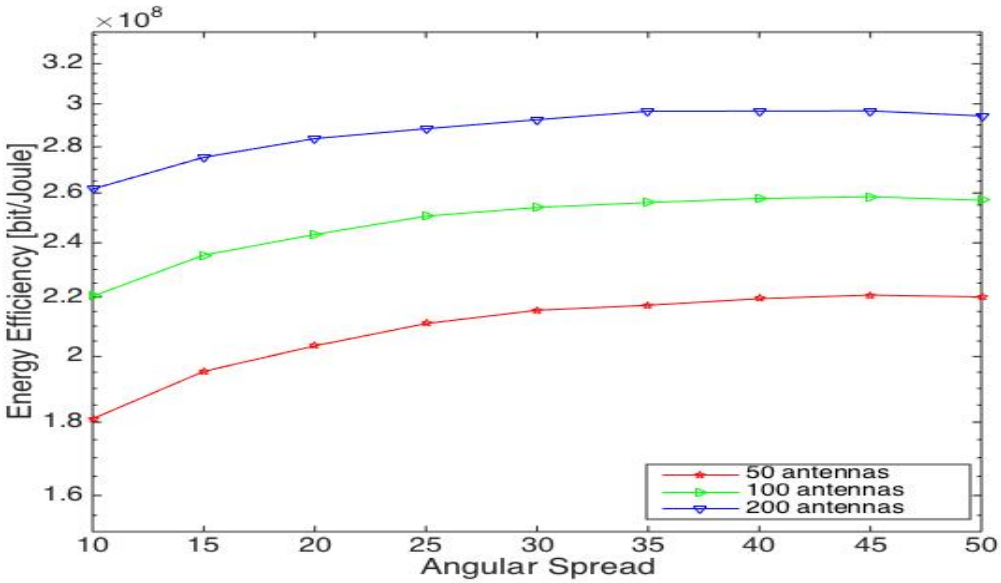

Figure 3.16 (a) Achievable EE as function of the angle spread SNR: 25 dB [63].

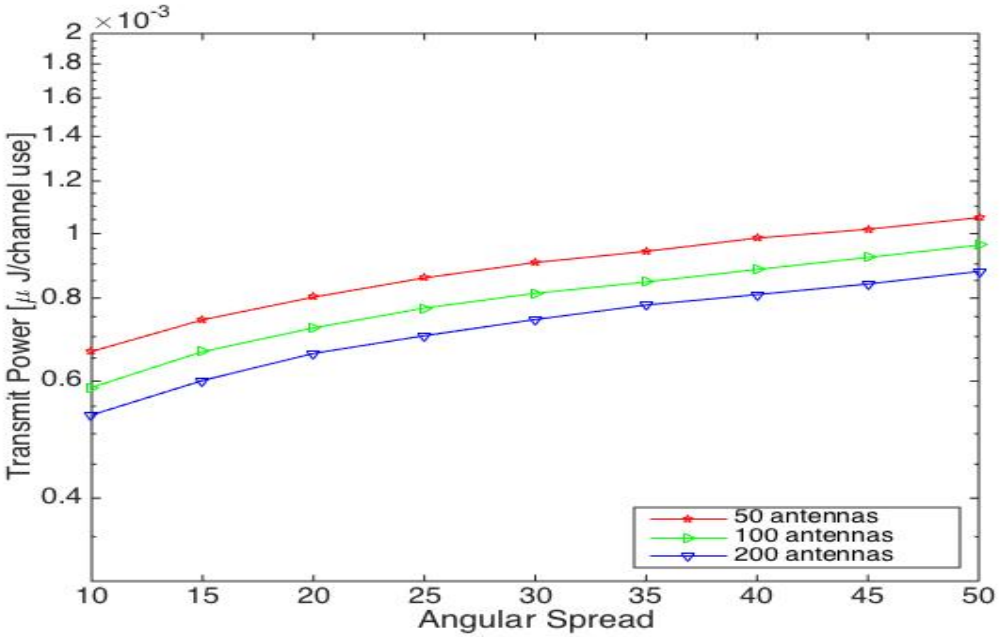

Figure 3.16 (b) The corresponding transmit power of the curves in Figure 3.16 (a) [63].

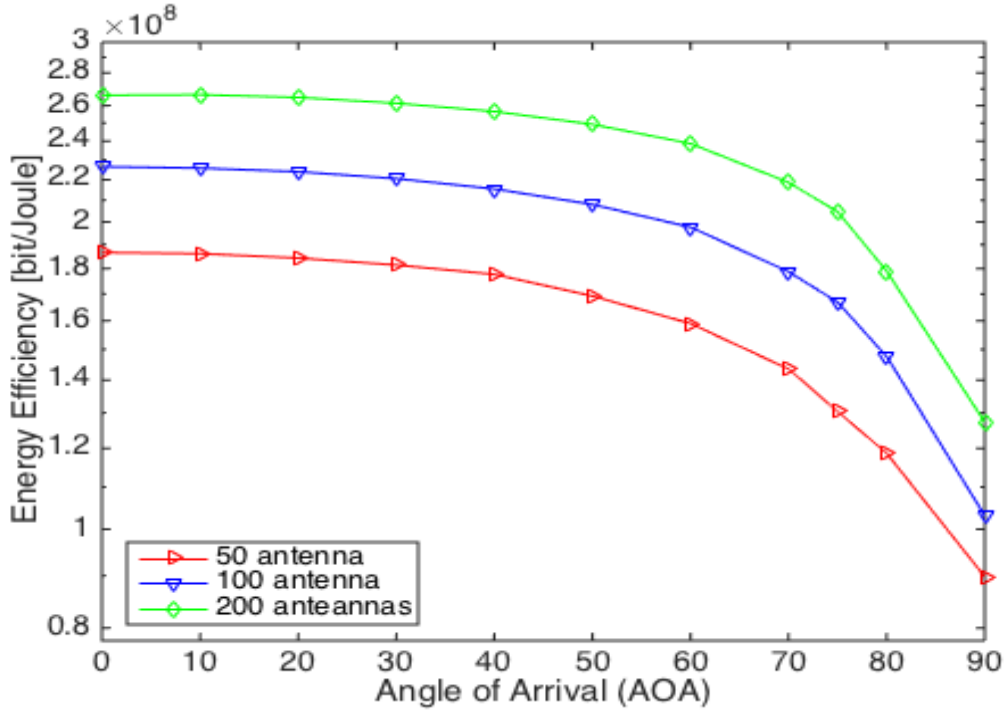

Figure 3.17 (a) Achievable EE as function of the angle spread SNR: 25 dB [99].

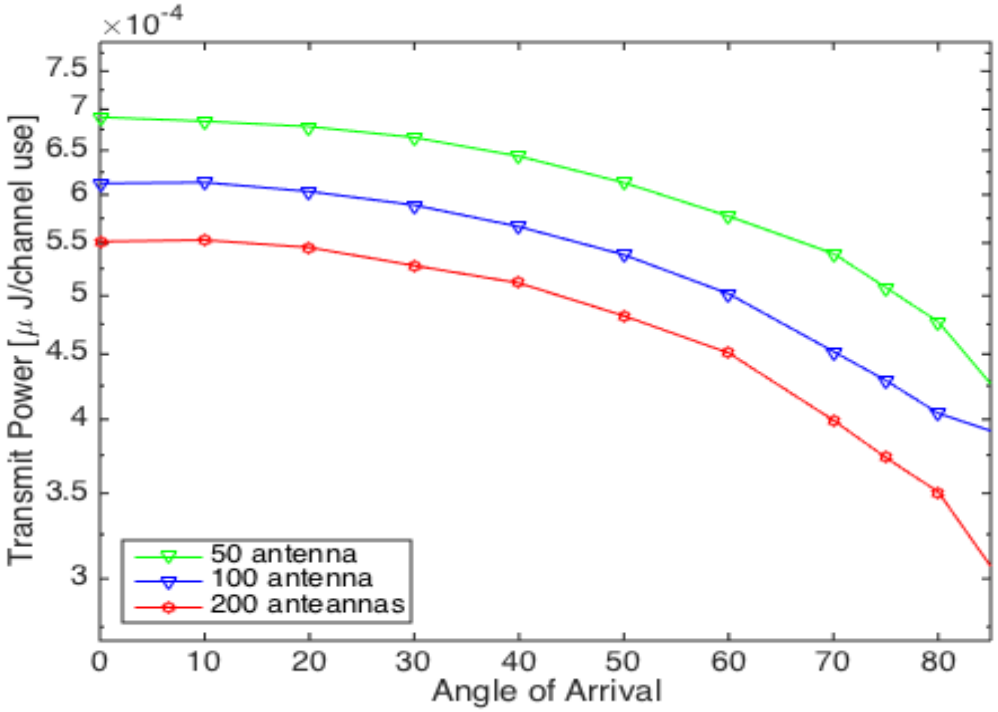

Figure 3.17 (b) The corresponding transmit power of the curves in Figure 3.17 (a) [99]

Figure 3.17 (a) shows the average EE of the DL and the UL for three different number of BS antennas using the capacities in 3.12 and 3.13. EE improves as the number of antennas goes up. Hence, EE is very important feature of massive MIMO. Also, it is oblivious that as the AOA to the BS increases, EE decreases as a result. The impact of increasing the AOA can notices when it exceeds 50 degrees.

Figure 3.17(b) shows the power allocations corresponding to the curves in Figure 3.17 (b). Although higher number of antennas N is more energy efficient, more transmit power is required as the number of antennas is increased and when the AOA is very small.

The average EE of the DL and the UL for three different number of antennas using the capacities in 3.12 and 3.13 are shown in Figure 3.18 (a) as a function of the antenna spacing. EE can be increased by adding more number of antennas to the BS. This confirms one of the most important properties of massive MIMO. Improvement in EE can be also achieved by increasing the spacing between the antenna elements. Figure 3.18 (b) shows the power allocations corresponding to the curves in Figure 3.17 (a). The transmit power grows as the separation between the antennas increases.

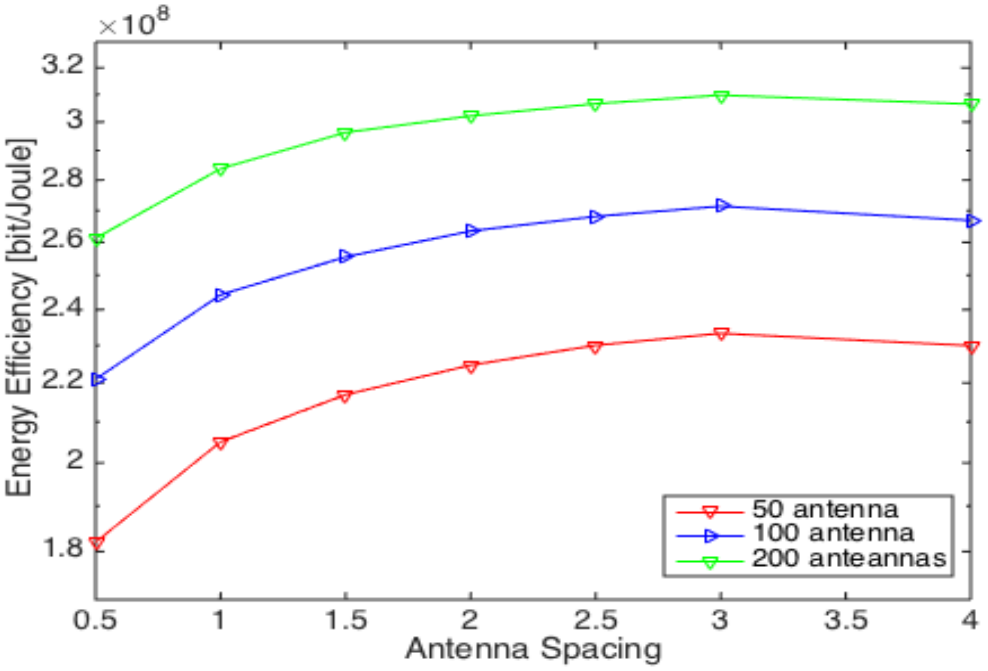

Figure 3.18 (a) Achievable EE as function of the angle spread SNR: 25 dB [99].

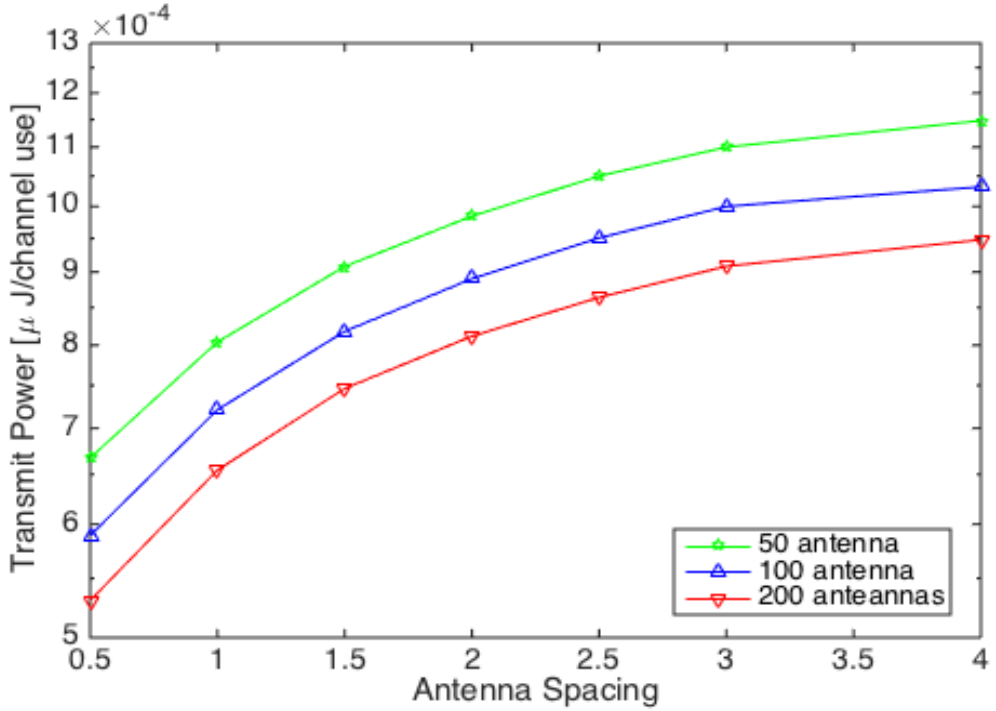

Figure 3.18 (b) The corresponding transmit power of the curves in Figure 3.18 (a) [99]

3.6 Conclusion

This chapter considered the impact of non-ideal channel conditions on the capacity and energy efficacy of massive MIMO. The analysis was based on a system model that considers for these channel conditions. Numerical results showed that the gain of the enormous antenna array in massive MIMO systems depends on the CSI. Results also showed the impact of the angle spread, AOA, antenna spacing and SNR on the channel estimation accuracy, capacity and EE were the channel covariance matrix was generated using the one ring model. The channel estimation accuracy can be improved if the angle spread and the spacing between antenna are decreased and if the AOA, pilot length, SNR and the number of BS antenna are increased. While The channel capacity is proportional to the angle spread, SNR, number of BS antennas, and antenna spacing, it is inversely proportional to the AOA. The EE is improved as the angle spread, SNR, antenna spacing, and number of antennas are increased but decreases at lower AOA.

It can be concluded that one of consequence of the non-ideal channels is the degradation in capacity and energy efficiency of massive MIMO systems. This can be combated by increasing the transmit power to increase the SNR, increase the spacing of the antenna array and by adding more number of antenna at the BS.

Chapter Four The Effect of Users Allocation on The Capacity of Massive MIMO

4.1 Introduction

Current research on massive MIMO concentrates on the benefits of employing hundreds of antennas at the BS that enable each cell of simultaneously serving large number of users. [27], [29], [100]. It has already been shown that significant improvement in the channel capacity can be achieved though simple linear processing techniques that can give almost near optimal performance. However, too many users might want to use their devices in the same location especially in large cities. Therefore, it is very important to analyze the performance of massive MIMO systems in these circumstances to understand the effect of the large number of users in the cell. Extensive studies about the capacity of the small scale MIMO systems with too many users have already been conducted with the assumption of having a perfect channel state information (CSI) [101], [102]. Imperfect CSI in point to point and multiuser MIMO systems are considered in [103]–[105], however, it is still needed to investigate large system in order to study the behavior of massive MIMO.

In this chapter, the estimated CSI is used to analyze the capacity of Massive MIMO for any number of users. Hence, the UL and the DL lower bounds of the sum capacity which can be achieved with per user basis MMSE detectors and the uplink pilots are

derived. The analysis shows that the capacity can be improved by increasing the number of users when the BS is equipped with a large number of antennas. However, when the number of users exceeds a certain number the overall sum capacity of the system start decreasing.

4.2 System Model

Again, a single cell scenario where *K* single antennas users are served with a BS with *M* antenna is considered. It is assumed that each coherence block consists of *S* transmission symbols and that the users' channels do not change during every block. Within the coherence block, the response of channel from the user *k* to the BS is denoted $\mathbf{C}_k \in \mathbb{C}^{M\times N}$. The small spacing between antennas and the lack of enough scattering in the channel can cause spatially correlated fading. Thus, spatial correlation is described using the kronecker model.

$$\mathbf{C}_k = \mathbf{R}_{r,k}^{\frac{1}{2}} \mathbf{C}_{\omega,k} \mathbf{R}_{t,k}^{\frac{1}{2}} \tag{4.1}$$

Where the elements of the matrix $\mathbf{C}_{\omega,k} \in \mathbb{C}^{M\times N}$ are i.i.d. The spatial correlation at the BS and the user *k* are denoted $\mathbf{R}_{r,k}$ and $\mathbf{R}_{t,k}$ respectively. The eigenvalue decomposition of $\mathbf{R}_{t,k}$ is $\mathbf{V}_k \mathbf{A}_k \mathbf{V}_k^H$ where $\mathbf{A}_k$ is the matrix containing the eigenvalues diag $\{\lambda_{k,1} \ldots, \lambda_{k,N}\}$ and $\mathbf{V}_k$ denote the unitary matrix.

4.2.1 UL Channel Estimation

The number of orthogonal sequences during the UL pilot signaling to estimate all the channels at the BS is $B=NK$. Thus, the matrix that contains the pilots of user k is denoted $\mathbf{T}_k \in \mathbb{C}^{N\times B}$. Where $\mathrm{tr}(\mathbf{T}_k\mathbf{T}_k^H) \leq BP_k$ is the pilot energy constraint to minimize the MSE of channel estimation using the pilot matrix $\mathbf{T}_k = \mathbf{V}_k\mathbf{L}_k^{\frac{1}{2}}\mathbf{U}_k^T$. Where $\mathbf{L}_k = \mathrm{diag}\{\ell_{k,1}, \ldots., \ell_{k,N}\}$ is used to distribute the maximum power P_k between the N dimensions of the channel. $\mathbf{U}_k \in \mathbb{C}^{B\times N}$ satisfies $\mathbf{U}_k^H\mathbf{U}_k^T = B\mathbf{I}_N$ and $\mathbf{U}_k^H\mathbf{U}_\ell = 0$ when $k \neq \ell$. Hence, the received uplink signal at the BS is

$$\mathbf{Y} = \sum_{k=1}^{K} \mathbf{C}_k\, \mathbf{T}_k + \mathbf{N} = \sum_{k=1}^{K} \mathbf{H}_k\, \mathbf{D}_k^{\frac{1}{2}}\mathbf{U}_k^T + \mathbf{N} \tag{4.2}$$

where $\mathbf{D}_k = \mathbf{A}_k\mathbf{L}_k$ and $\mathbf{H}_k = \mathbf{R}_{r,k}^{\frac{1}{2}}\mathbf{C}_{\omega,k}\mathbf{V}_k$. $\mathbf{N}$ denotes the noise at the receiver. It the statistical information $\mathbf{D}_k$ is available at the receiver then the LMMSE estimate of the channel is

$$\hat{\mathbf{h}}_k = (\mathbf{D}_k^{\frac{1}{2}}\otimes\mathbf{R}_{r,k})\left(\left(\mathbf{D}_k\otimes\mathbf{R}_{r,k}\right) + \frac{\sigma^2}{B}\mathbf{I}_{MN}\right)^{-1}\mathbf{b}_k \tag{4.3}$$

where $\mathbf{b}_k = \mathrm{vec}(\frac{1}{B}\mathbf{Y}_k\mathbf{U}_k^*) = \mathrm{vec}(\mathbf{H}_k\mathbf{D}_k^{\frac{1}{2}} + \frac{1}{\sqrt{B}}\mathbf{N}\mathbf{U}_k^*)$. If the ith column of $\widehat{\mathbf{H}}_k$ is $\hat{\mathbf{h}}_{k,i}$, then

$$\mathbb{E}\left\{\hat{\mathbf{h}}_{k,i}\hat{\mathbf{h}}_{k,j}^H\right\} = \begin{cases}\boldsymbol{\Phi}_{k,i}, & i = j\\ 0, & i \neq j\end{cases} \tag{4.4}$$

where $\boldsymbol{\Phi}_{k,i} = \boldsymbol{\Phi}_{k,i} = d_{k,i}\mathbf{R}_{r,k}\left(d_{k,i}\mathbf{R}_{r,k}\frac{\sigma^2}{B}\mathbf{I}_M\right)^{-1}\mathbf{R}_{r,k}$.

4.2.1 UL Channel Capacity

When every user transmitter knows only its channel while the BS has perfect knowledge of the CSI to all users, every terminal pre-code its transmitted signal to maximize the capacity [106]. If the precoding matrix of user *k* during the transmission of the UL data is denoted $\overline{\mathbf{T}}_k \in \mathbb{C}^{N\times N}$, then $\overline{\mathbf{T}}_k = \mathbf{V}_k \mathbf{P}_k^{\frac{1}{2}}$ where $\mathbf{P}_k = \text{diag}\{p_{k,1} \dots, p_{k,N}\}$ denotes the power allocation matrix with $\text{tr}(\mathbf{P}_k) \leq \mathbf{P}_k$. Therefor, the received UL signal at the BS can be expressed as

$$\text{y} = \sum_{\boldsymbol{k=1}}^{\boldsymbol{K}} \mathbf{C}_k \, \overline{\mathbf{T}}_k \text{x}_k + \mathbf{n} = \sum_{k=1}^{K} \mathbf{H}_k \, \mathbf{A}_k^{\frac{1}{2}} \mathbf{P}_k^{\frac{1}{2}} \text{x}_k + \mathbf{n} \qquad 4.5$$

where the data symbol transmitted for the user *k* is denoted $\text{x}_k \sim \mathcal{CN}(0, \mathbf{I}_N)$ and the noise at the receiver noise is donated $\mathbf{n} \sim \mathcal{CN}(0, \sigma \mathbf{I}_M)$. The mutual information between y and $\text{x} = [\text{x}_k, \dots, \text{x}_k]$ has the following lower bound

$$I(\text{y}, \widehat{\mathbf{H}};\ \text{x}) \geq \sum_{k=1}^{K} \mathbb{E}\{\log_2 \left| \mathbf{I}_N + \text{O}_k \widehat{\text{H}}_k^H \sum_k \widehat{\text{H}}_k \right|\} \qquad 4.6$$

where $\widehat{\text{H}} = [\widehat{\text{H}}_{1,\dots,} \widehat{\text{H}}_k]$ is the imperfect BS at the receiver, $\text{O}_k = \mathbf{A}_k \mathbf{P}_k$ and $\sum_k = (\sum_{\ell \neq k} \widehat{\text{H}}_\ell \widehat{\text{O}}_\ell \widehat{\text{H}}_\ell^H + \text{Z} + \sigma^2 \mathbf{I}_M)^{-1}$ with $\text{Z} = \sum_\ell^K \sum_{n=1}^N \lambda_{\ell,n}\, p_{\ell,n} (\mathbf{R}_{r,\ell-} \boldsymbol{\Phi}_{\ell,n})$. UL capacity of the user *k* can be maximized using the following MMSE detector

$$\mathbf{t}_{k,i} = \sqrt{\lambda_{k,i}\, p_{k,i}} \sum \hat{\mathbf{h}}_{k,i} \qquad 4.7$$

where $\sum = (\sum_k^{-1} + \widehat{\text{H}}_k \text{O}_k \widehat{\text{H}}_k^H)^{-1}$. The UL channel capacity of user *k* after applying the MMSE detector to the signal in 4.5 is

$$\mathrm{C}_{\mathrm{UL},k} = \sum_{i=1}^{N} \mathbb{E}\left\{\log_2(1 + \mathrm{SINR}_{k,i}^{\mathrm{UL}})\right\} \quad 4.8$$

where SINR is

$$\mathrm{SINR}_{k,i}^{\mathrm{UL}} = \frac{\curlywedge_{k,i} p_{k,i} \left|\mathbf{t}_{k,i}^{H} \hat{\mathbf{h}}_{k,i}\right|^2}{\mathbb{E}\left\{\mathbf{t}_{k,i}(\mathrm{yy}^{H} - \curlywedge_{k,i} p_{k,i} \hat{\mathbf{h}}_{k,i} \widehat{\mathrm{H}}_k^{H}) \mathbf{t}_{k,i} | \widehat{\mathrm{H}}\right\}} \quad 4.9$$

4.2.2 DL Channel Capacity

The average effective channel at the user is $\overline{\mathrm{H}}_k \triangleq \mathbf{A}_k^{\frac{1}{2}} \mathbb{E}\{\mathbf{H}_k^{H} \mathbf{W}_k\} \Omega_\ell^{\frac{1}{2}}$ where $\mathbf{W}_k \in \mathbb{C}^{M \times N}$ denotes the user *k* DL precoding matrix and Ω_k allocate the transmit power between the *N* streams. At the *k*th user, the received signal is

$$\mathrm{y}_k = \mathbf{C}_k^{H} \sum_{\boldsymbol{\ell}=\mathbf{1}}^{\boldsymbol{K}} \mathbf{W}_{\boldsymbol{\ell}} \Omega_\ell^{\frac{1}{2}} \mathrm{x}_\ell + \mathbf{n}_k \quad 4.10$$

where $\mathrm{x}_\ell \sim \mathcal{CN}(0, \mathbf{I}_M)$ indicates the DL signal dedicated for ℓth user and $\mathbf{n}_k \sim \mathcal{CN}(0, \sigma \mathbf{I}_M)$ is the additive noise at the receiver. The processed received signal with user's *k* eigenvector of its correlation matrix $\mathbf{V}_k^{H}$ is

$$\mathbf{z}_k = \mathbf{V}_k^{H} \mathrm{y}_k = \mathbf{A}_k^{\frac{1}{2}} \mathbf{H}_k^{H} \sum_{\boldsymbol{\ell}=\mathbf{1}}^{\boldsymbol{K}} \mathbf{W}_{\boldsymbol{\ell}} \Omega_\ell^{\frac{1}{2}} \mathrm{x}_\ell + \mathbf{V}_k^{H} \mathbf{n}_k \quad 4.11$$

The mutual information between x_k and z_k has the following lower bound

$$I(\mathrm{z}_k, \mathrm{x}_k) \geq \log_2 \left| \mathbf{I}_N + \overline{\mathbf{H}}_k^{H} \overline{\Pi}_k \overline{\mathbf{H}}_k \right| \} \quad 4.12$$

where $\overline{\Pi}_k = (\mathbf{A}_k^{\frac{1}{2}} \mathbb{E}\{\mathbf{H}_k^H \sum_{\ell \neq k} (\mathbf{W}_\ell \Omega_\ell \mathbf{W}_\ell^H) \mathbf{H}_k\} \mathbf{A}_k^{\frac{1}{2}} + \sigma^2 \mathbf{I}_N)^{-1}$. The LMMSE of the *k*th user that maximizes the DL channel capacity is $\mathbf{r}_{k,i} = \overline{\Pi}_k \bar{\mathbf{h}}_{k,i}$, where $\Pi = \overline{\Pi}_k^{-1} + \overline{\mathbf{H}}_k \overline{\mathbf{H}}_k^H$ The DL channel capacity of user *k* after applying the MMSE detector to the signal in 4.11 is

$$\mathrm{C}_{\mathrm{DL},k} = \sum_{i=1}^{N} \mathbb{E}\{\log_2(1 + \mathrm{SINR}_{k,i}^{\mathrm{DL}})\} \quad 4.13$$

where SINR is

$$\mathrm{SINR}_{k,i}^{\mathrm{UL}} = \frac{|\mathbf{r}_{k,i}^H \bar{\mathbf{h}}_{k,i}|^2}{\mathbf{r}_{k,i}^r \mathbb{E}\{\mathbf{z}_k \mathbf{z}_k^H\} \mathbf{r}_{k,i} - |\mathbf{r}_{k,i}^H \bar{\mathbf{h}}_{k,i}|^2} \quad 4.14$$

where $\bar{\mathbf{h}}_{k,i}$ indicates the *i*th column of $\overline{\mathrm{H}}_k$

4.3 Results and Discussion

Certain cells might have to serve a large number users in some circumstances. In big cities, cells are always allocated a large number of users that must be served while cells in rural area might not be loaded at all. Figure 4.1 shows the capacity of a single cell massive MIMO as a function of the number of active users in the cell in three scenarios. The optimal capacities vary depending on the number of antennas in the BS. The first case is when the number of antennas at the BS is 50. In this case, the capacity start increasing until the number of users reaches 40. After this point, the capacity start degrading as more number of users are added to the cell. When the number of BS antennas is 100, the maximum capacity that can be reached is almost 125 bits/s/Hz with 65 users. Finally, the most suitable number of users on a cell where the BS is equipped with 200 antennas is 85

users as the channel capacity can reach up to 190 bit/s/Hz. Therefore, BS with large number of antennas perform better as it accommodates more user but, the capacity start degrading as the number of users exceeds a certain point. For example, the optimal capacities when the BS is equipped 50, 100 and 200 antennas occur at 40, 65 and 90 active terminals respectively. [107] studied the effect of number of users on the capacity of massive MIMO using different estimation techniques. Our results show that the optimal capacity of a single cell can be actually achieved with higher number of users using the LMMSE estimator.

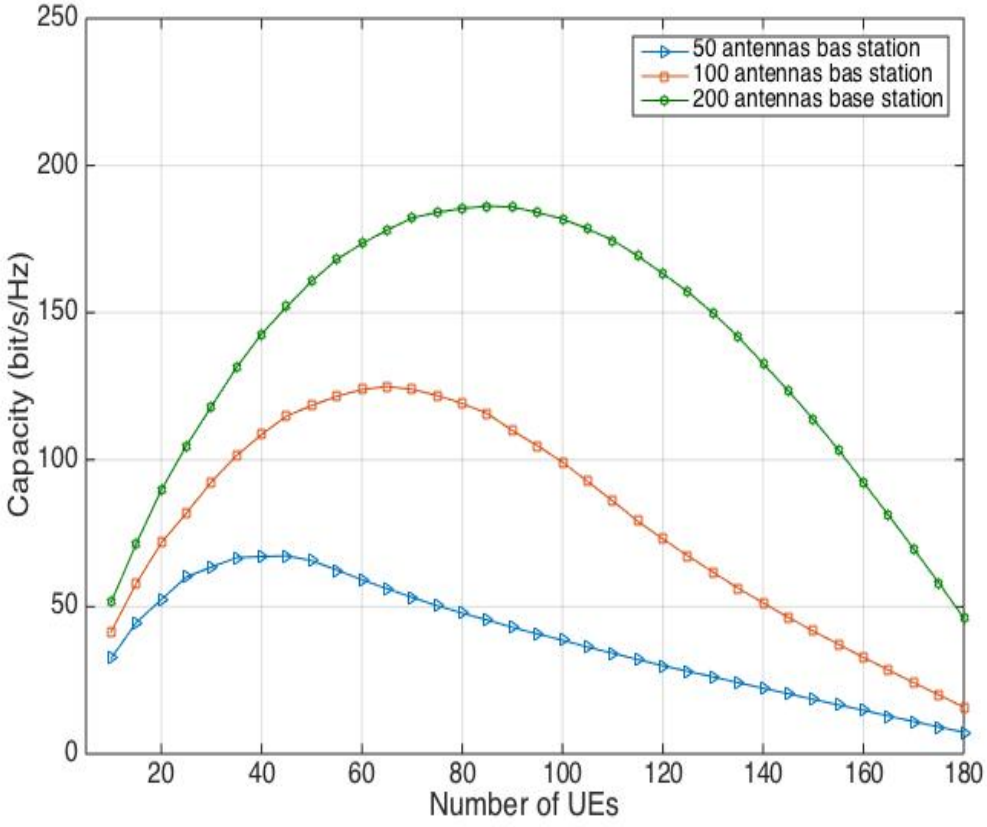

Figure 4.1 Capacity VS the number of scheduled UEs [108].

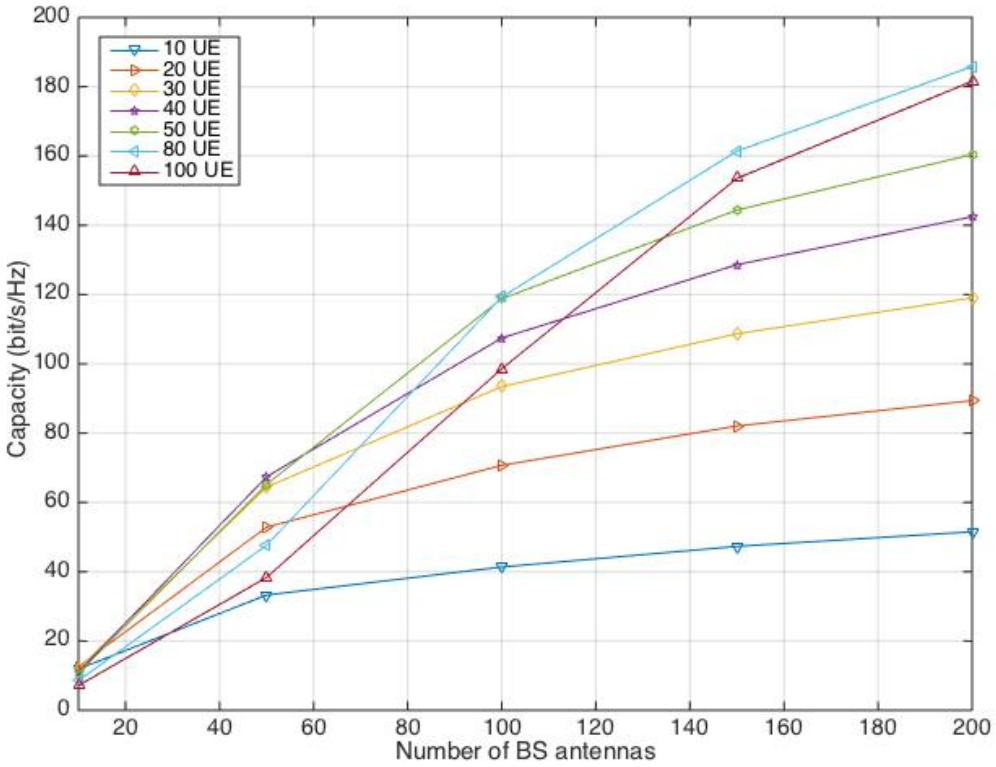

Figure 4.2 Capacity VS the number of BS antennas [108].

Figure 4.2 shows the impact of the number of user on the capacity as the number of antennas is increased. The capacity increase with a faster rate when the number of users is below 40 and the number of BS antennas is under 80. However, the capacity increase much in a much faster rate for BS with more than 80 antennas when the number of users is above 40. Although [47] claims that the channel capacity is proportional to the number of users and the BS, our simulation of massive MIMO using the LMMSE estimator can negatively affect the capacity of the cell.

One of the conventional solution to increase the system capacity is cell densification. Hence, massive MIMO system can be used as another network solution to increase the overall system capacity.

Massive MIMO can provide a good capacity even at low SNRs. Figure 4.3 shows the relation between the average SNR and the capacity of Massive MIMO. Starting from very low SNR below 0 dB, there is a small improvement as the SNR increases. However, capacity start saturating above 5 dB. Therefore, the transmit power of massive MIMO does not have to be very high to achieve its benefits. Our results are consistent with [107] where the performance of massive MIMO is analyzed using different processing techniques.

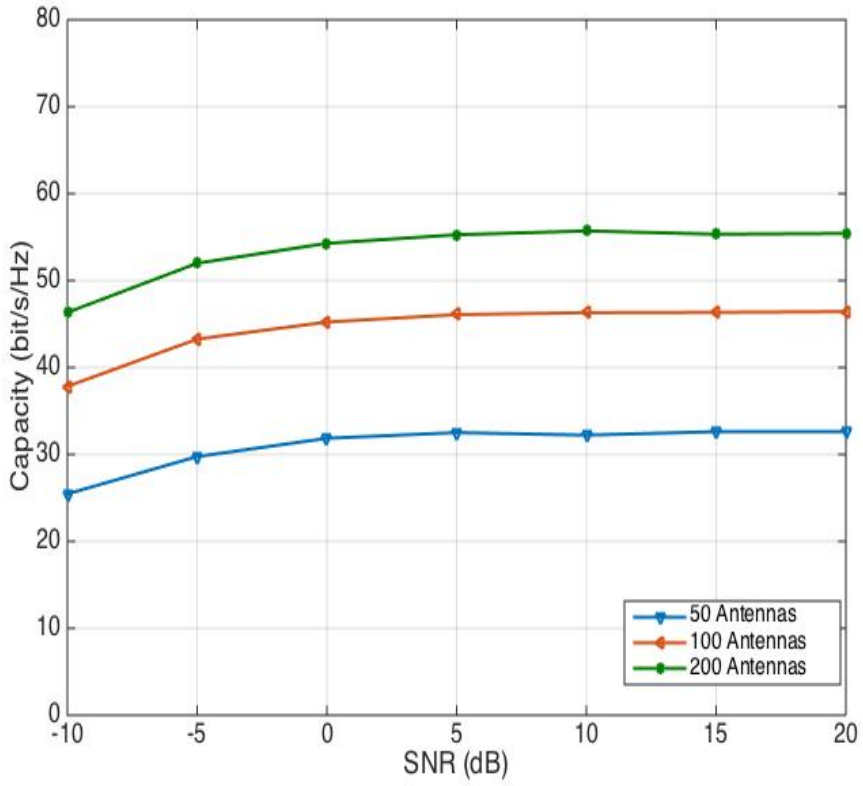

Figure 4.3 Effect of SNR variations on the capacity [108].

4.4 Conclusion

This chapter analyzed the channel capacity of massive MIMO in a single-cell scenario under the impact of variable number of scheduled users. Using the estimated CSI though the UL pilots, the ergodic sum capacity is calculated using the LMMSE detectors. Although it is assumed that the performance of massive MIMO improves as the number of users increases, the maximum number of users that can be served without affecting the performance depends on the number of BS antennas. Hence, the higher the number of antennas the better increasing the number of users improves the capacity of the system.

In general, high per cell channel capacity are achieved by allowing many users of transmitting simultaneously. While 40 users give a per cell capacity of 70 bit/s/Hz when the BS is equipped with 50 antennas, the performance increases to 110 bit/s/Hz and 145 bit/s/Hz when the BS is equipped with 100 and 200 antennas respectively.

Chapter Five: Summary and Future Work

5.1 Summary

Massive MIMO is a new technology that will be used in the 5th generation of wireless communications. There are a lot of issues that must to be considered before this new technology is put to practice. This research studied two aspects that can affect the performance of massive MIMO systems.

The first matter that affect the performance of massive MIMO is the quality of channel. It has been shown that one of the effects of the high channel correlation is the degradation in capacity and energy efficiency of massive MIMO systems. The effect of such channel conditions can be reduced by increasing the transmit power to improve the SNR. Increasing the spacing of the antenna array and adding more antennas at the BS can also lower the effects of channel by improving the channel capacity and the EE.

The impact of the user allocation on the capacity of massive MIMO was also investigated in this dissertation. It was shown that more number of terminals can be hosted in the cell when the number of BS antenna is increased. However, allocating too many users can negatively affect the capacity of massive MIMO.

5.2 Future Work

Massive MIMO is a new technology that comes with many challenges and issues that must be investigated. Therefore, there are plenty of possible research directions. The following list are providing some of the potential research directions in massive MIMO:

- Extend the Investigation to include issues such as higher numbers of BS antennas and different estimation method and compare their effects.
- Investigating the performance of massive MIMO in multi-cells scenario and compare it to the performance of the current small cells.
- Pilot contaminations: this is one of the things that significantly can limit the performance of massive MIMO. Dealing with this issue that happens during the training period because of interference from other cells is very important research directions. The effect of pilot contamination can be reduced using larger frequency reuse factors. However, this will decrease the spectral efficiency because it reduces the pre-log factor. Increasing the cell size can also reduce the effect of pilot contamination because the power of the signal inside the cell is going to be much stronger than interference from other cells. The problem is that the users at the edge of the cell might not be able to receive a decent quality of service. Therefore, an appropriate design to reduce the effect of pilot contamination that consider the size of the cell and pilot reuse factor should be investigated.

- The mechanism of acquiring the channel state information still need to be investigated to get an appropriate answer for many issues such as the possibility of blind estimations and the using FDD instead of TDD.

Bibliography

[1] C. V. N. I. Forecast, "Cisco visual networking index: Global mobile data traffic forecast update 2009-2014."

[2] Ericsson, "White paper: 5G systems enabling industry and society transformation."

[3] "Cisco Visual Networking Index." [Online]. Available: http://www.cisco.com/c/en/us/solutions/collateral/service-provider/visual-networking-index-vni/mobile-white-paper-c11-520862.html. [Accessed: 01-Jan-2017].

[4] H. Q. Ngo, A. Ashikhmin, H. Yang, E. G. Larsson, and T. L. Marzetta, "Cell-Free Massive MIMO versus Small Cells," *IEEE Trans. Wirel. Commun.*, vol. 16, no. 3, pp. 1–30, 2014.

[5] E. Telatar, "Capacity of multi-antenna Gaussian channels," *Eur. Trans. Telecommun*, vol. 10, no. 6, pp. 585–595, 1999.

[6] H. Weingarten, Y. Steinberg, and S. Shamai, "The capacity region of the gaussian MIMO broadcast channel," *Int. Symp. on Information Theory, 2004. ISIT 2004. Proceedings.*, vol. 52, no. March 2002, pp. 174–174, 2004.

[7] A.Nosratinia, T.Hunter, and A.Hedayat, "Cooperative communication in wireless networks," *IEEE Commun. Mag.*, vol. 42, no. 10, pp. 74–80, 2004.

[8] A. J. Paulraj, D. A. Gore, R. U. Nabar, and H. Bölcskei, "An Overview of MIMO Communications—A Key to Gigabit Wireless," in *proceedings of the IEEE*, 2004, vol. 92, no. 2.

[9] P. Viswanath and D. N. C. Tse, “Duality, achievable Rates and Sum Rate Capacity of Gaussian {MIMO} Broadcast Channel,” *Trans. Inform. Theory*, vol. 49, no. 10, pp. 2658–2668, 2003.

[10] A. Goldsmith, S. A. Jafar, N. Jindal, and S. Vishwanath, “Capacity Limits of MIMO Channels,” *IEEE J. Sel. Areas Commun.*, vol. 21, no. 5, pp. 684–702, 2003.

[11] L. Zheng and D. N. C. Tse, “Diversity and multiplexing: A fundamental tradeoff in multiple-antenna channels,” *IEEE Trans. Inf. Theory*, vol. 49, no. 5, pp. 1073–1096, 2003.

[12] D. Gesbert, M. Shafi, and D. Shiu, “From Theory to Practice : An Overview of MIMO Space – Time Coded Wireless Systems,” *Sel. Areas Commun. IEEE J.*, vol. 21, no. 3, pp. 281–302, 2003.

[13] C. N. Chuah, D. N. C. Tse, J. M. Kahn, and R. A. Valenzuela, “Capacity scaling in MIMO wireless systems under correlated fading,” *IEEE Trans. Inf. Theory*, vol. 48, no. 3, pp. 637–650, 2002.

[14] J. G. Andrews *et al.*, “What will 5G be?,” *IEEE J Sel Area Comm*, vol. 32, no. 6, pp. 1065–1082, 2014.

[15] A. Osseiran *et al.*, “Scenarios for the 5G Mobile and Wireless Communications: the Vision of the METIS Project,” *IEEE Commun. Mag.*, no. May, pp. 26–35, 2014.

[16] F. Boccardi, R. W. Heath, A. Lozano, T. L. Marzetta, and P. Popovski, “Five Disruptive Technology Directions for 5G,” *IEEE Commun. Mag*, vol. 52, no. 2, pp. 74–80, 2014.

[17] S. Fletcher and N. E. C. Telecom, “Cellular Architecture and Key Technologies for 5G Wireless Communication Networks,” *IEEE Commun. Mag.*, no. February, pp. 122–130, 2014.

[18] N. Michailow, R. Datta, S. Krone, M. Lentmaier, and G. Fettweis, “Generalized Frequency Division Multiplexing : A Flexible Multi-Carrier Modulation Scheme for 5th Generation Cellular Networks,” *Proc. Ger. Microw. Conf.*, vol. 62, no. 9, pp. 1–4, 2012.

[19] B. Bangerter, S. Talwar, R. Arefi, and K. Stewart, “Networks and devices for the 5G era,” *IEEE Commun. Mag.*, vol. 52, no. 2, pp. 90–96, 2014.

[20] N. Bhushan *et al.*, “Network densification: The dominant theme for wireless evolution into 5G,” *IEEE Commun. Mag.*, vol. 52, no. 2, pp. 82–89, 2014.

[21] I. Chih-Lin, C. Rowell, S. Han, Z. Xu, G. Li, and Z. Pan, “Toward green and soft: A 5G perspective,” *IEEE Commun. Mag.*, vol. 52, no. 2, pp. 66–73, 2014.

[22] E. GUSTAFSSON and A. JONSSON, “ALWAYS BEST CONNECTED EVA,” *IEEE Wirel. Commun.*, no. February, pp. 36–41, 2003.

[23] G. Wunder *et al.*, “5G NOW: Non-Orthogonal, Asynchronous Waveforms for Future Mobile Applications,” *IEEE Commun. Mag.*, no. February, pp. 97–105, 2014.

[24] S. Chen and J. Zhao, “The requirements, challenges, and technologies for 5G of terrestrial mobile telecommunication,” *IEEE Commun. Mag.*, vol. 52, no. 5, pp. 36–43, 2014.

[25] Z. Ding, Z. Yang, P. Fan, and H. V. Poor, "On the performance of non-orthogonal multiple access in 5G systems with randomly deployed users," *IEEE Signal Process. Lett.*, vol. 21, no. 12, pp. 1501–1505, 2014.

[26] M. N. Tehrani, M. Uysal, and H. Yanikomeroglu, "Device-to-device communication in 5G cellular networks: challenges, solutions, and future directions," *Commun. Mag. IEEE*, vol. 52, no. 5, pp. 86–92, 2014.

[27] T. L. Marzetta, "Noncooperative Cellular Wireless with Unlimited Numbers of Base Station Antennas," vol. 9, no. 11, pp. 3590–3600, 2010.

[28] E. Bjornson, E. G. Larsson, and T. L. Marzetta, "Massive MIMO: ten myths and one critical question," *IEEE Commun. Mag.*, vol. 54, no. 2, pp. 114–123, 2016.

[29] H. Q. Ngo, E. G. Larsson, and T. L. Marzetta, "Energy and Spectral Efficiency of Very Large Multiuser MIMO Systems," *IEEE Trans. Commun.*, vol. 61, no. 4, pp. 1436–1449, 2013.

[30] E. G. Larsson, O. Edfors, F. Tufvesson, and T. L. Marzetta, "Massive MIMO for Next Generation Wireless Systems," no. February, pp. 1–19, 2013.

[31] T. L. Marzetta, E. G. Larsson, H. Yang, and H. Q. Ngo, *Fundamentals of Massive MIMO*. New York: Cambridge University Press, 2016.

[32] J. Li, D. Wang, and P. Zhu, "Uplink Spectral Efficiency Analysis of Distributed Massive MIMO With Channel Impairments," vol. 5, 2017.

[33] W. Tan, S. Jin, C. K. Wen, and Y. Jing, "Spectral Efficiency of Mixed-ADC Receivers for Massive MIMO Systems," *IEEE Access*, vol. 4, pp. 7841–7846, 2016.

[34] H. Q. Ngo, “Massive MIMO : Fundamentals and System Designs,” Linköping University, 2015.

[35] A. Swindlehurst, E. Ayanoglu, P. Heydari, and F. Capolino, “Millimeter-wave massive MIMO: The next wireless revolution?,” *IEEE Commun. Mag.*, vol. 52, no. 9, pp. 56–62, 2014.

[36] J. Spiess, Y. T. Joens, R. Dragnea, and P. Spencer, “Using Big Data to Improve Customer Experience and Business Performance,” *Bell Labs Tech. J.*, vol. 18, no. 4, pp. 3–17, 2014.

[37] L. Lu, G. Y. Li, A. Ashikhmin, R. Zhangand, and A. L. Swindlehurst, “An Overview of Massive MIMO : Benefits and Challenges,” *IEEE J. Sel. Top. Signal Process.*, vol. 8, no. 5, pp. 742–758, 2014.

[38] D. Persson, B. K. Lau, and E. G. Larsson, “Scaling Up MIMO,” *IEEE Signal Process. Mag.*, vol. 30, no. 1, pp. 40–60.

[39] E. Bjornson, J. Hoydis, M. Kountouris, and M. Debbah, “Massive MIMO systems with non-ideal hardware: Energy efficiency, estimation, and capacity limits,” *IEEE Trans. Inf. Theory*, vol. 60, no. 11, pp. 7112–7139, 2014.

[40] S. Schwarz and M. Rupp, “Performance Evaluation of Low Complexity Double-Sided Massive MIMO Transceivers,” 2016.

[41] R. C. De Lamare, “Massive MIMO Systems : Signal Processing Challenges and Research Trends,” pp. 1–9.

[42] J. G. Andrews *et al.*, “What Will 5G Be?,” *IEEE J. Sel. Areas. Commun*, vol. 32, no. 6, pp. 1065–1082, 2014.

[43] G. P. Fettweis, “The tactile internet: Applications and challenges,” *IEEE Veh. Technol. Mag.*, vol. 9, no. 1, pp. 64–70.

[44] A. Alshammari, S. Albdran, and M. A. Matin, “Channel Capacity of Next Generation Large Scale MIMO Systems,” in *SPIE*, 2016.

[45] L. He, S. Member, J. Wang, and S. Member, “Bandwidth Efficiency Maximization for Single-Cell Massive Spatial Modulation MIMO : An Adaptive Power Allocation Perspective,” vol. 5, 2017.

[46] M. Xiao *et al.*, “Millimeter Wave Communications for Future Mobile Networks,” vol. 8716, no. c, pp. 1–7, 2017.

[47] T. L. Marzetta, “Massive MIMO: An Introduction,” *Bell Labs Tech. J.*, vol. 20, pp. 11–22, 2015.

[48] D. Gesbert, M. Kountouris, R. W. HeathJr., C. Chae, and T. Chae, “Shifting the MIMO Paradigm,” *IEEE Signal Process. Mag.*, vol. 24, no. 5, p. 36–46, 2007.

[49] T. L.Marzetta, “How much training is required formultiuserMIMO?,” in *ACSSC 40th Asilomar Conference on Signals, Systems and Computers.*, 2006, pp. 359–363.

[50] P. Elias, A. Feinstein, and C. Shannon, “A note on the maximum flow through a network,” *IRE Trans. Inf. Theory*, vol. 2, no. 4, pp. 117–119, 1956.

[51] P. F. Driessen and G. J. Foschini, “On the capacity formula for multiple input-multiple out-put wireless channels: a geometric interpretation,” in *IEEE International Conference on Communications (ICC)*, 1999, pp. 1603–1607.

[52] C. F. BRAUN, “Electrical oscillations and wireless telegraphy,” in *Nobal Lecture*, 1909, pp. 239–240.

[53] H. Beverage and H. O. Peterson, “Diversity Receiving System of R.C.A. Communications, Inc., for Radiotelegraphy,” in *Proceedings of the Institute of Radio Engineers*, 1931, pp. 529–561.

[54] A Wittneben, “Basetation modulation diversity for digital simulcast,” in *Vehicular Technology Conference, 1991, Gateway to the Future Technology in Motion, 41st IEEE*, 1991, pp. 848–853.

[55] N. Seshadri, C. E. W. Sundberg, and V. Weerackody, “Advanced technologies for modulation, error correction , channel equalization and diversity,” *ATT Tech. J.*, 1993.

[56] S M Alamouti, “A simple transmit diversity technique for wireless communications,” *IEEE J. Sel. Areas Commun.*, vol. 16, no. 8, pp. 1451–1458, 1998.

[57] G. Fochini, “Layered space time architecture for wireless communication in a fading environment when using multi-element antennas,” *Bell Labs Tech. J.*, pp. 41–59, 1996.

[58] G. J. Foschini, “V-BLAST: an architecture for realizing very high data rates over the rich scattering wireless channel,” in *International symposium on signal, systems and electronics, ISSSE*, 1998, pp. 295–300.

[59] J. R. Hapton, *Intoduction To MIMO Communications*, 1st ed. New York: Cambridge University Press, 2014.

[60] A. Goldsmith, S. A. Jafar, N. Jindal, and S. Vishwanath, “Capacity Limits of MIMO Channels,” *IEEE J. Sel. Areas Commun.*, vol. 21, no. 5, pp. 684–702, 2003.

[61] Q. H. Spencer, C. B. Peel, A. L. Swindlehurst, and M. Haardt, “An introduction to the multi-user MIMO downlink,” *Commun. Mag. IEEE*, vol. 42, no. 10, pp. 60–67, 2004.

[62] Y. Cho, J. Kim, W. Yang, and C. Kang, *MIMO-OFDM WIRELESS COMMUNICATIONS WITH MATLAB*. Singapore: Wiley, 2010.

[63] A. Alshammari, S. Albdran, and M. A. Matin, “The Effect of Channel Spatial Correlation on Capacity and Energy Efficiency of Massive MIMO Systems,” in *The 7th IEEE annual Comuting and Communication Workshop and Conferernce*, 2017.

[64] S. ten B. Jakob Hoydis Merouane Debbah, “Massive MIMO in the UL/DL of Cellular Networks: How Many Antennas Do We Need?,” *Ieee J. Sel. Areas Commun.*, vol. 31, no. 2, pp. 160–171, 2013.

[65] T. L.Marzetta, “Noncooperative cellularwireless with unlimited numbers of base station antennas,” *IEEE Trans. Wirel. Commun*, vol. 9, no. 11, pp. 3590–3600, 2010.

[66] L. M. Systems, H. Yin, D. G. Fellow, M. Filippou, and Y. Liu, “A Coordinated Approach to Channel Estimation in,” *IEEE J. Sel. Areas Commun.*, vol. 31, no. 2, pp. 264–273, 2013.

[67] L. Liu, D. W. Matolak, C. Tao, and Y. Li, “Analysis of an Upper Bound on the Effects of Large Scale Attenuation on Uplink Transmission Performance for Massive MIMO Systems,” *IEEE Access*, pp. 1–1, 2017.

[68] E. Bjornson, J. Hoydis, M. Kountouris, and M. Debbah, “Hardware Impairments in Large-scale MISO Systems : Energy Efficiency , Estimation , and Capacity Limits,” in *Proceedings of International Conference on Digital Signal Processing*, 2013.

[69] A. Alshammari, S. Albdran, M. A. R. Ahad, and M. Matin, “Impact of Angular Spread on Massive MIMO Channel Estimation,” in *The 19th International Conference on Computer and Information Technology (ICCIT)*, 2016.

[70] J. Hoydis, S. Ten Brink, and M. Debbah, “Massive MIMO: How many antennas do we need?,” *2011 49th Annu. Allert. Conf. Commun. Control. Comput. Allert. 2011*, pp. 545–550, 2011.

[71] S. Biswas, J. Xue, F. A. Khan, and Tharmalingam Rantnarajah, “Performance Analysis of Correlated Massive MIMO Systems With Spatially Distributed Users,” *IEEE Syst. J.*, vol. PP, no. 99, pp. 1–12.

[72] X. Jia, P. Deng, L. Yang, and H. Zhu, “Spectrum and Energy Efficiencies for Multiuser Pairs Massive MIMO Systems With Full-Duplex Amplify-and-Forward Relay,” *IEEE Access*, vol. 3, pp. 1907–1918, 2015.

[73] J. C. Shen, J. Zhang, K. C. Chen, and K. B. Letaief, “High-Dimensional CSI Acquisition in Massive MIMO: Sparsity-Inspired Approaches,” *IEEE Syst. J.*, vol. 11, no. 1, pp. 32–40, 2017.

[74] H. Xie, F. Gao, and S. Jin, "An Overview of Low-Rank Channel Estimation for Massive MIMO Systems," *IEEE Access*, vol. 4, pp. 7313–7321, 2016.

[75] X. Gao, O. Edfors, F. Rusek, and F. Tufvesson, "Linear pre-coding perfor- mance in measured very-large MIMO channels," in *Proc. IEEE Vehicular Technology Conf. (VTC)*, 2011.

[76] V. et Al., "A Flexible 100-Antenna Testbed for Massive MIMO," in *Proc. IEEE Globecom Wksp. — Massive MIMO: From Theory to Practice*, 2014.

[77] R. C. de Lamare, "Massive MIMO Systems: Signal Processing Challenges and Research Trends," *URSI Radio Sci. Bull.*, vol. cs.IT, pp. 1–9, 2013.

[78] S. Albdran, A. Alshammari, and M. A. Matin, "Uplink Channel Estimation Error for Large Scale MIMO System," in *SPIE*, 2016.

[79] V. Jungnickel *et al.*, "The role of small cells, coordinated multipoint, and massive MIMO in 5G," *IEEE Commun. Mag.*, vol. 52, no. 5, pp. 44–51, 2014.

[80] K. T. Truong and R. W. Heath, "Effects of Channel Aging in Massive MIMO Systems," *J. Commun. Networks*, vol. 15, no. 4, pp. 338–351, 2014.

[81] S. Noh, M. D. Zoltowski, Y. Sung, and D. J. Love, "Training signal design for channel estimation in massive MIMO systems," *2014 IEEE Int. Conf. Acoust. Speech Signal Process.*, vol. 8, no. 5, pp. 6499–6503, 2014.

[82] Y. Long, Z. Chen, and J. Fang, "Nonasymptotic Analysis of Capacity in Massive MIMO Systems," *IEEE Wirel. Commun. Lett.*, vol. 4, no. 5, pp. 541–544, 2015.

[83] J. Liu, A. Eryilmaz, N. B. Shroff, and E. S. Bentley, "Understanding the impact of limited channel state information on massive MIMO network performances," *Proc. 17th ACM Int. Symp. Mob. Ad Hoc Netw. Comput. - MobiHoc '16*, vol. 8716, no. c, pp. 251–260, 2016.

[84] J. Jose, A. Ashikhmin, T. L. Marzetta, and S. Vishwanath, "Pilot contam- ination and precoding in multi-cell TDD systems," *IEEE Trans. Wirel. Commun.*, vol. 10, no. 8, p. 2640 2651, 2011.

[85] A. Ashikhmin and T. L. Marzetta, "Pilot contamination precoding in multi- cell large scale antenna systems," in *Proc. IEEE International Symposium on Information Theory (ISIT)*, 2012.

[86] R. Müeller, L. Cottatellucci, and M. Vehkaperä, "Blind pilot decontamination," *IEEE J. Sel. Sig. Process*, vol. 8, no. 5, p. 773 786, 2014.

[87] H. Q. Ngo and E. G. Larsson, "EVD-based channel estimations for multicell multiuser MIMO with very large antenna arrays," in *EEE International Conference on Acoustics, Speech and Signal Processing (ICASSP)*, 2012.

[88] H. Yin, D. Gesbert, M. Filippou, and Y. Liu, "A coordinated approach to channel estimation in large-scale multiple-antenna systems," *IEEE J. Sel. Areas Commun*, vol. 31, no. 2, 2013.

[89] O. Elijah, C. Y. Leow, T. A. Rahman, S. Nunoo, and S. Z. Iliya, "A Comprehensive Survey of Pilot Contamination in Massive MIMO-5G System," *IEEE Commun. Surv. Tutorials*, vol. 18, no. 2, pp. 905–923, 2016.

[90] S. Albdran, A. Alshammari, M. Ahad, and M. Matin, “Effect of Exponential Correlation Model on Channel Estimation fo Massive MIMO,” in *The 19th International Conference on Computer and Information Technology (ICCIT)*, 2016.

[91] M. Agiwal, A. Roy, and N. Saxena, “Next generation 5G wireless networks: A comprehensive survey,” *IEEE Communications Surveys and Tutorials*, vol. 18, no. 3. pp. 1617–1655, 2016.

[92] S. Albdran, A. Alshammari, and M. A. Matin, “Spectral and Energy Efficiency for Massive MIMO Systems Using Exponential Correlation Model,” in *The 7th IEEE annual Comuting and Communication Workshop and Conferernce*, 2017.

[93] B. S. Paul and R. Bhattacharjee, “Effect of Array Geometry on the Capacity of Outdoor MIMO Communication: A Study,” in *India Conference, 2006 Annual IEEE*, 2006.

[94] W. C. Jakes, *Microwave Mobile Communications*. Piscataway, NJ: IEEE Press, 1993.

[95] D.-S. Shiu, G. J. Faschini, and M. J. Gans, “Fading correlation and its effect on the capacity of multi-element antenna systems,” in *Universal Personal Communications, 1998. ICUPC ’98. IEEE 1998 International Conference on*, 1998.

[96] M. P¨tzold and B. O. Hogstad, “A Wideband Space-Time MIMO Channel Simulator Based on the Geometrical One-Ring Model,” in *Personal, Indoor and Mobile Radio Communications, 2004. PIMRC 2004. 15th IEEE International*

Symposium on, 2004.

[97] A. Adhikary, J. Nam, J. Y. Ahn, and G. Caire, "Joint Spatial Division and Multiplexing—The Large-Scale Array Regime," *IEEE Trans. Inf. Theory*, vol. 59, no. 10, pp. 6441–6463, 2013.

[98] J. Gong, J. F. Hayes, and M. R. Soleymani, "The effect of antenna physics on fading correlation and the capacity of multielement antenna systems," *IEEE Trans. Veh. Technol.*, vol. 56, no. 4 I, pp. 1591–1599, 2000.

[99] A. Alshammari and M. A. Matin, "Mitigating The Effect Spatial Correlation in Massive MIMO Systems," *To be Submitt.*

[100] J. Hoydis, S. Ten Brink, and M. Debbah, "MassiveMIMOin the UL/DL of cellular networks: How many antennas do we need?," *IEEE J. Sel. Areas Commun*, vol. 31, no. 2, pp. 160–171, 2013.

[101] N. Jindal and A. Goldsmith, "Dirty -paper coding versus TDMA fpr <O<P brpadcast channels," *IEEE Trans. Inf. Theory*, vol. 51, no. 5, pp. 1783–1794, 2005.

[102] Y. Taesng and A. Goldsmith, "On the optimality of multiantenna broadcast scheduling using zero forcing beamforming," *IEEE J. Sel. Areas Commun*, vol. 24, no. 3, pp. 528–541, 2006.

[103] T. Yoo and A. Goldsmith, "Capacity and power allocation for fading MIMO channels with channel estimation error," *IEEE Trans. Inf. Theory*, vol. 52, no. 5, pp. 2203–2214, 2006.

[104] P. Layec, P. Piantanida, R Visoz, and A. O. Bertheh, “Capacity bounds for MIMO multiple access channel with imperfect channel state information,” in *in prc. IEEE ITW*, 2008, pp. 21–25.

[105] L. Musavian, M. R. Nakhai, M. Dohler, and A. H. Aglvami, “Effect of channel uncertainty on the mutual information of MIMO fading channels,” *ieee trans. Veh. Tech*, vol. 56, no. 5, pp. 2798–2806, 2007.

[106] X. Li, Q. Gao, and R. M. M, “Capacit bounds and low complexity transceiver design for double scattering MIMO multiple access channels,” *IEEE Trans. Signal Process*, vol. 58, no. 5, pp. 2809–2822, 2010.

[107] E. Bjӧrnson, E. G. Larsson, and M. Debbah, “Massive MIMO for Maximal Spectral Efficiency: How Many Users and Pilots Should Be Allocated?,” *IEEE Trans. Wirel. Commun.*, vol. 15, no. 2, pp. 1293–1308, 2016.

[108] A. Alshammari, S. Albdran, and M. A. Matin, “Optimal Capacity and Energy Efficiency of Massive MIMO Systems,” *Intenational J. Comput. Scince Inf. Secur.*, vol. 15, no. 6, 2017.

Appendix A

(List of Publication)

Journals

1. A. Alshammari, S. Albdran and M. Matin, " Optimal Capacity and Energy Efficiency of Massive MIMO Systems" *Intenational Journal of Computer Scince and information security.* vol. 15, no. 6. 2017.
2. S. Albdran, A. Alshammari and M. Matin, " On The Channel Estimation and Spectral Efficincey of Massive MIMO Systems". *Intenational Journal of Computer Scince and information security.* vol. 15, no. 6. 2017.

Conference proceedings

1. A. Alshammari, S. Albdran and M. Matin, "The Effect of Channel Spatial Correlation on Capacity and Energy Efficiency of Massive MIMO Systems," in *The 7th IEEE annual Comuting and Communication Workshop and Conferernce*, 2017.
2. A. Alshammari, S. Albdran, M. A. R. Ahad, and M. Matin, "Impact of Angular Spread on Massive MIMO Channel Estimation," in *The 19th IEEE International Conference on Computer and Information Technology (ICCIT)*, 2016.
3. A. Alshammari, S. Albdran and M. Matin, "Channel Capacity of Next Generation Large Scale MIMO Systems," *in Proc. SPIE 9970, Optics and Photonics for Information Processing X,* 99701F. September 2016.

4. S. Albdran, A. Alshammari and M. Matin, “Spectral and Energy Efficiency for Massive MIMO Systems Using Exponential Correlation Model,” in *The 7th IEEE annual Comuting and Communication Workshop and Conferernce*, 2017.
5. S. Albdran , A. Alshammari, M. A. R. Ahad, and M. Matin, “Effect of Exponential Correlation Model on Channel Estimation of Massive MIMO,” in *The 19th IEEE International Conference on Computer and Information Technology (ICCIT)*, 2016.
6. S. Albdran, A. Alshammari and M. Matin, “Uplink Channel Estimation Error for Large Scale MIMO System,” *in Proc. Proc. SPIE 9970, Optics and Photonics for Information Processing X,* 99701J. September 2016.

Appendix B

(Conference Proceedings)

The Effect of Channel Spatial Correlation on Capacity and Energy Efficiency of Massive MIMO Systems

Ahmed Alshammari,*Student Member, IEEE*, Saleh Albdran, *Student Member, IEEE*, and Mohammad Matin, *Senior Member, IEEE*
Department of Electrical Engineering, Daniel Felix Ritchie School of Engineering & Computer Science
University of Denver
Ahmad0046@yahoo.com

***Abstract*— Massive MIMO is an emerging technology that has the potential of bringing huge improvements to wireless communications in the future. This paper investigates the effects of spatial correlation on the capacity and energy efficiency of massive MIMO. We use a channel covariance matrix that is generated according to the one ring model. We consider linear minimum mean square error (LMMSE) for estimating channel properties with pilot signals. The impact of channels spatial correlation on the capacity and energy efficiency of the massive MIMO model used in this paper are demonstrated using computer simulation. We show that the capacity and energy efficacy improve as the correlation between the channels is reduced.**

Index Terms*— *Massive MIMO, Channel Estimation, Capacity, Energy efficiency Angular Spread, LMMSE

I. INTRODUCTION

The amount of data delivered over wireless networks has increased considerably during the recent years [1]. This growth in data exchange is going to continue in the future driven by new technologies such as augmented reality and device to device communications [2], [3]. This will represent a major challenge because the amount of available spectrum is limited and it will never increase [4]. Future wireless communications systems must be efficient in exploiting these resources. Hence, new technologies should substantially increase the transmission capacity without requiring additional bandwidth or consuming more energy.

Massive MIMO is a promising new technology that can help overcome the future challenges and meet the expected demand for higher data rates [5]. The idea of scaling up MIMO is relatively new [6]. This technology will play an important role of increasing the spectral efficiency of wireless communications. It is going to be an order of magnitude scale up of multi user MIMO technology. The concept of massive MIMO is illustrated in Fig. 1 where the base station (BS) that has a large number of antennas communicate with terminals equipped with single antenna each [2]. With the help of the huge antenna array, transmit beamforming focus the downlink signal at a certain terminal. As the number of antennas is increased, the accuracy of this focus improves [2]. Hence, the main feature of massive MIMO is that every user should only get the signal that is intended for him with the least interference possible from other terminals [7].

Exploiting time division duplex (TDD) scheme, Uplink and downlink transmission of Massive MIMO happen on same frequency but at different times [8]. Massive MIMO takes advantage of channel reciprocity which means channel state information (CSI) is the same for the uplink and the downlink. Therefore, the CSI estimated on the uplink is used to combine the received single on the uplink and also to beamform downlink data [9].

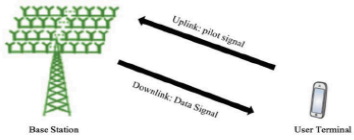

Fig.1. Massive MIMO base station (BS) equipped with hundreds of antennas while only one antenna is used in the user terminal.

Massive MIMO will send information only on the direction of the intended user. Therefore, transmit beamforming requires a good knowledge of the channel at the base station. Also, accurate CSI leads to reducing the bit error rate (BER) that result in enhanced spectral efficiency [10]. There are various channel estimation methods that can be used to obtain a good CSI. The most popular methods used for channel estimation use pilot signal. The quality of the estimated channel are affected by the environment and the channels spatial correlation (SC) [10]. The SC depends on the scattering objects that are present in the propagation environment and the antennas configuration.

Notations: $\mathbf{x}$, $\mathbf{X}$ denote column vectors and matrices respectively. $\mathbf{X}^{T}$ denote transpose, $\mathbf{X}^{H}$ denote conjugate transpose and $\mathbf{X}^{*}$ indicate. Trace of matrix $\mathbf{X}$ is indicated as $\mathrm{tr}(\mathbf{X})$. $\mathbf{x}\sim\mathcal{CN}(\bar{\mathbf{x}},\mathbf{R})$ is circular symmetric complex Gaussian vector where the mean and covariance matrix are $\bar{\mathbf{x}}$ and $\mathbf{R}$ respectively.

978-1-5090-4228-9/17/$31.00 ©2017 IEEE

II. System And Channel Model

In this paper, we study the impact of spatial correlation on the capacity and energy efficacy of a single link under the effect of a random interference conditions. The base station (BS) in this link contain N-antennas whereas the terminals only have a single antenna each. The key principle in this study is that we can increase the quantity of antennas N in the base station to a very large number. We consider a TDD scheme that uses the same flat fading subcarrier when switching the transmission between the uplink and the downlink. This makes the process of channel estimation more efficient [11]. This is because the estimation accuracy and the amount of the overhead required in the uplink are independent of the number of antennas [12], [9]. Channel reciprocity of the TDD protocol is illustrated in Fig.2 where the estimated channel is used for detecting the uplink data and then to transmit data on the downlink.

We assume that the channel is fixed during a coherence period T_{coher} with channel realizations that are random and independent between fading blocks. We are considering the TDD mode in Fig. 2 that was used in many sources such as [13], [14]. Every block starts with uplink pilots, followed by uplink data. After that, the system switches to the downlink which begins with downlink pilot that enable the terminals of estimating their channels and the existing interference conditions. The downlink signaling does not scale with the number of antenna N because their numbers are scalar regardless of N. The downlink data transmission concludes the coherence period for T_{Data}^{DL} uses of the channel. The following equation is valid for the TDD protocol $T_{\text{pilot}}^{\text{UL}} + T_{data}^{UL} + T_{pilot}^{DL} + T_{Data}^{DL} = T_{coher}$.

We model the random channel $\mathbf{h} \in \mathbb{C}^{N\times 1}$ between the base station and the terminal as an ergodic random process that has a constant independent realization for every coherence time $\mathbf{h} \sim \mathcal{CN}(\mathbf{0}, \mathbf{R})$. The covariance matrix is denoted as $\mathbf{R} = \mathbb{E}\{\mathbf{hh}^{\boldsymbol{H}}\} \in \mathbb{C}^{N\times N}$. We assume that the spectral norm of the covariance matrix $\mathbf{R}$ is uniformly bounded.

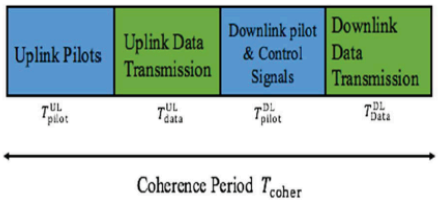

Fig. 2. Illustration of TDD protocol where the coherence time is divided between uplink/downlink pilot and data transmissions.

A. Downlink/Uplink channel model

The task of the downlink channel is transmitting data and estimating channels based on pilots. The received downlink signal $z \in \mathbb{C}$ for multiple input single outputs flat fading channel is modeled as

$$z = \mathbf{h}^{\boldsymbol{T}}\mathbf{d} + v \tag{1}$$

where $\mathbf{d} \in \mathbb{C}^{N\times 1}$ can be a training sequence to estimate the channel or a random data signal with zero mean. The covariance matric is indicated as $\mathbf{X} = \mathbb{E}\{\mathbf{dd}^{\boldsymbol{H}}\}$ and $p^{\text{BS}} = \text{tr}(\mathbf{X})$ is the average power. $\mathbf{X}$ is a parameter that depends on the realization of the channel $\mathbf{h}$. Hence, $\mathbf{X}$ remains constant for every coherence time but changes after that because the channel realization changes. The v term in (2) is a random process that contains the noise of the receiver $v_{noise} \sim \mathcal{CN}(0, {\sigma_{\text{UE}}}^2)$ and interference from other terminals $v_{\boldsymbol{interf}}$ which is independent of the data signal and has zero mean.

$$v = v_{\boldsymbol{noise}} + v_{\boldsymbol{interf}} \tag{2}$$

The uplink channel is used to send training sequences for channel estimation and to transmit data; see Fig. 1. The system model that we consider in the uplink with a received signal $\mathbf{y} \in \mathbb{C}^N$ at the base station is

$$\mathbf{y} = \mathbf{h}s + \mathbf{n} \tag{3}$$

where $s \in \mathbb{C}$ can be a random data signal or a training signal to estimate the channel. The average power of that signal is $p^{UE} = \mathbb{E}\{|s|^2\}$. The term $\mathbf{n} \in \mathbb{C}^{N\times 1}$ in (4) consists of the receiver noise $\mathbf{n}_{\boldsymbol{noise}}$ and interference of the transmission from other terminals. The interference depends on the channel realization but does not depend on s.

$$\mathbf{n} = \mathbf{n}_{\boldsymbol{noise}} + \mathbf{n}_{\boldsymbol{interf}} \tag{4}$$

B. One ring model

We consider the one ring model from [15] to investigate the impact of spatial correlation on the capacity and energy efficacy of massive MIMO. The model assumes that the terminal is surrounded by a ring of scattering objects with radius r as shown in Fig. 3. However, no scattering objects is around the base station according to the one ring model. It also assumes that the terminal is located at distance d and has an azimuth angle θ with the base station. The angular spread of the multipath components is denoted as Δ. The channel covariance matrix $\mathbf{R}$ for the antennas $1 \le n, p \le N$ is given in (5) [16].

$$[\mathbf{R}]_{n,p} = \frac{\mathbf{1}}{\mathbf{2\Delta}} \int_{-\Delta}^{\Delta} e^{jk^T(\alpha+\theta)(u_n - u_p)}\, d\alpha \tag{5}$$

where

$$k(\alpha) = -\frac{2\pi}{\lambda}(\cos(\alpha), \sin(\alpha))^{\text{T}}$$

u_n, u_p denote the position vectors of the BS

The antenna spacing is assumed to be half the wavelength with a uniform linear array (ULA). The channel covariance matrix is given in its Toeplitz form in (6).

$$[\mathbf{R}]_{n,p} = \frac{1}{2\Delta}\int_{-\Delta+\theta}^{\Delta+\theta} e^{-j2\pi D(n-p)sin(\alpha)}\, d\alpha \qquad (6)$$

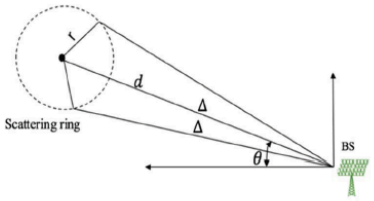

Fig. 3. A terminal at distance d from the base station that is surrounded by a ring of a scattering objects.

III. Uplink Channel Estimation

The channel state information $\mathbf{h}$ is estimated on the uplink by comparing an already known uplink training sequence s with the received uplink signal $\mathbf{y}$ in (3). We are considering Rayleigh fading channel which is affected by independent complex Gaussian noise [17]. The channel $\mathbf{h}$ is estimated at the base station using linear minimum mean square error estimator (LMMSE) from the received uplink signal in (3).

$$\hat{\mathbf{h}} = s^{*}\mathbf{R}\bar{\mathbf{Y}}^{-1}\mathbf{y} \qquad (7)$$

where $\mathbf{R}$ indicates the covariance matrix and $\bar{\mathbf{y}}$ is given in (8)

$$\bar{\mathbf{Y}} = \mathbb{E}\{\mathbf{y}\mathbf{y}^{H}\} = p^{UE}\boldsymbol{R} + \boldsymbol{S}+\sigma_{BS}{}^{2}\mathbf{I} \qquad (8)$$

The MSE is

$$\mathrm{MSE} = \mathrm{tr}(\mathbf{G}) = \mathbb{E}\left\|\hat{\mathbf{h}} - \mathbf{h}\right\|_{2}^{2} \qquad (9)$$

$$\mathbf{G} = \mathbb{E}\{(\hat{\mathbf{h}} - \mathbf{h})\left(\hat{\mathbf{h}} - \mathbf{h}\right)^{H}\} = \mathbf{R} - p^{UE}\mathbf{R}\bar{\mathbf{Y}}^{-1}\mathbf{R} \qquad (10)$$

where $\mathbf{G}$ indicate the error covariance matrix. The channels consists of the LMMSE estimate in (7) pulse an unknown estimation error.

$$\mathbf{h} = \hat{\mathbf{h}} + \boldsymbol{\epsilon} \qquad (11)$$

where $\boldsymbol{\epsilon} \in \mathbb{C}^{N\times 1}$ indicate the estimation error.

IV. DL/UL Data Transmission

We now analyze the channel capacity of the downlink in (1) and the uplink in (3). The analysis is based on having an imperfect pilot estimated channel as we discussed in the previous section. Therefore, the capacity depends on the CSI acquired using the LMMSE estimator. We are considering the channel capacities (in bit/channel use) of the downlink in (1) and the uplink in (3) for a random knowledge of CSI at the base station (BS) and the user equipment (UE). In every coherence period، the base station is assumed to have a random knowledge $\mathcal{H}^{\mathrm{BS}}$ of the channel $\mathcal{H}$. The base station uses this knowledge to choose the conditional distribution of the transmitted signal $\mathbf{d}$ $f = (\mathbf{d}|\mathcal{H}^{\mathrm{BS}})$. Also, UE has a different random knowledge of the channel $\widetilde{\mathcal{H}}^{UE}$. Therefore, the downlink capacity is

$$\mathrm{C}^{\mathrm{DL}} = \frac{\tau_{\mathrm{data}}^{\mathrm{DL}}}{T_{\mathrm{coher}}}\mathbb{E}\left\{\max_{f=(\mathbf{d}|\mathcal{H}^{\mathrm{BS}}):\,\mathbb{E}\|\mathbf{d}\|_{2}^{2}\,\le\,p^{\mathrm{BS}}} \mathfrak{I}\left(\mathbf{d};z|\mathcal{H},\mathcal{H}^{\mathrm{BS}},\widetilde{\mathcal{H}}^{\mathrm{UE}}\right)\right\} \qquad (12)$$

where $\mathfrak{I}(\mathbf{d};z|\mathcal{H},\mathcal{H}^{\mathrm{BS}},\widetilde{\mathcal{H}}^{\mathrm{UE}})$ indicates the mutual information between the received signal z and the transmitted signal $\mathbf{d}$. Also the capacity of the uplink system in (3) is

$$\mathrm{C}^{\mathrm{UL}} = \frac{\tau_{\mathrm{data}}^{\mathrm{UL}}}{T_{\mathrm{coher}}}\mathbb{E}\left\{\max_{f=(s|\mathcal{H}^{\mathrm{UE}}):\,\mathbb{E}\{\|s\|_{2}^{2}\}\,\le\,p^{\mathrm{BS}}} \mathfrak{I}\left(\mathbf{d};\mathbf{y}|\mathcal{H},\mathcal{H}^{\mathrm{BS}},\widetilde{\mathcal{H}}^{\mathrm{UE}}\right)\right\} \qquad (13)$$

where $\mathfrak{I}(\mathbf{d};\mathbf{y}|\mathcal{H},\mathcal{H}^{\mathrm{BS}},\widetilde{\mathcal{H}}^{\mathrm{UE}})$ is also the mutual information between the received signal $\mathbf{y}$ and the transmitted signal s. The joint distribution of $\mathcal{H},\mathcal{H}^{\mathrm{BS}},\widetilde{\mathcal{H}}^{\mathrm{UE}}$ is used to find the expectation in (13). Note also that $\frac{\tau_{\mathrm{data}}^{\mathrm{DL}}}{T_{\mathrm{coher}}}$ and $\frac{\tau_{\mathrm{data}}^{\mathrm{UL}}}{T_{\mathrm{coher}}}$ denote the fraction of channel uses given for downlink and uplink data transmissions.

Assuming that $\widetilde{\mathcal{H}}^{UE}$ and $\widetilde{\mathcal{H}}^{BS}$ are the channel estimated at the receiver for the DL/UL respectively. These estimates are not identical to the actual $\mathcal{H}^{\mathrm{BS}}$ and $\mathcal{H}^{\mathrm{UE}}$. The capacities in (12) and (21) become

$$\mathrm{C}^{\mathrm{DL}} = \frac{\tau_{\mathrm{data}}^{\mathrm{DL}}}{T_{\mathrm{coher}}}\mathbb{E}\left\{\log_{2}(1+\mathrm{SINR}^{\mathrm{DL}}(\mathbf{x}^{\mathrm{DL}}))\right\} \qquad (14)$$

$$\mathrm{C}^{\mathrm{UL}} = \frac{\tau_{\mathrm{data}}^{\mathrm{UL}}}{T_{\mathrm{coher}}}\mathbb{E}\left\{\log_{2}(1+\mathrm{SINR}^{\mathrm{UL}}(\mathbf{x}^{\mathrm{UL}}))\right\} \qquad (15)$$

where $\mathbf{x}^{\mathrm{DL}} = [u_1^{\mathrm{DL}} \dots u_k^{\mathrm{DL}}]^{T}$ and $\mathbf{x}^{\mathrm{UL}} = [u_1^{\mathrm{UL}} \dots u_k^{\mathrm{UL}}]^{T}$ indicate the beamformig and receive combining vectors that are both a function of $\hat{\mathbf{h}}$ and have a unit norms respectively. The SINR for the downlink and the uplink are given in (16) and (17) respectively.

$$\mathrm{SINR}^{\mathrm{DL}}(\mathbf{x}^{\mathrm{DL}}) = \frac{\left|\mathbb{E}\{\mathbf{h}^{H}\mathbf{x}^{\mathrm{DL}}|\widetilde{\mathcal{H}}^{\mathrm{UE}}\}\right|^{2}}{\mathbb{E}\left\{\left|\mathbf{h}^{H}\mathbf{x}^{\mathrm{DL}}\right|^{2}\middle|\widetilde{\mathcal{H}}^{\mathrm{UE}}\right\}-\left|\mathbb{E}\{\mathbf{h}^{H}\mathbf{x}^{\mathrm{DL}}|\widetilde{\mathcal{H}}^{UE}\}\right|^{2}+\frac{\mathbb{E}\{I_{\mathcal{H}}^{\mathrm{UE}}|\widetilde{\mathcal{H}}^{UE}\}}{p^{\mathrm{BS}}}+\frac{\sigma_{\mathrm{UE}}^{2}}{p^{\mathrm{BS}}}} \qquad (16)$$

$$\mathrm{SINR}^{\mathrm{UL}}(\mathbf{x}^{\mathrm{UL}}) = \frac{\left|\mathbb{E}\{\mathbf{h}^{H}\mathbf{x}^{\mathrm{UL}}|\widetilde{\mathcal{H}}^{\mathrm{BS}}\}\right|^{2}}{\mathbb{E}\left\{\left|\mathbf{h}^{H}\mathbf{x}^{\mathrm{UL}}\right|^{2}\middle|\widetilde{\mathcal{H}}^{\mathrm{BS}}\right\}-\left|\mathbb{E}\{\mathbf{h}^{H}\mathbf{x}^{\mathrm{UL}}|\widetilde{\mathcal{H}}^{BS}\}\right|^{2}+\frac{\mathbb{E}\{(\mathbf{x}^{\mathrm{UL}})^{H}(\mathrm{Q}_{\mathcal{H}}+\sigma_{\mathrm{BS}}^{2}\mathrm{I})\mathbf{x}^{\mathrm{UL}}|\widetilde{\mathcal{H}}^{\mathrm{BS}}\}}{p^{\mathrm{UE}}}} \qquad (17)$$

Capacities on (14) and (15) can be calculated numerically for any downlink beamforming vector and any uplink receive combining vector for the estimated channel $\hat{\mathbf{h}}$.

A. Numerical Results

In this section we illustrate the effect of channel spatial correlation on the capacity of massive MIMO. The average SNRs we consider for the downlink and the uplink are defined

as $p^{\mathrm{BS}}\frac{\mathrm{tr}(\mathbf{R})}{N\sigma^2{}_{\mathrm{UE}}}$ and $p^{\mathrm{UE}}\frac{\mathrm{tr}(\mathbf{R})}{N\sigma^2{}_{\mathrm{BS}}}$ respectively. We vary the angular spread and the number of antennas, while we fix the SNR values. In order to make the downlink and uplink capacities identical and we fix the ratio of the downlink and uplink data $\frac{\tau_{\mathrm{data}}^{\mathrm{DL}}}{T_{\mathrm{coher}}} = \frac{\tau_{\mathrm{data}}^{\mathrm{UL}}}{T_{\mathrm{coher}}} = 0.45$.

Fig 4. considers spatially correlated scenario for three different numbers of antennas: 50,100 and 300 where SNR is fixed at 0 dB. Simulation results shows the capacity as a function of angular spread of the one ring model for the three cased. The capacity grows as the angular spread is increased. This means that the least correlated channels give the best performance while the lowest performance happens with the strongly correlated channels. The figure also shows that capacity grows as we add more antennas to the base station. Fig. 5. is similar to Fig. 4 but with different SNR value. The overall capacity is increased for all the antennas as a result of increasing the SNR to 25 dB. Also, the capacity is more sensitive to changes in the spatial correlation between the channels.

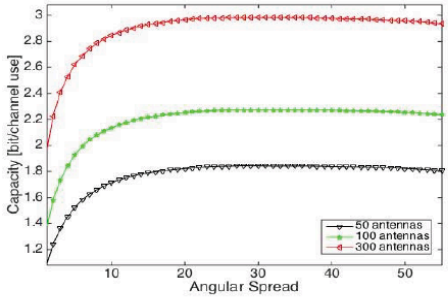

Fig. 4. Channel capacity as a function of the angular spread for different number of antennas SNR:0 dB.

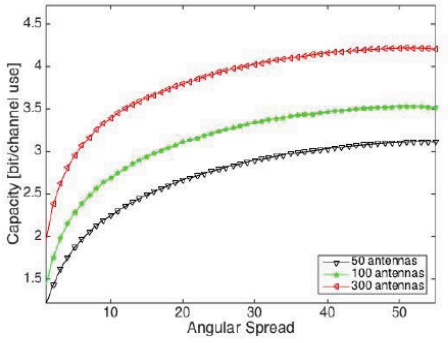

Fig. 5. Channel capacity as a function of the angular spread for different number of antennas SNR:25 dB.

V. Energy Efficiency

Energy efficiency (EE) of massive MIMO is considered in this section. The energy efficiency can be found by taking the ratio capacity (bit/channel use) and the transmitted power which is measured in (joule/channel use). Thus, the measurement unit of EE is bit/Joule. With the TDD mode, the energy used by the amplifiers in the transmitters in every coherence time is

$$E_{\mathrm{amp}} = \left(\tau_{\mathrm{pilot}}^{\mathrm{DL}} + \tau_{\mathrm{data}}^{\mathrm{DL}}\right)\frac{p^{\mathrm{BS}}}{\omega^{\mathrm{BS}}} + \left(\tau_{\mathrm{pilot}}^{\mathrm{UL}} + \tau_{\mathrm{data}}^{\mathrm{UL}}\right)\frac{p^{UE}}{\omega^{\mathrm{UE}}} \tag{18}$$

where $\omega^{\mathrm{BS}}, \omega^{\mathrm{UE}}$ denote the efficiency of the amplifiers at the base station and the user equipment respectively. The average power (Joule/channel use) is given as

$$\frac{E_{\mathrm{amp}}}{T_{\mathrm{coher}}} = \underbrace{\alpha_{\mathrm{DL}}\left(\frac{\tau_{\mathrm{pilot}}^{\mathrm{DL}}}{T_{\mathrm{coher}}}\frac{p^{\mathrm{BS}}}{\omega^{\mathrm{BS}}} + \frac{\tau_{\mathrm{pilot}}^{\mathrm{UL}}}{T_{\mathrm{coher}}}\frac{p^{\mathrm{UE}}}{\omega^{\mathrm{UE}}}\right) + \frac{\tau_{\mathrm{data}}^{\mathrm{DL}}}{T_{\mathrm{coher}}}\frac{p^{\mathrm{BS}}}{\omega^{\mathrm{BS}}}}_{\text{DL power}}$$

$$+ \underbrace{\alpha_{\mathrm{UL}}\left(\frac{\tau_{\mathrm{pilot}}^{\mathrm{DL}}}{T_{\mathrm{coher}}}\frac{p^{\mathrm{BS}}}{\omega^{\mathrm{BS}}} + \frac{\tau_{\mathrm{pilot}}^{\mathrm{UL}}}{T_{\mathrm{coher}}}\frac{p^{\mathrm{UE}}}{\omega^{\mathrm{UE}}}\right) + \frac{\tau_{\mathrm{data}}^{\mathrm{UL}}}{T_{\mathrm{coher}}}\frac{p^{\mathrm{UE}}}{\omega^{\mathrm{UE}}}}_{\text{UL power}} \tag{19}$$

where α_{DL} and α_{UL} are the ratios of the downlink and the uplink transmission respectively

$$\alpha_{\mathrm{DL}} = \frac{\tau_{\mathrm{data}}^{\mathrm{DL}}}{\tau_{\mathrm{data}}^{\mathrm{DL}} + \tau_{\mathrm{data}}^{\mathrm{UL}}} \tag{20}$$

$$\alpha_{\mathrm{UL}} = \frac{\tau_{\mathrm{data}}^{\mathrm{UL}}}{\tau_{\mathrm{data}}^{\mathrm{DL}} + \tau_{\mathrm{data}}^{\mathrm{UL}}} \tag{21}$$

The EE (in bit/Joule) of massive MIMO system is defined as the following.

$$\mathrm{EE}^{\mathrm{DL}} = \frac{\mathrm{C}^{\mathrm{DL}}}{\alpha_{\mathrm{DL}}\left(\frac{\tau_{\mathrm{pilot}}^{\mathrm{DL}}}{T_{\mathrm{coher}}}\frac{p^{\mathrm{BS}}}{\omega^{\mathrm{BS}}} + \frac{\tau_{\mathrm{pilot}}^{\mathrm{UL}}}{T_{\mathrm{coher}}}\frac{p^{\mathrm{UE}}}{\omega^{\mathrm{UE}}} + N\rho + \zeta\right) + \frac{\tau_{\mathrm{data}}^{\mathrm{DL}}}{T_{\mathrm{coher}}}\frac{p^{\mathrm{BS}}}{\omega^{\mathrm{BS}}}} \tag{22}$$

$$\mathrm{EE}^{\mathrm{DL}} = \frac{\mathrm{C}^{\mathrm{UL}}}{\alpha_{\mathrm{UL}}\left(\frac{\tau_{\mathrm{pilot}}^{\mathrm{DL}}}{T_{\mathrm{coher}}}\frac{p^{\mathrm{BS}}}{\omega^{\mathrm{BS}}} + \frac{\tau_{\mathrm{pilot}}^{\mathrm{UL}}}{T_{\mathrm{coher}}}\frac{p^{\mathrm{UE}}}{\omega^{\mathrm{UE}}} + N\rho + \zeta\right) + \frac{\tau_{\mathrm{data}}^{\mathrm{UL}}}{T_{\mathrm{coher}}}\frac{p^{\mathrm{UE}}}{\omega^{\mathrm{UE}}}} \tag{23}$$

where $N\rho + \zeta$ denote the baseband circuit power consumption.

A. Numerical Results

Now, we illustrate how EE behave depending on the number of antenna, spatial correlation, transmit power. We setup: $\rho + \zeta = 0.02\frac{\mu\mathrm{J}}{\text{Channel use}}$ which represent the power consumed by the circuit if only one antenna is used. However, the circuit power for any number of antennas N is $N\rho + \zeta$. Therefore, we use splitting between ρ and ζ: $\frac{\rho}{\rho+\zeta} = 0$. We also set the amplifiers efficiencies to $\omega^{\mathrm{BS}} = \omega^{\mathrm{UE}} = 0.3$. The covariance matrix of the channel is generated using the one ring

model in (6) with angel spread that varies between 10 to 50. In order to make the EE of the downlink and the uplink equal, we let $\alpha_{\mathrm{DL}} = \alpha_{\mathrm{UL}} = 0.5$ and $\frac{\tau_{\mathrm{data}}^{\mathrm{UL}}}{T_{\mathrm{coher}}} = \frac{\tau_{\mathrm{data}}^{\mathrm{DL}}}{T_{\mathrm{coher}}} = 0.05$.

Fig. 6 shows EE of the downlink and the uplink for three different number of antennas using the capacities in (12) and (13). EE increase as the number of antennas goes up. Hence, EE is very important feature of massive MIMO. The figure also shows that the performance improves as the angular spread is increased. Thus, EE improves as the correlation between the channels is decreased.

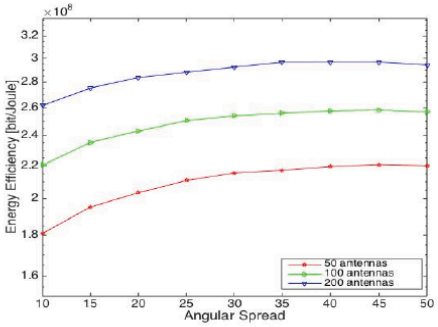

Fig. 6. Achievable energy efficiency as function of the angular spread for three different scenarios N (50, 100, 200) and a fixed SNR: 20 dB.

Fig. 7 shows the power allocations that corresponded to the curves in Figure. 6. Although higher number of antennas N is more energy efficient, more transmit power is required as the number of antennas is increased. The transmit power grows as the correlation between the channels is decreased.

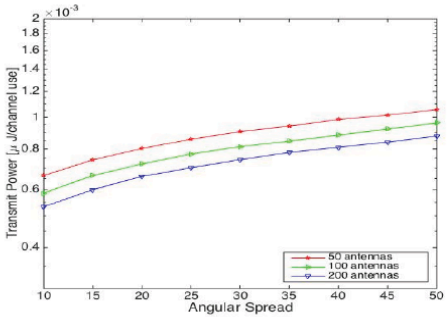

Fig. 7. The corresponding transmit power of the curves in Fig. 6.

VI. Conclusion

This paper studied the impact of channel spatial correlation on the capacity and energy efficacy of massive MIMO. The study was founded on a system model which considers spatial correlation between the channels. We showed that the performance of the enormous antenna array gain of massive MIMO systems might vary depending on the degree of channel correlation. Simulation results show that the capacity and energy efficiency can be limited by the channel correlation matrix that was generated using the one ring model. We showed that higher levels of channel spatial correlation results in a degradation in capacity and energy efficiency of massive MIMO systems.

References

[1] T. L. Marzetta, "Massive MIMO: An Introduction," *Bell Labs Tech. J.*, vol. 20, pp. 11–22, 2015.

[2] E. Bjornson, E. G. Larsson, and T. L. Marzetta, "Massive MIMO: ten myths and one critical question," *IEEE Commun. Mag.*, vol. 54, no. 2, pp. 114–123, 2016.

[3] J. G. Andrews *et al.*, "What Will 5G Be?," *IEEE J. Sel. Areas. Commun*, vol. 32, no. 6, pp. 1065–1082, 2014.

[4] A. Alshammari, S. Albdran, M. A. R. Ahad, and M. Matin, "Impact of Angular Spread on Massive MIMO Channel Estimation," in *The 19th International Conference on Computer and Information Technology (ICCIT)*, In Press, 2016.

[5] L. Lu, G. Y. Li, A. Ashikhmin, R. Zhangand, and A. L. Swindlehurst, "An Overview of Massive MIMO : Benefits and Challenges," *IEEE J. Sel. Top. Signal Process.*, vol. 8, no. 5, pp. 742–758, 2014.

[6] T. L. Marzetta, "Noncooperative Cellular Wireless with Unlimited Numbers of Base Station Antennas," vol. 9, no. 11, pp. 3590–3600, 2010.

[7] S. Albdran, A. Alshammari, M. Ahad, and M. Matin, "Effect of Exponential Correlation Model on Channel Estimation fo Massive MIMO," in *The 19th International Conference on Computer and Information Technology (ICCIT)*, In Press, 2016.

[8] E. G. Larsson, O. Edfors, F. Tufvesson, and T. L. Marzetta, "Massive MIMO for Next Generation Wireless Systems," no. February, pp. 1–19, 2013.

[9] M. Agiwal, A. Roy, and N. Saxena, "Next Generation 5G Wireless Networks : A Comprehensive Survey," vol. 18, no. 3, pp. 1617–1655, 2016.

[10] X. Liu, M. E. Bialkowski, and F. Wang, "Investigations into the Effect of Spatial Correlation on Channel Estimation and Capacity of Multiple Input Multiple Output System," *Int'l J. Commun. Netw. Syst. Sci.*, vol. 2, no. 4, pp. 267–275, 2009.

[11] S. Biswas, J. Xue, F. A. Khan, and Tharmalingam Rantnarajah, "Performance Analysis of Correlated Massive MIMO Systems With Spatially Distributed Users," *IEEE Syst. J.*, vol. PP, no. 99, pp. 1–12.

[12] R. C. De Lamare, "Massive MIMO Systems : Signal Processing Challenges and Research Trends," pp. 1–9.

[13] G. Caire, N. Jindal, M. Kobayashi, and N. Ravindran, "Multiuser MIMO achievable rates with downlink training and channel state feedback," *IEEE Trans. Inf. Theory*, vol. 56, no. 6, pp. 2845–2866, 2010.

[14] E. Björnson, M. Kountouris, M. Bengtsson, and B. Ottersten, "Receive combining vs. multi-stream multiplexing in downlink systems with multi-antenna users," *IEEE Trans. Signal Process*, vol. 61, no. 13, pp. 3431–3446, 2013.

[15] A. Adhikary, J. Nam, J. Y. Ahn, and G. Caire, "Joint Spatial Division and Multiplexing—The Large-Scale Array Regime," *IEEE Trans. Inf. Theory*, vol. 59, no. 10, pp. 6441–6463, 2013.

[16] J. Gong, J. F. Hayes, and M. R. Soleymani, "The effect of antenna physics on fading correlation and the capacity of multielement antenna systems," *IEEE Trans. Veh. Technol.*, vol. 56, no. 4 I, pp. 1591–1599, 2000.

[17] T. L.Marzetta, "How much training is required formultiuserMIMO?," in *ACSSC 40th Asilomar Conference on Signals, Systems and Computers.*, 2006, pp. 359–363.

Impact of Angular Spread on Massive MIMO Channel Estimation

Ahmed Alshammari[1], Saleh Albdran[1], Md. Atiqur Rahman Ahad[2] and Mohammad Matin[1], *Senior Member, IEEE*
[1]Department of Electrical Engineering ,University of Denver
[2]Department of Electrical and Electronic Engineering, University of Dhaka

***Abstract*— large scale antenna arrays technology has the potential of bringing many advantages to future wireless systems. Energy and spectral efficiency are going to be the most important features. Hence, accurate estimate of channel state information (CSI) makes these advantages achievable. This paper investigates the effects of angular spread on the accuracy of channel estimation for massive multiple input multiple output (MIMO) wireless communication systems. The model we consider consists of user equipment (UE) and a base station with large antenna array. Linear minimum mean square error (LMMSE) is used to estimate the uplink channel of a massive MIMO system using a pilot signal. It is shown that higher spatial correlation (SC) positively affects the accuracy of channel estimation when the signal to noise ratio is kept constant.**

Keywords—Massive MIMO, channel estimation, channel state information, angular spread, LMMSE.

I. INTRODUCTION

The quantity of electromagnetic spectrum is always going to be same, but the demand for wireless throughput will always be growing [1], [2], [3]. Therefore, new technologies are always emerging. Massive multiple input multiple output (MIMO) is a new promising network architecture that recently has been proposed [4]. It has a great potential of increasing spectral and energy efficiency in order to meet the growing demand for wireless services [5],[6]. Massive MIMO is considered to be a multiuser MIMO where each base station is equipped with a large number of antennas that communicate with a single antenna user equipments (UEs) [7], [8], [9].

Spectral efficiency can be limited by channel estimation accuracy [3],[10],[11]. Therefore, accurate estimate of the channel state information (CSI) is important for the base station (BS) and the user equipment (UE) to achieve the advantages of Massive MIMO[12], [13]. However, acquiring CSI in Massive MIMO is not an easy task because the overhead required to estimate the channel is overwhelming [1], [14]. In order to avoid this issue, time division duplexing (TDD) is used instead of Frequency Division duplexing (FDD). To exploit channel reciprocity in TDD mode, channels are only estimated for the uplink where all UEs synchronously send uplink data signals followed by pilot sequences [5], [15]. CSI is then estimated by the BS using these pilot sequences [16].

Propagation environment and spatial correlation (SC) vary according to antennas configuration and objects between the transmitter and the receiver which affect channel properties [17]. Most massive MIMO analysis in literature is based on the assumption that channels are independent [9]. This assumption is not practical in reality where we have large number of antennas at the BS. This paper investigates the relation between SC and channel estimation accuracy of massive MIMO systems. Due to its low complexity and near optimal performance, (LMMSE) estimator is used to obtain CSI.

The rest of the paper is organized as the following: Section II introduces the system model and illustrates the one ring model that is used to simulate the effect of SC. Section III describe the LMMSE uplink channel estimation. Numerical results are shown in section IV. Finally, section V concludes the paper.

Notation: Column vectors $\mathbf{x}$ and matrices $\mathbf{X}$ are represented by lower and upper case boldface respectively. $\mathbf{X}^{T}$, $\mathbf{X}^{H}$ and $\mathbf{X}^{*}$ indicate transpose, conjugate transpose and conjugate respectively. $\mathrm{tr}(\mathbf{X})$ is the trace of matrix $\mathbf{X}$. $\mathbf{x}\sim\mathcal{CN}(\bar{\mathbf{x}},\mathbf{R})$ denote circular symmetric complex Gaussian stochastic vector where $\bar{\mathbf{x}}$ and $\mathbf{R}$ are the mean and covariance matrix respectively. $\|\mathbf{x}\|_2$ indicate spectral norm.

II. SYSTEM AND CHANNEL MODEL

This paper investigates the accuracy of channel estimation for massive MIMO. We consider a single uplink established between one BS with array of N antennas and a single antenna UE. The attractive thing about UE with single antennas is that they are cheap, simple and consume less power while they still provide high throughput. Moreover, the assumption of single antenna UE can be considered as a special case of UE with multiple antennas when each antenna is treated as a separate autonomous user [9].

We assume a block fading structure which makes the channel between the base station and UEs $\mathbf{h} \in \mathbb{C}^{N\times 1}$ stay constant for a coherence period T_{coher}. $\mathbf{h}$ is considered to be ergodic process that has independent realization $\mathbf{h}\sim\mathcal{CN}(\mathbf{0},\mathbf{R})$. $\mathbf{R}=\mathbb{E}\{\mathbf{h}\mathbf{h}^{H}\}\in\mathbb{C}^{N\times N}$ is the covariance matrix. Regardless of the number of antennas, spectral norm of $\mathbf{R}$ is assumed to be uniformly bounded.

978-1-5090-4090-2/16/$31.00 ©2016 IEEE

ISBN 978-1-5090-4089-6

The received signal $\mathbf{y} \in \mathbb{C}^N$ at the BS is given by the following uplink system model

$$\mathbf{y} = \mathbf{h}s + \mathbf{n} \tag{1}$$

Where $s \in \mathbb{C}$ can either be known pilot signal to estimate channel or data signal. The average transmitted power is $p^{UE} = \mathbb{E}\{|s|^2\}$. $\mathbf{n} = \mathbf{n}_{noise} + \mathbf{n}_{interf} \in \mathbb{C}^{N\times 1}$ indicates an additive term which is composed of receiver noise $\mathbf{n}_{noise} \sim \mathcal{CN}(\mathbf{0}, {\sigma_{BS}}^2\mathbf{I})$ and the interference $\mathbf{n}_{interf}$ from other users. Interference varies depending on the channel realizations $\mathcal{H}$, but it is independent of s. Therefore, the covariance matrix $\mathrm{W} = \mathbb{E}\{\mathbf{n}_{noise}\mathbf{n}^H{}_{interf}\}$ for pilot transmission is assumed to have a zero mean. W is assumed to have a uniform bounded spectral norm $\|\mathrm{W}\|_2 = O(1)$.

We use the one ring model from [18] in order to explore the influence of SC on the channel estimation accuracy of massive MIMO. The one ring model is depicted in Fig. 1 where a ring of scattering objects of radius r is surrounding the UE while the BS station is not surrounded by anything. UE is located at distance d from the BS at azimuth angel θ. The multipath components arrive with angular spread (AS) Δ from the main angle of arrival. The channel coefficients of antennas $1 \le n, p \le N$ are correlated as illustrated in [19].

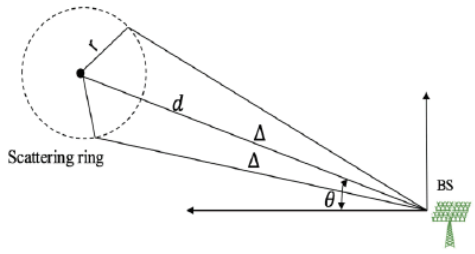

Fig. 1. UE located at distance d from BS with azimuth angel θ and AS Δ due to a ring of scatterers with radius r.

$$[\mathbf{R}]_{n,p} = \frac{1}{2\Delta}\int_{-\Delta}^{\Delta} e^{jk^T(\alpha+\theta)(u_n-u_p)}\, d\alpha \tag{2}$$

where

$$k(\alpha) = -\frac{2\pi}{\lambda}(\cos(\alpha), \sin(\alpha))^{\mathrm{T}}$$

u_n, u_p indicate the position vectors of the base station antennas in the two dimensional coordinate.

The BS in this model is assumed to have uniform linear array (ULA) with antenna spacing of half wavelength. The Toeplitz form of the covariance matrix for channel of a user at Angle of Arrival θ, and AS Δ has the form

$$[\mathbf{R}]_{n,p} = \frac{1}{2\Delta}\int_{-\Delta+\theta}^{\Delta+\theta} e^{-j2\pi D(n-p)sin(\alpha)}\, d\alpha \tag{3}$$

Where $n, p \in \{0, 1, \dots, N-1\}$

III. UPLINK CHANNEL ESTIMATION

Estimating the current CSI $\mathbf{h}$ is done by making a comparison between a known pilot signal s and the received UL signal $\mathbf{y}$ in (1). Rayleigh fading channels are the kind of channels considered in this paper. They are observed under the effect of independent complex Gaussian noise [20]. Linear minimum mean square error (LMMSE) estimator $\mathbf{h}$ is used to estimate $\mathbf{h}$ form the received signal $\mathbf{y}$ in (1).

$$\hat{\mathbf{h}} = s^*\mathbf{R}\bar{\mathbf{y}}^{-1}\mathbf{y} \tag{4}$$

Where $\mathbf{R}$ is the covariance matrix of $\mathbf{h}$ and the covariance matrix of $\mathbf{y}$ is

$$\bar{Y} = \mathbb{E}\{\mathbf{y}\mathbf{y}^H\} = p^{UE}\boldsymbol{R} + \boldsymbol{S} + {\sigma_{BS}}^2\mathbf{I} \tag{5}$$

Where $\boldsymbol{S}$ denotes interference

The mean squared error is $\mathrm{MSE} = \mathbb{E}\|\hat{\mathbf{h}} - \mathbf{h}\|_2^2 = \mathrm{tr}(\mathbf{G})$ and $\mathbf{G}$ is given by

$$\mathbf{G} = \mathbb{E}\{(\hat{\mathbf{h}} - \mathbf{h})(\hat{\mathbf{h}} - \mathbf{h})^H\} = \mathbf{R} - p^{UE}\mathbf{R}\bar{\mathbf{y}}^{-1}\mathbf{R} \tag{6}$$

The channel can be decomposed as $\mathbf{h} = \hat{\mathbf{h}} + \boldsymbol{\epsilon}$ where $\hat{\mathbf{h}}$ is the estimation in (4) and $\boldsymbol{\epsilon} \in \mathbb{C}^{N\times 1}$ indicate the estimation error. $\mathbb{E}\{\hat{\mathbf{h}}\mathbf{h}^H\} = \mathbf{R} - \mathbf{G}$ and $\mathbb{E}\{\boldsymbol{\epsilon}\boldsymbol{\epsilon}^H\} = \mathbf{G}$ are the covariance matrices where $\mathbf{G}$ is given in (6).

The length of the pilot signal can influence the accuracy of channel estimation [6]. The LMMSE estimator in (4) uses a scalar pilot signal $\mathbf{y}$ to excite all the channel dimensions in the UL. Increasing the length of the pilot can improve the MSE.

Assume that the training signal is $\mathbf{y} \in \mathbb{C}^{1\times B}$ where $1 \le \boldsymbol{B} \le \boldsymbol{T}^{UL}_{pilot}$. Separate LMMSE estimates need to be calculated for every element B, $\hat{\mathbf{h}}_i = \mathbf{h} - \boldsymbol{\epsilon}_i$ **for** $i = 1, \dots, B$ and taking the average we get.

$$\bar{\hat{\mathbf{h}}} = \frac{1}{B}\sum_{i=1}^{B}\hat{\mathbf{h}}_i = \mathbf{h} - \frac{1}{B}\sum_{i=1}^{B}\boldsymbol{\epsilon}_i \tag{7}$$

Then the MSE becomes

$$\mathbb{E}\left\{\left(\frac{1}{B}\sum_{i=1}^{B}\boldsymbol{\epsilon}_i\right)^H\left(\frac{1}{B}\sum_{i=1}^{B}\boldsymbol{\epsilon}_i\right)\right\} = \frac{\mathrm{tr}(\mathbf{G})}{B} \tag{8}$$

Hence, the MSE is inversely proportional to the pilot length. It goes to zero with increasing the length of the pilot B.

978-1-5090-4090-2/16/$31.00 ©2016 IEEE

ISBN 978-1-5090-4089-6

IV. NUMERICAL RESULTS

This section shows the effect of SC on the accuracy of the estimated channel.

The relative estimation error per antenna, $\text{MSE}_{rel} = \frac{\text{MSE}}{\text{tr}(\mathbf{R})}$, for different numbers of antennas at the BS is presented as a function of angular spread in Fig. 2. We consider N= (2,4,16,128) antennas at the BS and we fix the SNR at 5dB. The one ring model [19] is used to generate the channel covariance matrix **R**. This model assumes that the multipath components arrive to the BS with an angle spread between 0 to 90 degrees from the main angle of arrival. It is also assumed that spacing between the adjacent antennas is half wavelength where the BS has ULA.

Fig. 2 confirms that in the case of low angular spread where the spatial correlation is high, estimation accuracy is improved when the number of antennas at the BS is large. However, there is no big difference in estimation accuracy between BSs with high and low number of antennas when the channels are uncorrelated.

The Relative estimation error for the linear MMSE estmatator as a function of angular spread for different SNRs= (5, 10, 15)dB where the BS have 50 antennas is shown in Fig. 3. Estimation accuracy is improved at higher uplink SNR. Fig. 3 proves that increasing the uplink SNR can always makes the estimate of the channel more accurate regardless how correlated the channels are.

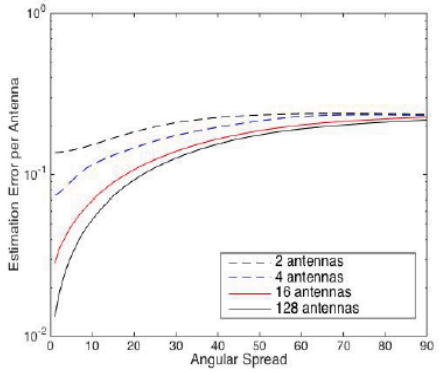

Fig. 2. Relative estimation error for the linear MMSE estmatator as a function of angular spread for different numbers of antennas at the BS with uplink SNR= 5dB.

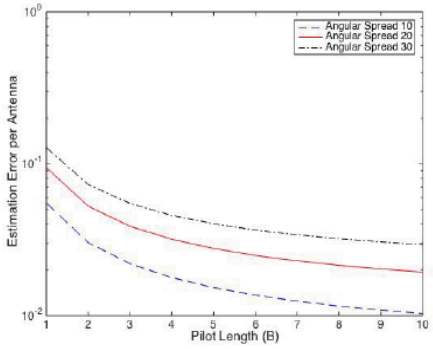

Fig. 4. Relative estimation error for the linear MMSE estmatator as a function of pilot length for different angular spreads (10, 20, 30) degrees with uplink SNR of 5dB

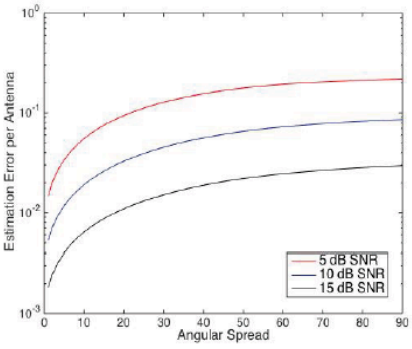

Fig. 3. Relative estimation error for the linear MMSE estmatator as a function of angular spread for different SNRs= (5, 10, 15)dB with BS of 50 antennas.

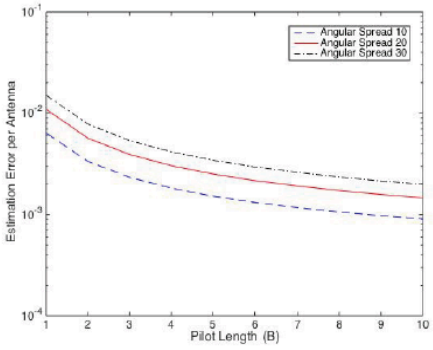

Fig. 5. Relative estimation error for the linear MMSE estmatator as a function of pilot length for different angular spreads (10, 20, 30) degrees with uplink SNR of 15dB.

978-1-5090-4090-2/16/$31.00 ©2016 IEEE

ISBN 978-1-5090-4089-6

Longer pilot signals that span B≥1 channel uses can reduce errors per antenna. Fig. 4 and Fig. 5 show the relative estimation error for the linear MMSE estmatator as a function of pilot length for different angular spreads (10, 20, 30) degrees where the uplink SNRs are 5 dB and 15 dB repectively. Correlated channels can exist when the angular spread of one ring model is low. It is clear that highly correlated channels can be estimated with more accurrcy. This conclusion is consistant with the results of [19]. It is also obvious that increasing the length of the pilot bring additional improvement to the channel estimation accurcy.

V. CONCLUSION

We investigated the accuracy of channel estimation for massive MIMO systems. The investigation was established on an uplink system model where the BS has a large number of antennas while the user has a single antenna. We studied the effects of spatial correlation on the estimation error per antenna for massive MIMO. We also used the one ring model in order to analyze the impact of SC between antennas. Simulation results showed that increasing the number of antennas makes channel estimation more accurate especially when the antennas are highly correlated.

REFERENCES

[1] T. L. Marzetta, "Massive MIMO: An Introduction," *Bell Labs Tech. J.*, vol. 20, pp. 11–22, 2015.

[2] F. Boccardi, R. W. Heath, A. Lozano, T. L. Marzetta, and P. Popovski, "Five Disruptive Technology Directions for 5G," *IEEE Commun. Mag*, vol. 52, no. 2, pp. 74–80, 2014.

[3] J. G. Andrews, S. Buzzi, W. Choi, S. V. Hanly, A. Lozano, A. C. K. Soong, and J. C. Zhang, "What Will 5G Be?," *IEEE J. Sel. Areas. Commun*, vol. 32, no. 6, pp. 1065–1082, 2014.

[4] T. L.Marzetta, "Noncooperative cellularwireless with unlimited numbers of base station antennas," *IEEE Trans. Wirel. Commun*, vol. 9, no. 11, pp. 3590–3600, 2010.

[5] L. Lu, G. Y. Li, A. Ashikhmin, R. Zhangand, and A. L. Swindlehurst, "An Overview of Massive MIMO : Benefits and Challenges," *IEEE J. Sel. Top. Signal Process.*, vol. 8, no. 5, pp. 742–758, 2014.

[6] E. Bjornson, J. Hoydis, M. Kountouris, and M. Debbah, "Massive MIMO systems with non-ideal hardware: Energy efficiency, estimation, and capacity limits," *IEEE Trans. Inf. Theory*, vol. 60, no. 11, pp. 7112–7139, 2014.

[7] E. Bjornson, E. G. Larsson, and T. L. Marzetta, "Massive MIMO: ten myths and one critical question," *IEEE Commun. Mag.*, vol. 54, no. 2, pp. 114–123, 2016.

[8] D. Persson, B. K. Lau, and E. G. Larsson, "Scaling Up MIMO," *IEEE Signal Process. Mag.*, vol. 30, no. 1, pp. 40–60.

[9] H. Q. Ngo, E. G. Larsson, and T. L. Marzetta, "Energy and Spectral Efficiency of Very Large Multiuser MIMO Systems," *IEEE Trans. Commun.*, vol. 61, no. 4, pp. 1436–1449, 2013.

[10] E. Bjornson, J. Hoydis, M. Kountouris, and M. Debbah, "Hardware Impairments in Large-scale MISO Systems : Energy Efficiency , Estimation , and Capacity Limits," in *Proceedings of International Conference on Digital Signal Processing*.

[11] E. Telatar, "Capacity of multi-antenna Gaussian channels," *Eur. Trans. Telecommun*, vol. 10, no. 6, pp. 585–595, 1999.

[12] B. Lv, Z. Yang, and Y. Feng, "Temporally and Spatially Correlated Uplink Channel Estimation for Massive MIMO Systems," in *International Conference on Wireless Communications & Signal Processing (WCSP)*, 2015

[13] R. C. de Lamare, "Massive MIMO Systems: Signal Processing Challenges and Research Trends," *URSI Radio Sci. Bull,* pp. 1–9, 2013.

[14] D. Tse and P. Viswanath, *Fundamentals of Wireless Communications*, 1st ed. Cambridge, UK: Cambridge University Press, 2005.

[15] T. L.Marzetta, "How much training is required formultiuserMIMO?," in *ACSSC 40th Asilomar Conference on Signals, Systems and Computers.*, 2006, pp. 359–363.

[16] S. Biswas, J. Xue, F. A. Khan, and Tharmalingam Rantnarajah, "Performance Analysis of Correlated Massive MIMO Systems With Spatially Distributed Users," *IEEE Syst. J.*, vol. PP, no. 99, pp. 1–12.

[17] X. Liu, M. E. Bialkowski, and F. Wang, "Investigations into the Effect of Spatial Correlation on Channel Estimation and Capacity of Multiple Input Multiple Output System," *Int'l J. Commun. Netw. Syst. Sci.*, vol. 02, no. 04, pp. 267–275, 2009.

[18] A. Adhikary, J. Nam, J. Y. Ahn, and G. Caire, "Joint Spatial Division and Multiplexing—The Large-Scale Array Regime," *IEEE Trans. Inf. Theory*, vol. 59, no. 10, pp. 6441–6463, 2013.

[19] J. Gong, J. F. Hayes, and M. R. Soleymani, "The effect of antenna physics on fading correlation and the capacity of multielement antenna systems," *IEEE Trans. Veh. Technol.*, vol. 56, no. 4 I, pp. 1591–1599, 2000.

[20] B. Hassibi and B. M. Hochwald, "How much training is needed in multiple-antenna wireless links?," *IEEE Trans. Inf. Theory*, vol. 49, no. 4, pp. 951–963, 2003.

978-1-5090-4090-2/16/$31.00 ©2016 IEEE

ISBN 978-1-5090-4089-6

Appendix C

(Journals)

International Journal of Computer Science and Information Security (IJCSIS),
Vol. 15, No. 6, June 2017

Impact of Spatial Correlation and Users Allocation on The Performance of Massive MIMO Systems

Ahmed Alshammari, Saleh Albdran, and Mohammad Matin

***Abstract*— The next generation of wireless networks must substantially improve the area data throughput, to meet the expected growth on the demand of wireless communications. The area data throughput can at least be ten times improved using the Massive MIMO technology that increases the spectral efficiency without using more bandwidth or increasing the density of the cells. These phenomenal improvements can be made possible using large numbers of antennas in the base station (BS) to enable spatial multiplexing of a big number of terminals. In this paper, we study the relation between the number of terminals, channel spatial correlation, number of BS antennas, other system parameters and the performance of Massive MIMO systems. The system analysis is based on the derived spectral and energy efficiencies expressions that can be achieved using the channel estimates. Simulations are used to show the ergodic channel capacity and the energy efficiency, in different channel spatial correlation scenarios and different number of user terminals. We notice that the energy efficiency and the capacity improve as the channels starts de-correlating. We also note that the improvement in the channel capacity varies depending on the numbers of terminals and the BS antennas.**

***Index Terms*— Massive MIMO, Capacity, LMMSE, Wireless, Correlation, spectral efficiency.**

I. Introduction

DATA traffic has doubled almost every 30 months since the invention of wireless communications according to the observation that Martin Cooper made in the nineties [1], [2]. The current exponential increase is led by the escalating demand driven by the huge growth wireless data traffic. Nothing indicate that this demand will slow down anytime soon. Thus, future cellular networks must have higher capacity to meet the continuously growing need for wireless communications [3]. It is preferred to achieve this goal without increasing the number of base stations or using additional bandwidth. Thus, one of the main goals of the 5G technologies is being more efficient in bandwidth usage by orders of magnitude [4]–[6].

Three different components can be used to increase the efficiency of wireless systems: (1) using more of the frequency spectrum (2) densification of the cellular networks by increasing the numbers of cells that operate with independent base stations and (3) increasing the efficiency of bandwidth usage [7]. The first two components have greatly contributed to the improvement of spectral efficiency of the previous network generations. However, bands below 5 GHz that can provide good network service are so scarce because most of it has already been allocated to existing services. Moreover, although it is still possible to increase the cell density, the option of cell densification is reaching a saturation point. On the other hand, no major improvements were made on the spectral efficiency in the past network generations. Therefore, this factor might be the only way to bring higher area throughput to the next generation of wireless networks [8].

During the last decade, the technology of multiple input multiple output (MIMO) has considerably contributed to the improvements in the reliability and the capacity of wireless systems [8]. Although the initial form of the MIMO technology was designed for devices equipped with several antennas to communicate with each other in point to point links, it has been developed to more general form known as multi-user MIMO where the BS serves users with single antenna terminals to share the multiplexing gain [9]. In general, the impact of the propagation environment on Multi user MIMO is less than the case of point to point MIMO due to the multi-user diversity. Therefore, Multi user MIMO became an important component of most communication standards [8]. Typically, the number of BS antennas are not so big for MIMO applications. Hence. it does not bring significant improvements for spectral efficiency.

Massive multiple input multiple output (MIMO) which is a scale up of MIMO technology has recently been proposed [10]. This technology provides the means that can potentially enhance spectral efficiency by orders of magnitudes [11]. It can achieve this goal by equipping the BS with tens or even hundreds of antennas [12], [13]. According to the theory of random matrix, [14] asymptotically shows that increasing the antennas eliminate the impact of the uncorrelated noise and the small scale fading. The cell size and the number of users with massive MIMO are independent. Moreover, simple linear signal processing like match filtering is sufficient to achieve the advantageous of massive MIMO [15]. These unprecedented gains allow serving tens of users in every cell simultaneously,

while the robustness against inter-user interference is maintained [16], [17].

https://sites.google.com/site/ijcsis/
ISSN 1947-5500

The downlink (DL) and uplink (UL) operations of Massive MIMO are shown in Fig.1 that can be considered cell singled out of a network of cells. Single antenna users K are served through a BS that contains an array of antennas [18]. Different BS serve the other cell sites without cooperating with each other except for power control and the assignment of pilots [10]. Every user can take the advantage of the full time-frequency resources for the UL and DL transmissions. On the UL, the BS recovers the signals sent by individual users. On the DL, users only receive the signals aimed for them. At the BS, availability of the channel state information (CSI) enable multiplexing. between users.

Time division duplex (TDD) mode in Fig. 2 has several advantageous. First, channel knowledge is only needed at the BS for coherent antenna processing [1], [19]. Second, the necessary overhead required for channel estimation and the number of BS antennas are independent. Hence, TDD is preferred for massive MIMO because it is possible to use the same frequency resource for UL and DL transmissions when they are separated in time [18]. TDD operation exploit the fact that propagation channels can be reciprocal which makes the channel response identical for both directions [20]. The property of channel reciprocity enable massive MIMO systems of using the same channel for combining the received UL signal and the precoding of the DL transmission.

This paper studies the effect of spatially correlated channels and the number of users of Massive MIMO systems on its capacity and energy efficiency. The remainder of this paper is structured as the following. The system model is introduced in section II. Section III discusses the channel estimator used to estimate the Massive MIMO channel. section IV shows the numerical results that illustrate the limitations that channel spatial correlations and user allocation impose on the capacity on the Massive MIMO system. Section V investigates energy efficiency of the model introduced in section II. Section VI is the final part which conclude this paper.

Notations: column vectors and matrices are indicated with boldface lowercase $\mathbf{x}$ and uppercase $\mathbf{X}$ respectively. $\mathbf{X}^{\boldsymbol{H}}$ is used to denote conjugate transpose, $\mathbf{X}^{\boldsymbol{T}}$ denote transpose, $\mathbf{X}^{*}$ indicate conjugate and $\mathrm{tr}(\mathbf{X})$ is used to indicate the trace of matrix $\mathbf{X}$ is denoted

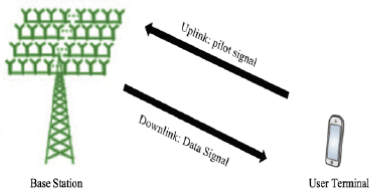

Fig.1. Channel reciprocity between base station (BS) with a large number of antennas and a single antennas terminal.

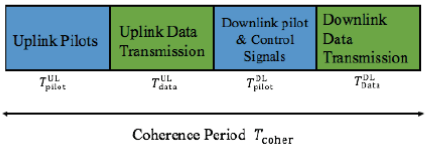

Fig. 2. Time division duplex (TDD) protocol

II. System Model

This paper investigates the performance of Massive MIMO systems considering the effect of channel spatial correlation and the number of users in a single cell scenario. The BS is equipped with M-antennas while the users have a single antenna each. The BS antennas M can be increased to a very large number. Hence, to enable efficient channel estimation, time division duplex (TDD) mode is used to transmit DL and UL signals through one flat fading subcarrier [11]. The overhead needed for channel estimation and the number of BS antennas are independent because of channel reciprocity according to the TDD protocol.

A. Downlink/Uplink channel model

The received signal $z \in \mathbb{C}$ on the DL for multi input single output flat fading channel are modeled as

$$z = \mathbf{h}^{\boldsymbol{T}}\mathbf{d} + v \tag{1}$$

where $\mathbf{d} \in \mathbb{C}^{N\times 1}$ denotes the pilot signal or the zero mean stochastic data signal. $\mathbf{X} = \mathbb{E}\{\mathbf{d}\mathbf{d}^{\boldsymbol{H}}\}$ indicates the covariance matrix where the average power is $p^{\mathrm{BS}} = \mathrm{tr}(\mathbf{X})$. The parameter $\mathbf{X}$ depends on the channel realization. Therefore, it stays the same during the coherence period but varies between blocks since the channel realization differs. v represents a stochastic process that consists of the receiver noise and the zero-mean interference caused by other users

$$v = v_{\boldsymbol{noise}} + v_{\boldsymbol{interf}} \tag{2}$$

The received UL signal $\mathbf{y} \in \mathbb{C}^{N}$ which also can be used for pilot and data transmissions is modeled as in (3).

$$\mathbf{y} = \mathbf{h}s + \mathbf{n} \tag{3}$$

where $s \in \mathbb{C}$ represents the pilot signal used for channel estimation or the stochastic data signal with average power $p^{UE} = \mathbb{E}\{|s|^2\}$. The term $\mathbf{n} \in \mathbb{C}^{N\times 1}$ in (4) is also a representation of the stochastic process containing the receiver noise and the zero-mean interference caused by other users

$$\mathbf{n} = \mathbf{n}_{\boldsymbol{noise}} + \mathbf{n}_{\boldsymbol{interf}} \tag{4}$$

B. One ring model

To analyze the capacity of Massive MIMO channels, we consider the one ring model [21]. Fig. 3 shows that model with

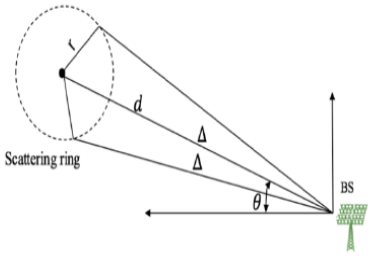

Fig. 3. The one ring model

the assumption that the location of the user is surrounded with a ring of radius r of scattering objects whereas the BS is not surrounded with any scattering objects. The model also assumes an azimuth angle θ between the BS and user which is located at distance d. The covariance matrix $\mathbf{R}$ of channel for $1 \leq n, p \leq N$ is given in (5) [22].

$$[\mathbf{R}]_{n,p} = \frac{1}{2\Delta}\int_{-\Delta}^{\Delta} e^{jk^T(\alpha+\theta)(u_n-u_p)}\, d\alpha \qquad (5)$$

where Δ denotes the angle spread of the multipath components, u_n, u_p indicate the position vector of the BS and

$$k(\alpha) = -\frac{2\pi}{\lambda}(\cos(\alpha), \sin(\alpha))^{\mathrm{T}}$$

The antennas are assumed to be distributed with a half wavelength spacing in a uniform linear array (ULA). Hence, The Toeplitz form of the channel covariance matrix is given in (6).

$$[\mathbf{R}]_{n,p} = \frac{1}{2\Delta}\int_{-\Delta+\theta}^{\Delta+\theta} e^{-j2\pi D(n-p)sin(\alpha)}\, d\alpha \qquad (6)$$

III. Uplink Channel Estimation

Estimating the UL channel $\mathbf{h}$ is done using the UL pilot transmission. We consider Rayleigh fading channel under the effect of i.i.d noise [9]. We use the linear minimum mean square error estimator (LMMSE) to estimate the UL channel using the received UL signal

$$\hat{\mathbf{h}} = s^{*}\mathbf{R}\bar{\mathbf{Y}}^{-1}\mathbf{y} \qquad (7)$$

where $\bar{\mathbf{y}}$ is given in (8) and $\mathbf{R}$ denote the covariance matrix

$$\bar{\mathbf{Y}} = \mathbb{E}\{\mathbf{y}\mathbf{y}^{H}\} = p^{UE}\boldsymbol{R} + \boldsymbol{S} + \sigma_{BS}{}^{2}\mathbf{I} \qquad (8)$$

The mean square error (MSE) is

$$\mathrm{MSE} = \mathrm{tr}(\mathbf{G}) = \mathbb{E}\left\|\hat{\mathbf{h}} - \mathbf{h}\right\|_2^2 \qquad (9)$$

Where the error covariance matrix $\mathbf{G}$

$$\mathbf{G} = \mathbb{E}\{(\hat{\mathbf{h}} - \mathbf{h})\left(\hat{\mathbf{h}} - \mathbf{h}\right)^{H}\} = \mathbf{R} - p^{UE}\mathbf{R}\bar{\mathbf{Y}}^{-1}\mathbf{R} \qquad (10)$$

The actual channel consists of the LMMSE channel estimate and the estimation error as shown in (7)

$$\mathbf{h} = \hat{\mathbf{h}} + \boldsymbol{\epsilon} \qquad (11)$$

where $\boldsymbol{\epsilon} \in \mathbb{C}^{N\times 1}$ denotes error of the LMMSE estimator.

A. Numerical Results

Simulation results that show the influence of spatial correlation on accuracy of channel estimation are discussed in this section.

We consider various numbers of BS antennas (2, 4, 16, 128) and different uplink SNRs. Fig. 4 shows the per antenna relative estimation errors with respect to the angle spread. The multipath components are received at the BS with angle spread that varies between 0 and 55 degrees according to the one ring model which is used to generate the covariance matrix of the channel $\mathbf{R}$. The most important observation from Fig. 4 is that the channel spatial correlation has a great effect on the estimation accuracy. According to the one ring model, decreasing the angle spread results in higher spatial correlation.

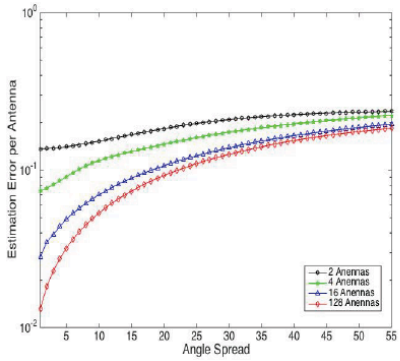

Fig. 4. Estimation error per antenna vs angle spread with UL SNR= 5dB

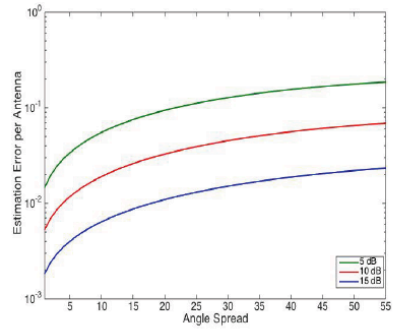

Fig. 5. Estimation error vs angle spread for 50 BS antennas with SNR (5, 10, 15) dBs.

Our results show that it is easier to estimate the spatially correlated channel because they have smaller errors as shown in Fig. 5. We also notice that the estimation error per antenna is improved if the antennas number *N* is increased in the one ring model. The reason for that is the lack of richness in the propagation that can be encountered in practice as in the one ring model.

Fig. 5. shows the estimation error per antenna using the one ring model for *N*=50 antennas for various SNRs=(5,10, 15) dB. Estimation accuracy is presented as a function of angle spread. Higher SNRs reduce the errors in channel estimation per antenna.

IV. DL/UL Data Transmission

This section investigates the capacity of massive MIMO channel. We focus on the impact of spatial correlation and the user allocation. We evaluate the capacity of the system based on the imperfect pilot based estimated channel that was studied in section II. Hence, the system capacity will depend on the channel state information obtained with the LMMSE estimator. We start by considering random knowledge of the channel at the user equipment and the BS to evaluate the DL and UL channel capacities in (1) and (3) respectively. Therefore, random knowledge $\mathcal{H}^{\mathrm{BS}}$is available at the BS of the channel $\mathcal{H}$ during each coherence time. This knowledge is used to select conditional distribution of the transmit data $f = (\mathbf{d}|\mathcal{H}^{\mathrm{BS}})$. Moreover, different knowledge of the channel $\widehat{\mathcal{H}}^{UE}$ is available at the user equipment. The capacity of DL channel is

$$\mathrm{C}^{\mathrm{DL}} = \frac{\tau_{\mathrm{data}}^{\mathrm{DL}}}{T_{\mathrm{coher}}} \mathbb{E}\left\{ f = (\mathbf{d}|\mathcal{H}^{\mathrm{BS}}) : \max \mathbb{E}\|\mathbf{d}\|_2^2 \le p^{\mathrm{BS}} \quad \mathfrak{T}\left(\mathbf{d}; z|\mathcal{H}, \mathcal{H}^{\mathrm{BS}}, \widehat{\mathcal{H}}^{\mathrm{UE}}\right)\right\} \tag{12}$$

The mutual information between the transmitted and the received DL signals is $\mathfrak{T}\left(\mathbf{d}; z|\mathcal{H}, \mathcal{H}^{\mathrm{BS}}, \widehat{\mathcal{H}}^{\mathrm{UE}}\right)$. The capacity of the UL channel is calculated as

$$\mathrm{C}^{\mathrm{UL}} = \frac{\tau_{\mathrm{data}}^{\mathrm{UL}}}{T_{\mathrm{coher}}} \mathbb{E}\left\{ f = (s|\mathcal{H}^{\mathrm{UE}}) : \max \mathbb{E}\{\|s\|_2^2\} \le p^{\mathrm{BS}} \quad \mathfrak{T}\left(\mathbf{d}; \mathbf{y}|\mathcal{H}, \mathcal{H}^{\mathrm{BS}}, \widehat{\mathcal{H}}^{\mathrm{UE}}\right)\right\} \tag{13}$$

The mutual information between the transmitted and the received UL signals is $\mathfrak{T}\left(\mathbf{d}; \mathbf{y}|\mathcal{H}, \mathcal{H}^{\mathrm{BS}}, \widehat{\mathcal{H}}^{\mathrm{UE}}\right)$. The expectation in (13) can be calculated using the joint distribution of $\mathcal{H}, \mathcal{H}^{\mathrm{BS}}, \widehat{\mathcal{H}}^{\mathrm{UE}}$. $\frac{\tau_{\mathrm{data}}^{\mathrm{DL}}}{T_{\mathrm{coher}}}$ and $\frac{\tau_{\mathrm{data}}^{\mathrm{UL}}}{T_{\mathrm{coher}}}$ indicate the portion of channel uses allocated for UL and DL transmissions respectively.

If $\widehat{\mathcal{H}}^{UE}$and $\widehat{\mathcal{H}}^{BS}$ are the available estimations of the DL/UL channel at the receiver that do not match $\mathcal{H}^{\mathrm{BS}}$and $\mathcal{H}^{\mathrm{UE}}$, capacities in (12) and (13) become

$$\mathrm{C}^{\mathrm{DL}} = \frac{\tau_{\mathrm{data}}^{\mathrm{DL}}}{T_{\mathrm{coher}}} \mathbb{E}\left\{\log_2(1 + \mathrm{SINR}^{\mathrm{DL}}(\mathbf{x}^{\mathrm{DL}}))\right\} \tag{14}$$

$$\mathrm{C}^{\mathrm{UL}} = \frac{\tau_{\mathrm{data}}^{\mathrm{UL}}}{T_{\mathrm{coher}}} \mathbb{E}\left\{\log_2(1 + \mathrm{SINR}^{\mathrm{UL}}(\mathbf{x}^{\mathrm{UL}}))\right\} \tag{15}$$

where $\mathbf{x}^{\mathrm{UL}} = [u_1^{\mathrm{UL}} \dots u_k^{\mathrm{UL}}]^T$ and $\mathbf{x}^{\mathrm{DL}} = [u_1^{\mathrm{DL}} \dots u_k^{\mathrm{DL}}]^T$ denote the receive combining and the transmit beamforming vectors which have unit norm and are a function of $\hat{\mathbf{h}}$. Capacities on (14) and (15) can be numerically computed for any beamforming vector and any combining vector of the estimated channel $\hat{\mathbf{h}}$. The SINR for DL & UL are given in (16) and (17) respectively.

$$\mathrm{SINR}^{\mathrm{DL}}(\mathbf{x}^{\mathrm{DL}}) = \frac{\left|\mathbb{E}\left\{\mathbf{h}^H \mathbf{x}^{\mathrm{DL}} | \widehat{\mathcal{H}}^{\mathrm{UE}}\right\}\right|^2}{\mathbb{E}\left\{\left|\mathbf{h}^H \mathbf{x}^{\mathrm{DL}}\right|^2 | \widehat{\mathcal{H}}^{\mathrm{UE}}\right\} - \left|\mathbb{E}\left\{\mathbf{h}^H \mathbf{x}^{\mathrm{DL}} | \widehat{\mathcal{H}}^{UE}\right\}\right|^2 + \frac{\mathbb{E}\left\{I_{\mathcal{H}}^{\mathrm{UE}} | \widehat{\mathcal{H}}^{UE}\right\}}{p^{\mathrm{BS}}} + \frac{\sigma^2{}_{\mathrm{UE}}}{p^{\mathrm{BS}}}} \tag{16}$$

$$\mathrm{SINR}^{\mathrm{UL}}(\mathbf{x}^{\mathrm{UL}}) = \frac{\left|\mathbb{E}\left\{\mathbf{h}^H \mathbf{x}^{\mathrm{UL}} | \widehat{\mathcal{H}}^{\mathrm{BS}}\right\}\right|^2}{\mathbb{E}\left\{\left|\mathbf{h}^H \mathbf{x}^{\mathrm{UL}}\right|^2 | \widehat{\mathcal{H}}^{\mathrm{BS}}\right\} - \left|\mathbb{E}\left\{\mathbf{h}^H \mathbf{x}^{\mathrm{UL}} | \widehat{\mathcal{H}}^{BS}\right\}\right|^2 + \frac{\mathbb{E}\left\{(\mathbf{x}^{\mathrm{UL}})^H (\mathrm{Q}_{\mathcal{H}} + \sigma_{\mathrm{BS}}^2 \mathrm{I}) \mathbf{x}^{\mathrm{UL}} | \widehat{\mathcal{H}}^{\mathrm{BS}}\right\}}{p^{\mathrm{UE}}}} \tag{17}$$

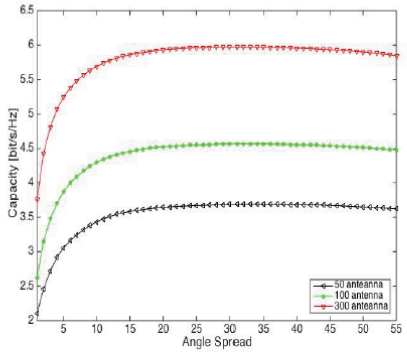

Fig. 6. Channel capacity vs angle spread SNR:0 dB.

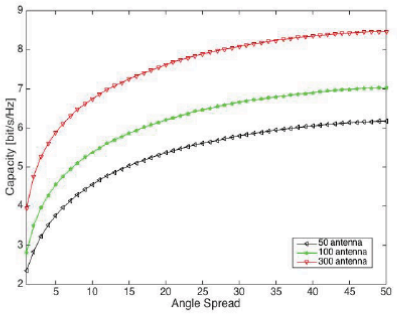

Fig. 7. Channel capacity vs angle spread SNR:25 dB.

A. Numerical Results

Next, we show the impact of spatial correlation and users allocation on the channel capacity of massive MIMO in a single

A. Numerical Results

Energy efficiency of massive MIMO can be affected by many factors such as the transmit power, spatial correlation, the number of antennas and the circuit power parameters ρ and ζ. The power consumed by the system with N=1 antennas is assumed to be $\rho + \zeta = 0.02 \frac{\mu J}{\text{Channel use}}$. Hence, for any number of antennas N, $N\rho + \zeta$ is the consumed power at the circuit. $\frac{\rho}{\rho+\zeta} = 0$ is used to split between ρ and ζ. Also, the amplifiers efficiencies $\omega^{\text{BS}}, \omega^{\text{UE}}$is fixed at 0.3. The one ring model in (6) is used to generate the channel covariance matrix with varying the angle spread between 10 and 50. Setting up $\alpha_{\text{DL}} = \alpha_{\text{UL}} = 0.5$ and $\frac{T^{\text{UL}}_{\text{data}}}{T_{\text{coher}}} = \frac{T^{\text{DL}}_{\text{data}}}{T_{\text{coher}}} = 0.05$ result in identical DL and UL EE.

Fig. 9 shows the energy efficiencies of DL/UL for three different number of antennas scenario using (12) and (13). Increasing the number of antennas in the BS improve the energy efficacy. The figure also shows that the increased channel spatial correlation has a negative effect on the energy efficiency of massive MIMO.

The corresponding power allocations of the three cases in Fig. 9 are shown in Fig 10. Despite the enhanced energy efficacy, more transmit power is needed when increasing the number of antennas in the BS and when the channels are less correlated.

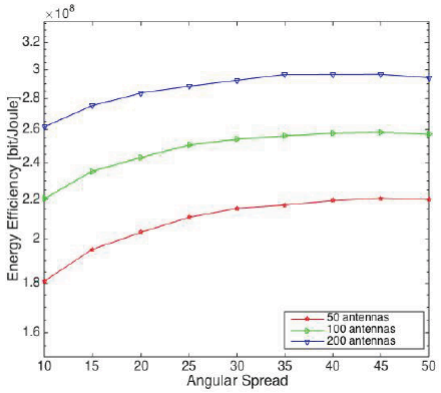

Fig. 10. Energy efficiency vs the angle spread at SNR: 20 dB.

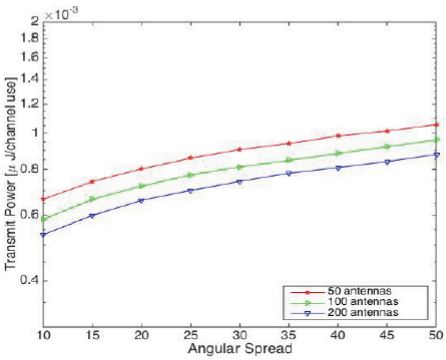

Fig. 11. Transmit power as a function of angle spread

VI. Conclusion

The effect of spatial correlation and the user allocations on massive MIMO systems were studied in this paper. The analysis is based on a system model that considers the spatial correlation and the number of users in a single cell scenario. Our results show that the benefits of the gains that comes with the large antenna array varies based on the channel condition and the number of users being served. It has been shown that the capacity and the energy efficiency are negatively affected when the channel spatial correlation is increased. It was shown that more users can be served when the number of base station antennas is increased. However, exceeding a certain number of users negatively affects the performance of Massive MIMO system.

References

[1] A. Alshammari, S. Albdran, and M. A. Matin, "The Effect of Channel Spatial Correlation on Capacity and Energy Efficiency of Massive MIMO Systems," in *The 7th IEEE annual Comuting and Communication Workshop and Conferernce*, 2017.

[2] T. Van Chien and E. Björnson, "Massive MIMO Communications," in *5G Mobile Communications*, E. W. Xiang, K. Zheng, and X. Shen, Eds. Springer, 2017, pp. 77–116.

[3] T. Van Chien and E. Björnson, "Massive MIMO Communications," in *5G Mobile Communications*, E. W. Xiang, K. Zheng, and X. Shen, Eds. Springer, 2017, pp. 77–116.

[4] T. L. Marzetta, "Massive MIMO: An Introduction," *Bell Labs Tech. J.*, vol. 20, pp. 11–22, 2015.

[5] F. Boccardi, R. W. Heath, A. Lozano, T. L. Marzetta, and P. Popovski, "Five Disruptive Technology Directions for 5G," *IEEE Commun. Mag*, vol. 52, no. 2, pp. 74–80, 2014.

[6] S. Albdran, A. Alshammari, M. Ahad, and M. Matin, "Effect of Exponential Correlation Model on Channel Estimation fo Massive MIMO," in *The 19th International Conference on Computer and Information Technology (ICCIT)*, 2016.

[7] T. L. Marzetta, E. G. Larsson, H. Yang, and H. Q. Ngo, *Fundamentals of Massive MIMO*. New York: Cambridge University Press, 2016.

[8] L. Lu, G. Y. Li, A. Ashikhmin, R. Zhangand, and A. L. Swindlehurst, "An Overview of Massive MIMO : Benefits and Challenges," *IEEE J. Sel. Top. Signal Process.*, vol. 8, no. 5, pp. 742–758, 2014.

[9] T. L.Marzetta, "How much training is required formultiuserMIMO?," in *ACSSC 40th Asilomar Conference on Signals, Systems and Computers.*, 2006, pp. 359–363.

[10] T. L. Marzetta, "Noncooperative Cellular Wireless with Unlimited Numbers of Base Station Antennas," vol. 9, no. 11, pp. 3590–3600, 2010.

[11] E. G. Larsson, O. Edfors, F. Tufvesson, and T. L. Marzetta, "Massive MIMO for Next Generation Wireless Systems," no. February, pp. 1–19, 2013.

[12] R. C. De Lamare, "Massive MIMO Systems : Signal Processing Challenges and Research Trends," pp. 1–9.

[13] A. Alshammari, S. Albdran, M. A. R. Ahad, and M. Matin, "Impact of Angular Spread on Massive MIMO Channel Estimation," in *The 19th International Conference on Computer and Information Technology (ICCIT)*, 2016.

[14] T. L.Marzetta, "Noncooperative cellularwireless with unlimited numbers of base station antennas," *IEEE Trans. Wirel. Commun*, vol. 9, no. 11, pp. 3590–3600, 2010.

[15] H. Q. Ngo, E. G. Larsson, and T. L. Marzetta, "Energy and Spectral Efficiency of Very Large Multiuser MIMO Systems," *IEEE Trans. Commun.*, vol. 61, no. 4, pp. 1436–1449, 2013.

[16] E. Björnson, E. G. Larsson, and M. Debbah, "Massive MIMO for Maximal Spectral Efficiency: How Many Users and Pilots Should Be Allocated?," *IEEE Trans. Wirel. Commun.*, vol. 15, no. 2, pp. 1293–1308, 2016.

[17] S. Albdran, A. Alshammari, and M. A. Matin, "Spectral and Energy Efficiency for Massive MIMO Systems Using Exponential Correlation Model," in *The 7th IEEE annual Comuting and Communication Workshop and Conferernce*, 2017.

[18] D. Persson, B. K. Lau, and E. G. Larsson, "Scaling Up MIMO," *IEEE Signal Process. Mag.*, vol. 30, no. 1, pp. 40–60.

[19] E. Bjornson, J. Hoydis, M. Kountouris, and M. Debbah, "Hardware Impairments in Large-scale MISO Systems : Energy Efficiency , Estimation , and Capacity Limits," in *Proceedings of International Conference on Digital Signal Processing*, 2013.

[20] E. Bjornson, E. G. Larsson, and T. L. Marzetta, "Massive MIMO: ten myths and one critical question," *IEEE Commun. Mag.*, vol. 54, no. 2, pp. 114–123, 2016.

[21] A. Adhikary, J. Nam, J. Y. Ahn, and G. Caire, "Joint Spatial Division and Multiplexing—The Large-Scale Array Regime," *IEEE Trans. Inf. Theory*, vol. 59, no. 10, pp. 6441–6463, 2013.

[22] J. Gong, J. F. Hayes, and M. R. Soleymani, "The effect of antenna physics on fading correlation and the capacity of multielement antenna systems," *IEEE Trans. Veh. Technol.*, vol. 56, no. 4 I, pp. 1591–1599, 2000.